CO_2 Capture by Absorption with Potassium Carbonate
First Quarterly Report 2007

Quarterly Progress Report
Reporting Period Start Date: January 1, 2007
Reporting Period End Date: March 31, 2007
Authors: Gary T. Rochelle,
Andrew Sexton, Jason Davis, Marcus Hilliard, Qing Xu, David Van Wagener, Jorge M. Plaza,
Amornvadee Veawab (University of Regina), Manjula Nainar (University of Regina)

April 27, 2007
DOE Award #: DE-FC26-02NT41440
Department of Chemical Engineering
The University of Texas at Austin

Disclaimer

Abstract

The objective of this work is to improve the process for CO_2 capture by alkanolamine absorption/stripping by developing an alternative solvent, aqueous K_2CO_3 promoted by piperazine. The best K^+/PZ solvent, 4.5 m K^+/4.5 m PZ, requires equivalent work of 31.8 kJ/mole CO_2 when used with a double matrix stripper and an intercooled absorber. The oxidative degradation of piperazine or organic acids is reduced significantly by inhibitor A, but the production of ethylenediamine is unaffected. The oxidative degradation of piperazine in 7 m MEA/2 m PZ is catalyzed by Cu^{++}. The thermal degradation of MEA becomes significant at 120^{o}C. The solubility of potassium sulfate in MEA/PZ solvents is increased at greater CO_2 loading.

The best solvent and process configuration, matrix with MDEA/PZ, offers 22% and 15% energy savings over the baseline and improved baseline, respectively, with stripping and compression to 10 MPa. The energy requirement for stripping and compression to 10 MPa is about 20% of the power output from a 500 MW power plant with 90% CO_2 removal. The stripper rate model shows that a "short and fat" stripper requires 7 to 15% less equivalent work than a "tall and skinny" one. The stripper model was validated with data obtained from pilot plant experiments at the University of Texas with 5m K^+/2.5m PZ and 6.4m K^+/1.6m PZ under normal pressure and vacuum conditions using Flexipac AQ Style 20 structured packing. Experiments with oxidative degradation at low gas rates confirm the effects of Cu^{+2} catalysis; in MEA/PZ solutions more formate and acetate is produced in the presence of Cu^{+2}. At 150^{o}C, the half life of 30% MEA with 0.4 moles CO_2/mole amine is about 2 weeks. At 100^{o}C, less than 3% degradation occurred in two weeks. The solubility of potassium sulfate in MEA solution increases significantly with CO_2 loading and decreases with MEA concentration. The base case corrosion rate in 5 M MEA/1.2M PZ is 22 mpy. With 1 wt% heat stable salt, the corrosion rate increases by 50% to 160% in the order: thiosulfate< oxalate<acetate<formate. Cupric carbonate is ineffective in the absence of oxygen, but 50 to 250 ppm reduces corrosion to less than 2 mpy in the presence of oxygen.

Contents

List of Figures

List of Tables

Introduction

The objective of this work is to improve the process for CO_2 capture by alkanolamine absorption/stripping by developing an alternative solvent, aqueous K_2CO_3 promoted by piperazine. This work expands on parallel bench-scale work with system modeling and pilot plant measurements to demonstrate and quantify the solvent process concepts.

Gary Rochelle is supervising the bench-scale and modeling work. Six graduate students (Andrew Sexton, Marcus Hilliard, Jason Davis, Jorge Plaza, David Van Wagener, Qing Xu) have received a portion of their support during this quarter for direct effort on the scope of this contract. These students have also been supported on related activities by the TXU Carbon Management Program. Subcontract work was performed by Manjula Nainar at the University of Regina under the supervision of Amy Veawab.

Experimental and Modeling Methods

Subtask 1.8a describes development of a model in RateSep™ for the absorber.

Subtask 1.8b describes further development of a rate model in ACM for the double matrix stripper.

Subtask 3.2 presents methods for analyzing amine degradation products by anion and cation chromatography. It describes a new method for preparing samples of degraded solutions by reaction with hydrogen peroxide.

Subtask 3.3 describes a method of gas chromatography for amine degradation products.

Subtask 3.4 describes methods for using the high temperature gas FTIR to determine amine and CO_2 vapor pressure over loaded solutions of piperazine.

Subtask 4.1 describes a method for measuring the solubility of potassium sulfate in loaded amine solutions with ion conductivity.

Task 5 describes electrochemical methods for measuring corrosion.

Results and Discussion

Progress has been made on five subtasks in this quarter:

Subtask 1.8a – Predict Absorber Flowsheet Options

The RateSep™ model of the absorber has been used to develop a heat and material balance for 4.5 m K+/4.5 m PZ used at loadings provided by a matrix stripper. This absorber uses split feed with intercooling at two points. The balance will be used by Trimeric to estimate costs for this configuration.

Subtask 1.8b – Predict Stripper Flowsheet Options

The rate-based model in Aspen Custom Modeler has been used to develop a heat and material balance for 4.5 m K+/4.5 m PZ with a matrix stripper. This balance, with that of the absorber, will be used by Trimeric to estimate costs for this configuration.

Subtask 3.2 – Oxidative Degradation

Analyses have been completed on earlier experiments with 2.5 m PZ/5 m $KHCO_3$ (with V), 2.5 m PZ (with V and inhibitor A), 35% MEA (5 ppm Fe), and 7m MEA/2 m PZ (Fe and Cu).

Subtask 3.3 – Thermal Degradation

Samples of loaded MEA were degraded at 150°C and 100°C. These initial samples were analyzed by gas chromatography.

Subtask 3.4 – Amine Volatility

Measurements of CO_2 and amine vapor pressure have been completed for MEA, PZ, MEA/PZ, and K^+/PZ systems at 40 and 60°C.

Subtask 4.1 – Sulfate Precipitation

Measurements of potassium sulfate solubility were made at 25 and 40°C in loaded solutions of MEA and MEA/PZ.

Subtask 5.1 – Corrosion in base solution compared to MEA

Conclusions

1. Optimum semilean loading and intercooling increase absorber performance by a factor as high as 14%.

2. The best conditions found for 4.5 m K^+/4.5 m PZ in the matrix stripper required an equivalent work of 31.8 kJ/mol CO_2 with 230 kPa in the first stripper and a feed ratio of 0.185.

3. A second experiment with 5 M+/2.5 M PZ (500 ppm V) has confirmed its resistance to oxidative degradation, probably because the oxygen solubility is suppressed.

4. 100 mM Inhibitor A reduced the formation of detectable ionic degradation products in 2.5 m PZ with 500 ppm V by 50%. However, this inhibitor had no effect on the production of ethylenediamine.

5. The production rate of formate in 7m MEA/2m PZ (0.1 mM Fe and 5 mM Cu) was six times faster than 7 m MEA.

6. In preliminary experiments with oxidation by H_2O_2, Aminomethylpropanol (AMP) produced significantly less degradation product than MEA and PZ.

7. After four weeks of reaction, MEA losses were less than 5% at 100°C, 5 to 20% at 120°C, and 75% at 150°C. The reaction appears to be first order in MEA (with 3.5 to 11 m MEA). At 120°C the first order rate constant varies from 0.017e-2 to 0.058e-2 wk-1 as the CO_2 loading increases from 0.2 to 0.5.

8. The solubility of potassium sulfate in MEA/PZ solvents increases significantly with CO_2 loading and decreases with MEA and PZ concentration. It is a weak function of temperature which mirrors the effect of temperature on the solubility in water.

Future Work

We expect the following accomplishments in the next quarter:

Subtask 1.3b – Stripper Model

The absorber model in RateSep™ will be adapted to be used as a stripper model.

Subtask 1.7 – Simulate and Optimize Packing Effects

The absorber data from campaigns 1, 2, and 4 will be simulated with the RateSep™ model.

Subtask 1.8a – Predict Absorber Flowsheet Options

Additional work will be conducted to determine a feasible design and operating schemes using higher loading values for the lean and semilean feed streams.

Task 2 – Pilot Plant

Eric Chen will complete his Ph.D. dissertation in June. This document will be submitted as a topical report that will provide a comprehensive description of the pilot plant results with the K^+/PZ solvent.

Subtask 3.2 – Oxidative Degradation

Measurements of oxidative degradation will be made with these solvent compositions:

1. 3M AMP, $\alpha = 0.55$, 1 mM Fe
2. 7m MEA/2m PZ in the absence of copper and/or with the addition of inhibitor A
3. Higher weight percentage MEA solutions (40%)
4. Highly concentrated piperazine solutions (5 molal)
5. Higher loadings for 7m MEA solutions ($\alpha = 0.6$)

Subtask 3.3 – Thermal Degradation

The 120^{o}C data set for MEA will be completed in the next two weeks and a full data set for MEA at 135^{o}C will be completed over the next 8 weeks. A long term 100^{o}C data set will also be pursued in order to get some useful rate data from the current data set. A HPLC method is also being pursued in order to help identify higher boiling point degradation products that will not be seen by the current GC method. Thermal degradation will be measured in MEA at 135^{o}C and in MEA/PZ, PZ, and K^+/PZ at 120^{o}C. An HPLC method will be developed to quantify degradation products.

Subtask 3.4 – Amine Volatility

Amine volatility in loaded MEA and PZ solutions will be represented in AspenPlus with the electrolyte/NRTL model.

Subtask 4.1 – Sulfate Precipitation

AspenPlus® will be used to represent potassium sulfate solubility with the electrolyte/NRTL model.

Subtask 5.4 – Effects of corrosion inhibitors

Corrosion of MEA/PZ solutions will be measured with the addition of Cu^{++} and inhibitor A.

Task 1 – Modeling Performance of Absorption/Stripping of CO2 with Aqueous K2CO3 Promoted by Piperazine

Subtask 1.8a – Predicted Absorber Performance with 4.5 m K+/4.5 m PZ

by Jorge M. Plaza

(Supported by this contract and the TXU Carbon Management Program)

Introduction

Ongoing research carried out by Chen has developed a rate-based absorber model for the 5 m K^+ /PZ. The equilibrium submodel was originally generated from work carried out by Cullinane (2005) and later translated into AspenPlus® by Hillard (2005). Chen used the Data Regression System® in AspenPlus® to simultaneously regress equilibrium constants and interaction parameters to predict equilibrium and speciation. Furthermore, rate constants were calculated to allow the use of activity coefficients. This work uses the tools developed by Chen to analyze a system with 4.5 m K^+/ 4.5 m PZ solvent.

This model was used to develop a heat and material balance for economic Studies by Trimeric. First, a feasible system was proposed based on values given by Trimeric and results from the stripper optimization. Later, an absorber optimization based to maximize CO_2 removal was set up using a fixed packing height and varying the position of the semilean feed and an additional intercooling point. Results and conclusions are presented as well as an outline for future work.

Experimental

Base Case

Flue gas conditions were taken from a case study provided by Trimeric. Table 1 presents the conditions of the flue gas used for the modeling analysis.

Table 1: Flue gas conditions used for simulation cases

Variable	Value
Flow (kmol/s)	5.4879
Temperature (^oC)	40.0
Pressure (kPa)	111.33
Mol fraction	
H_2O	0.0670
CO_2	0.1270
N_2	0.7569
O_2	0.0491

Calculations were carried out using AspenPlus® and the rate model developed by Chen. The modeled system is shown in Figure 1. Since simulation of the stripper has been conducted using

Aspen Custom Modeler (ACM), it was not possible to completely connect the absorber/stripper system in AspenPlus®, so modeling of the absorber was done using data provided by the stripper optimization. Interconnection equipment such as pumps and cross-heat exchangers were included in the absorber model run, leaving only the stripper to be later included in the AspenPlus® modeling environment

Results from the stripper analysis provided a loading of 0.4012 moles CO_2/moles alkalinity for the lean stream and 0.4598 for the semilean stream. The flow split between the streams was 0.1850(mol semilean/mol lean). These values correspond to 0.5 kPa partial pressure of CO_2 in the lean stream. Additionally, stripper analysis provided an expected value of 0.4960 for the rich loading solvent stream leaving the absorber. Table 2 summarizes the design conditions for the absorber. Table 3 presents the conditions of the streams in the simulation. Heat duties and areas calculated for heat exchange equipment are presented in Table 4. Table 5 shows the specifications for the pumps in the system.

Table 2: Absorber design conditions for all modeling cases

Variable	Value
Diameter (m)	9.8
Height (m)	15.0
Packing Characteristics	
Type	CMR
Vendor	MTL
Material	Metal
Dimension	NO-2P
Liquid hold up (%)	5

Table 3: Stream conditions for the Trimeric modeling case

Variable	ABSLE	ABSLEAN	ABSLEAN1	ABSRICH	ABSRICHP	E1RICH	E2RICH
From:	E-2	ABSLE	EX-1	ABS-1	P-1	SP-1	SP-1
To:	ABSLEAN	ABS-1	E-1	P-1	FILTER-1	P-4	EX-1
Phase:	Liquid	Liquid	Liquid	Liquid	Liquid	Liquid	Liquid
Component Mole Flow (Kmol/h)							
H_2O	94094.28	94094.30	17424.54	111032.30	110730.10	93442.95	17286.93
K_2CO_3	0.00	0.00	0.00	0.00	0.00	0.00	0.00
$KHCO_3$	0.00	0.00	0.00	0.00	0.00	0.00	0.00
$PZ^{(a)}$	1039.96	1039.90	64.10	87.63	104.31	88.04	16.29
K^+	7401.73	7401.73	1377.71	8779.44	8779.44	7408.81	1370.63
H_3O^+	0.00	0.00	0.00	0.00	0.00	0.00	0.00
CO_2	0.095	0.10	0.14	2.26	1.810	1.5284	0.2827
HCO_3^-	681.21	681.19	243.54	1865.77	2128.36	1796.31	332.32
OH^-	0.1105	0.11	0.01	0.03	0.0301	0.0254	0.0047
CO_3^{2-}	377.74	377.75	43.19	168.92	208.47	175.92	32.55
PZH^+	654.64	654.67	191.98	983.54	1155.18	975.07	180.39
$PZCOO^-$	2335.79	2335.86	255.50	910.06	966.75	815.80	150.92
$PZ(COO^-)_2$	2141.89	2141.87	492.13	3324.65	3211.27	2709.94	501.34
H^+PZCOO^-	1229.45	1229.43	374.00	3.47E+03	3341.08	2819.24	521.56
N_2	0.00	0.00	0.00	0.43	0.43	0.367	0.0679
O_2	0.00	0.00	0.00	8.63	8.63	7.2791	1.3466

Variable	ABSLE	ABSLEAN	ABSLEAN1	ABSRICH	ABSRICHP	E1RICH	E2RICH
Component Mole Fraction							
H_2O	0.86	0.86	0.85	0.85	0.85	0.8476	0.8476
K_2CO_3	0.00	0.00	0.00	0.00	0.00	0.00	0.00
$KHCO_3$	0.00	0.00	0.00	0.00	0.00	0.00	0.00
$PZ^{(a)}$	0.0095	0.010	0.00	7.00E-04	0.0008	0.0008	0.0008
K^+	0.0673	0.07	0.07	0.07	0.0672	0.0672	0.0672
H_3O^+	0.00	0.00	0.00	0.00	0.00	0.00	0.00
CO_2	8.64E-07	8.64E-07	0.00	0.000	1.39E-05	1.39E-05	1.39E-05
HCO_3^-	0.0062	0.01	0.01	0.01	0.0163	0.0163	0.0163
OH^-	0.00	0.00	0.00	0.00	0.00	0.00	0.00
CO_3^{2-}	0.0034	0.0034	0.00	0.00	0.0016	0.0016	0.0016
PZH^+	0.0060	0.0060	0.01	0.01	0.0088	0.0088	0.0088
$PZCOO^-$	0.0212	0.0212	0.01	0.01	0.0074	0.0074	0.0074
$PZ(COO^-)_2$	0.0195	0.0195	0.02	0.03	0.0246	0.0246	0.0246
H^+PZCOO^-	0.0112	0.0112	0.02	2.66E-02	0.0256	0.0256	0.0256
N_2	0.00	0.00	0.00	0.00	0.00	0.00	0.00
O_2	0.00	0.00	0.00	0.00	0.00	0.0001	0.0001
Component Mass Flow (Kg/h)							
H_2O	1695135	1695135	313907.9	2000278	1994835	1683401	311428.8
K_2CO_3	0.00	0.00	0.00	0.00	0.00	0.00	0.00
$KHCO_3$	0.00	0.00	0.00	0.00	0.00	0.00	0.00

Variable	ABSLE	ABSLEAN	ABSLEAN1	ABSRICH	ABSRICHP	E1RICH	E2RICH
$PZ^{(a)}$	89579.10	89573.79	5521.25	7548.47	8985.30	7583.66	1402.97
K^+	289391.00	289391.00	53865.51	343256.50	343256.50	289668	53588.51
H_3O^+	0.00	0.00	0.00	0.00	0.00	0.00	0.00
CO_2	4.18	4.18	6.07	99.55	79.67	67.26	12.44
HCO_3^-	41565.97	41564.40	14860.39	113844.70	129867.50	109606.9	20277.26
OH^-	1.88	1.88	0.18	0.47	0.51	0.43	0.08
CO_3^{2-}	22668.28	22668.65	2591.69	10136.80	12510.49	10557.26	1953.09
PZH^+	57050.02	57052.09	16730.71	85712.88	100670.40	84974.01	15720.17
$PZCOO^-$	301646.00	301655.50	32996.02	117526.70	124847.60	105353.6	19490.39
$PZ(COO^-)_2$	368712.10	368708.90	84717.28	572315.50	552798.10	466498.6	86302.15
H^+PZCOO^-	160011.40	160009.10	48675.24	4.52E+05	434837.60	366921.3	67880.37
N_2	0.00	0.00	0.00	12.18	12.18	10.28	1.9
O_2	0.00	0.00	0.00	276.01	276.01	232.92	43.09
Component Mass Fraction							
H_2O	0.56	0.56	0.55	0.54	0.539	0.5387	0.5387
K_2CO_3	0.00	0.00	0.00	0.00	0.00	0.00	0.00
$KHCO_3$	0.00	0.00	0.00	0.00	0.00	0.00	0.00
$PZ^{(a)}$	0.03	0.030	0.01	2.00E-03	0.002	0.0024	0.0024
K^+	0.10	0.096	0.09	0.09	0.093	0.0927	0.0927
H_3O^+	0.00	0.00	0.00	0.00	0.00	0.00	0.00
CO_2	1.38E-06	1.38E-06	0.00	0.00	2.15E-05	2.15E-05	2.15E-05

Variable	ABSLE	ABSLEAN	ABSLEAN1	ABSRICH	ABSRICHP	E1RICH	E2RICH
HCO_3^-	0.014	0.01	0.03	0.03	0.035	0.0351	0.0351
OH^-	0.00	0.00	0.00	0.00	0.00	0.00	0.00
CO_3^{2-}	0.008	0.008	0.00	0.00	0.003	0.0034	0.0034
PZH^+	0.019	0.02	0.03	0.02	0.027	0.0272	0.0272
$PZCOO^-$	0.100	0.10	0.06	0.03	0.034	0.0337	0.0337
$PZ(COO^-)_2$	0.122	0.12	0.15	0.15	0.149	0.1493	0.1493
H^+PZCOO^-	0.053	0.05	0.08	1.22E-01	0.117	0.1174	0.1174
N_2	0.00	0.00	0.00	0.00	0.00	0.00	0.00
O_2	0.00	0.00	0.00	0.00	0.00	0.0001	0.0001
Mole Flow (kmol/h)	109956.9	109956.9	20466.8	130636.4	130635.9	110241.3	20394.6
Mass Flow (kg/h)	3025764	3025753	573872.2	3702976	3702976	3124875	578101.3
Volume Flow (m^3/h)	2588.6	2588.6	485.6	3113.1	3111.6	2625.8	485.8
Temperature (^oC)	40	40	48.85	43.59	43.28	43.29	43.29
Pressure (kPa)	100.03	100.03	230	99.91	788.91	719.96	719.96
Vapor Fraction	0	0	0	0	0	0	0
Liquid Fraction	1	1	1	1	1	1	1
Molar Enthalpy (J/kmol)	-303537600	-303537600	-307979000	-312040000	-312015900	-312016000	-312016000

Variable	ABSLE	ABSLEAN	ABSLEAN1	ABSRICH	ABSRICHP	E1RICH	E2RICH
Mass Enthalpy (J/kg)	-11030620	-11030660	-10983900	-11008380	-11007490	-11007500	-11007500
Molar Entropy (J/kmol-K)	-247321.8	-247322	-247124.1	-249494.2	-247759.3	-247755.7	-247755.7
Mass Entropy (J/kg-K)	-8987.73	-8987.77	-8813.55	-8801.84	-8740.61	-8740.48	-8740.48
Molar Density (kmol/m$^{3)}$	42.48	42.48	42.15	41.96	41.98	41.98	41.98
Mass Density (kg/m^3)	1168.87	1168.86	1181.87	1189.48	1190.08	1190.05	1190.05
Average Molecular Weight	27.52	27.52	28.04	28.35	28.35	28.35	28.35
Specific Heat (J/kg-K)	4387.34	4387.35	4404.59	4376.63	4352.74	4352.85	4352.85

[a] Piperazine (PZ)

Table 3: Stream conditions for the Trimeric modeling case (Continued)

Variable	EABSLEAN	ESTRLEAN	FABSRICH	GASIN	GASOUT	P1RICH	SEMI
From:	EX-2	P-3	FILTER-1		ABS-1	P-4	E-1
To:	E-2	EX-2	SP-1	ABS-1		EX-2	SEMILEAN
Phase:	Liquid	Liquid	Liquid	Vapor	Vapor	Liquid	Liquid
Component Mole Flow (Kmol/h)							
H_2O	93992.72	93183.54	110729.9	1323.68	1121.29	93442.39	17469.02
K_2CO_3	0	0	0	0	0	0	0
$KHCO_3$	0	0	0	0	0	0	0
$PZ^{(a)}$	1103.69	1588.976	104.3412	0	0.8509	88.1157	51.9337
K^+	7401.729	7401.729	8779.443	0	0	7408.814	1377.71
H_3O^+	0	0	0	0	0	0	0
CO_2	0.1614	9.9434	1.8113	2509.068	248.7574	1.5304	0.0615
HCO_3^-	796.6342	1788.808	2128.595	0	0	1796.915	195.6033
OH^-	0.1149	0.1945	0.0301	0	0	0.0254	0.0095
CO_3^{2-}	363.8685	180.8028	208.4599	0	0	175.8887	46.6454
PZH^+	685.2455	1084.887	1155.373	0	0	975.4085	165.4926
$PZCOO^-$	2293.275	1934.721	966.7463	0	0	815.9172	258.2326
$PZ(COO^-)_2$	2134.607	2200.644	3211.262	0	0	2709.794	498.0351
H^+PZCOO^-	1184.911	592.5008	3340.869	0	0	2818.861	404.0197
N_2	0	0	0.4349	14953.65	14953.21	0.367	0
O_2	0	0	8.6258	970.0412	961.4154	7.2791	0

Variable	EABSLEAN	ESTRLEAN	FABSRICH	GASIN	GASOUT	P1RICH	SEMI
Component Mole Fraction							
H_2O	0.8548	0.8474	0.8476	0.067	0.0649	0.8476	0.8535
K_2CO_3	0	0	0	0	0	0	0
$KHCO_3$	0	0	0	0	0	0	0
$PZ^{(a)}$	0.01	0.0144	0.0008	0	0	0.0008	0.0025
K^+	0.0673	0.0673	0.0672	0	0	0.0672	0.0673
H_3O^+	0	0	0	0	0	0	0
CO_2	1.47E-06	9.04E-05	1.39E-05	1.27E-01	1.44E-02	1.39E-05	3.01E-06
HCO_3^-	0.0072	0.0163	0.0163	0	0	0.0163	0.0096
OH^-	0	0	0	0	0	0	0
CO_3^{2-}	0.0033	0.0016	0.0016	0	0	0.0016	0.0023
PZH^+	0.0062	0.0099	0.0088	0	0	0.0088	0.0081
$PZCOO^-$	0.0209	0.0176	0.0074	0	0	0.0074	0.0126
$PZ(COO^-)_2$	0.0194	0.02	0.0246	0	0	0.0246	0.0243
H^+PZCOO^-	0.0108	0.0054	0.0256	0	0	0.0256	0.0197
N_2	0	0	0	0.7569	0.8651	0	0
O_2	0	0	0.0001	0.0491	0.0556	0.0001	0
Component Mass Flow (Kg/h)							
H_2O	1693305	1678728	1994831	23846.49	20200.34	1683391	314709.3
K_2CO_3	0	0	0	0	0	0	0
$KHCO_3$	0	0	0	0	0	0	0

Variable	EABSLEAN	ESTRLEAN	FABSRICH	GASIN	GASOUT	P1RICH	SEMI
$PZ^{(a)}$	95068.53	136869.5	8987.63	0	73.3	7590.02	4473.41
K^+	289391	289391	343256.5	0	0	289668	53865.51
H_3O^+	0	0	0	0	0	0	0
CO_2	7.11	437.61	79.72	110423.6	10947.76	67.35	2.71
HCO_3^-	48608.78	109148.9	129882	0	0	109643.6	11935.26
OH^-	1.95	3.31	0.51	0	0	0.43	0.16
CO_3^{2-}	21835.86	10850.03	12509.74	0	0	10555.14	2799.21
PZH^+	59717.02	94544.56	100687.2	0	0	85003.83	14422.17
$PZCOO^-$	296156	249852	124846.7	0	0	105368.4	33348.45
$PZ(COO^-)_2$	367458.1	378825.8	552797	0	0	466472.6	85733.35
H^+PZCOO^-	154214.9	77113.39	434810.8	0	0	366871.9	52582.76
N_2	0	0	12.18	418903.8	418891.6	10.28	0
O_2	0	0	276.01	31040.15	30764.14	232.92	0
Component Mass Fraction							
H_2O	0.5596	0.5548	0.5387	0.0408	0.042	0.5387	0.5484
K_2CO_3	0	0	0	0	0	0	0
$KHCO_3$	0	0	0	0	0	0	0
$PZ^{(a)}$	0.0314	0.0452	0.0024	0	0.0002	0.0024	0.0078
K^+	0.0956	0.0956	0.0927	0	0	0.0927	0.0939
H_3O^+	0	0	0	0	0	0	0
CO_2	2.35E-06	1.45E-04	2.15E-05	1.89E-01	2.28E-02	2.16E-05	4.72E-06

Variable	EABSLEAN	ESTRLEAN	FABSRICH	GASIN	GASOUT	P1RICH	SEMI
HCO_3^-	0.0161	0.0361	0.0351	0	0	0.0351	0.0208
OH^-	0	0	0	0	0	0	0
CO_3^{2-}	0.0072	0.0036	0.0034	0	0	0.0034	0.0049
PZH^+	0.0197	0.0312	0.0272	0	0	0.0272	0.0251
$PZCOO^-$	0.0979	0.0826	0.0337	0	0	0.0337	0.0581
$PZ(COO^-)_2$	0.1214	0.1252	0.1493	0	0	0.1493	0.1494
H^+PZCOO^-	0.051	0.0255	0.1174	0	0	0.1174	0.0916
N_2	0	0	0	0.717	0.8711	0	0
O_2	0	0	0.0001	0.0531	0.064	0.0001	0
Mole Flow (kmol/h)	109957	109966.7	130635.9	19756.44	17285.53	110241.3	20466.77
Mass Flow (kg/h)	3025764	3025764	3702976	584214	480877.1	3124875	573872.2
Volume Flow (m^3/h)	2596.76	2697.36	3111.62	461504.6	451179.9	2625.78	483.03
Temperature (^oC)	45.15	98.94	43.29	40	40.55	43.3	40
Pressure (kPa)	849	849	719.96	111.33	99.86	826.96	100.03
Vapor Fraction	0	0	0	1	1	0	0
Liquid Fraction	1	1	1	0	0	1	1
Molar Enthalpy (J/kmol)	-302872200	-296115600	-312016000	-65776430	-20912060	-312012300	-309147900

Variable	EABSLEAN	ESTRLEAN	FABSRICH	GASIN	GASOUT	P1RICH	SEMI
Mass Enthalpy (J/kg)	-11006450	-10761870	-11007490	-2224370	-751701.4	-11007370	-11025550
Molar Entropy (J/kmol-K)	-244793.6	-223379.9	-247755.4	4757.04	3109.5	-247746.7	-251742.7
Mass Entropy (J/kg-K)	-8895.86	-8118.4	-8740.47	160.87	111.77	-8740.16	-8978.23
Molar Density (kmol/m$^{3)}$	42.34	40.77	41.98	0.04	0.04	41.98	42.37
Mass Density (kg/m^3)	1165.21	1121.75	1190.05	1.27	1.07	1190.07	1188.07
Average Molecular Weight	27.52	27.52	28.35	29.57	27.82	28.35	28.04
Specific Heat (J/kg-K)	4379.22	4383.67	4352.86	1037.03	1066.45	4352.67	4406.64

[a] Piperazine (PZ)

Table 3: Stream conditions for the Trimeric modeling case. (Continued)

Variable	SEMILEAN	STR1RICH	STR2RICH	STRLEAN	STRSLEAN	STSLEANP
From:	SEMI	EX-2	EX-1	STRIPPER 2	STRIPPER 2 MID	P-2
To:	ABS-1	STRIPPER 1	STRIPPER 2	P-3	P-2	EX-1
Phase:	Liquid	Liquid	Mixed	Liquid	Liquid	Liquid
Component Mole Flow (Kmol/h)						
H_2O	17469.02	91917.37	17036.87	93184.66	17242.85	17242.44
K_2CO_3	0	0	0	0	0	0
$KHCO_3$	0	0	0	0	0	0
$PZ^{(a)}$	51.94	265.16	44.38	1588.05	111.54	111.71
K^+	1377.71	7408.81	1370.63	7401.73	1377.71	1377.71
H_3O^+	0	0.0001	0	0	0	0
CO_2	0.062	46.36	4.98	9.84	3.03	3.06
HCO_3^-	195.61	3401.78	594.512	1787.01	443.64	444.14
OH^-	0.0095	0.056	0.0092	0.1943	0.0171	0.0171
CO_3^{2-}	46.64	96.01	20.40	181.47	24.77	24.69
PZH^+	165.48	2368.57	400.87	1084.59	333.56	333.78
$PZCOO^-$	258.25	763.16	145.86	1934.88	224.91	224.91
$PZ(COO^-)_2$	498.02	2710.18	495.16	2200.64	496.58	496.53
H^+PZCOO^-	404.03	1301.03	284.24	593.57	211.12	210.78
N_2	0	0.367	0.0679	0	0	0

Variable	SEMILEAN	STR1RICH	STR2RICH	STRLEAN	STRSLEAN	STSLEANP
O_2	0	7.28	1.35	0	0	0
Component Mole Fraction						
H_2O	0.8535	0.8334	0.8352	0.8474	0.8424	0.8423
K_2CO_3	0	0	0	0	0	0
$KHCO_3$	0	0	0	0	0	0
$PZ^{(a)}$	0.0025	0.0024	0.0022	0.0144	0.0054	0.0055
K^+	0.0673	0.0672	0.0672	0.0673	0.0673	0.0673
H_3O^+	0	0	0	0	0	0
CO_2	3.01E-06	4.20E-04	2.44E-04	8.95E-05	1.48E-04	1.49E-04
HCO_3^-	0.0096	0.0308	0.0291	0.0163	0.0217	0.0217
OH^-	0	0	0	0	0	0
CO_3^{2-}	0.0023	0.0009	0.001	0.0017	0.0012	0.0012
PZH^+	0.0081	0.0215	0.0197	0.0099	0.0163	0.0163
$PZCOO^-$	0.0126	0.0069	0.0072	0.0176	0.011	0.011
$PZ(COO^-)_2$	0.0243	0.0246	0.0243	0.02	0.0243	0.0243
H^+PZCOO^-	0.0197	0.0118	0.0139	0.0054	0.0103	0.0103
N_2	0	0	0	0	0	0
O_2	0	0.0001	0.0001	0	0	0
Component Mass Flow (Kg/h)						
H_2O	314709.2	1655917	306924	1678748	310634.7	310627.3
K_2CO_3	0	0	0	0	0	0

Variable	SEMILEAN	STR1RICH	STR2RICH	STRLEAN	STRSLEAN	STSLEANP
$KHCO_3$	0	0	0	0	0	0
$PZ^{(a)}$	4473.67	22840.04	3822.36	136789.7	9607.95	9622.23
K^+	53865.51	289668	53588.51	289391	53865.51	53865.51
H_3O^+	0	0	0	0	0	0
CO_2	2.71	2040.21	219.37	433.23	133.38	134.66
HCO_3^-	11935.51	207568.7	36275.74	109039.4	27069.87	27100.13
OH^-	0.16	0.95	0.16	3.3	0.29	0.29
CO_3^{2-}	2799.03	5761.80	1224.35	10890.26	1486.62	1481.54
PZH^+	14420.83	206413.40	34934.42	94518.31	29069	29088.19
$PZCOO^-$	33350.18	98555.01	18836.53	249872.5	29045.26	29045.59
$PZ(COO^-)_2$	85731.02	466539.30	85237.71	378825.4	85483.17	85473.81
H^+PZCOO^-	52584.39	169327.60	36993.13	77252.74	27476.41	27432.92
N_2	0	10.28	1.9	0	0	0
O_2	0	232.92	43.09	0	0	0
Component Mass Fraction						
H_2O	0.5484	0.5299	0.5309	0.5548	0.5413	0.5413
K_2CO_3	0	0	0	0	0	0
$KHCO_3$	0	0	0	0	0	0
$PZ^{(a)}$	0.0078	0.0073	0.0066	0.0452	0.0167	0.0168
K^+	0.0939	0.0927	0.0927	0.0956	0.0939	0.0939
H_3O^+	0	0	0	0	0	0

Variable	SEMILEAN	STR1RICH	STR2RICH	STRLEAN	STRSLEAN	STSLEANP
CO_2	4.72E-06	6.53E-04	3.79E-04	1.43E-04	2.32E-04	2.35E-04
HCO_3^-	0.0208	0.0664	0.0627	0.036	0.0472	0.0472
OH^-	0	0	0	0	0	0
CO_3^{2-}	0.0049	0.0018	0.0021	0.0036	0.0026	0.0026
PZH^+	0.0251	0.0661	0.0604	0.0312	0.0507	0.0507
$PZCOO^-$	0.0581	0.0315	0.0326	0.0826	0.0506	0.0506
$PZ(COO^-)_2$	0.1494	0.1493	0.1474	0.1252	0.149	0.1489
H^+PZCOO^-	0.0916	0.0542	0.064	0.0255	0.0479	0.0478
N_2	0	0	0	0	0	0
O_2	0	0.0001	0.0001	0	0	0
Mole Flow (kmol/h)	20466.77	110286.1	20399.32	109966.6	20469.73	20469.76
Mass Flow (kg/h)	573869.7	3124875	578101.3	3025753	573869.7	573872.2
Volume Flow (m^3/h)	483.01	2699.56	496.77	2697.64	498.43	498.38
Temperature (^oC)	40	93.79	84.7	98.79	90.63	90.77
Pressure (kPa)	206.84	826.96	280	160	160	849
Vapor Fraction	0	0	0	0	0	0
Liquid Fraction	1	1	1	1	1	1

Variable	SEMILEAN	STR1RICH	STR2RICH	STRLEAN	STRSLEAN	STSLEANP
Molar Enthalpy (J/kmol)	-309146500	-305175500	-306436400	-296142100	-302472000	-302446000
Mass Enthalpy (J/kg)	-11025550	-10770550	-10813150	-10762860	-10789070	-10788110
Molar Entropy (J/kmol-K)	-251744	-225026.9	-228203.2	-223418.3	-228997.4	-228953.7
Mass Entropy (J/kg-K)	-8978.32	-7941.87	-8052.55	-8119.82	-8168.26	-8166.68
Molar Density (kmol/m$^{3)}$	42.37	40.85	41.06	40.76	41.07	41.07
Mass Density (kg/m^3)	1188.1	1157.55	1163.73	1121.63	1151.35	1151.48
Average Molecular Weight	28.04	28.33	28.34	27.52	28.04	28.04
Specific Heat (J/kg-K)	4406.44	4406.41	4383.44	4384.84	4438.91	4437.75

[a] Piperazine (PZ)

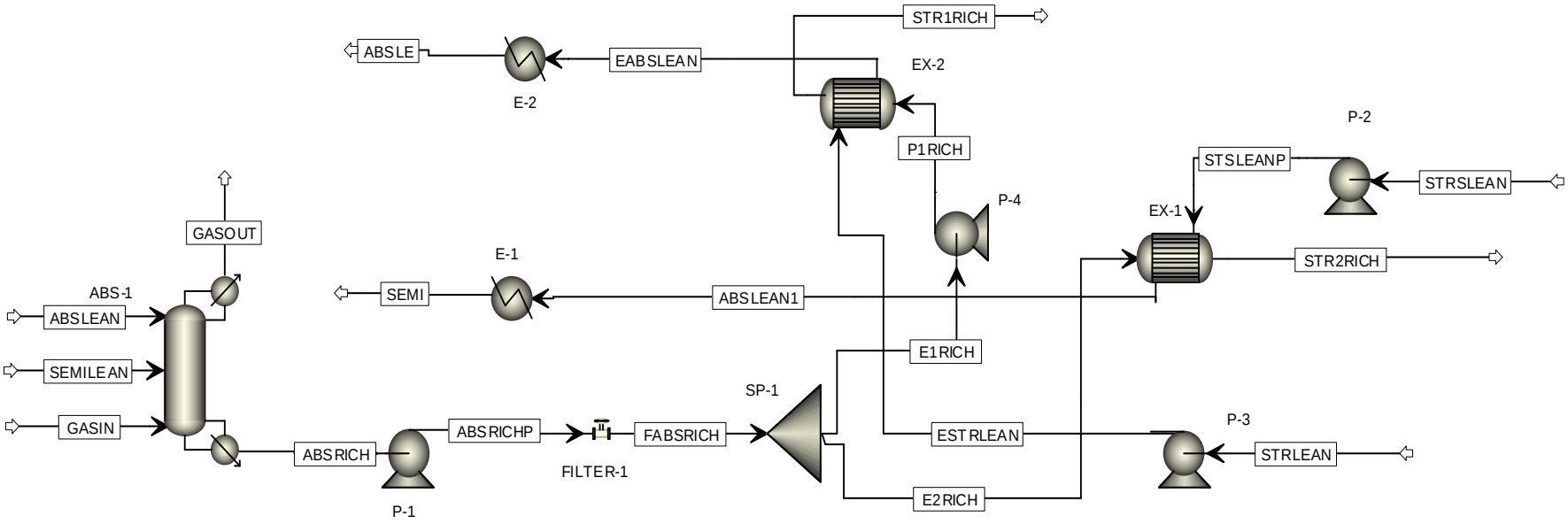

Figure 1: Absorber and stripper interconnection equipment for the base case model

Table 4: Heat Exchanger specifications for the Trimeric base modeling case

Equipment I.D	E-1	E-2	EX-1	EX-2
Heat Duty (kW)	-6,638.49	-20,336.41	31,211.44	205,549.40
Area (m^2)	NA	NA	6,300.49	74,978.73

For E-1 and E-2 AspenPlus® does not report area.

Table 5: Pump specifications for the Trimeric base modeling case

Equipment I.D.	**P-1**	**P-2**	**P-3**	**P-4**
Fluid Power (kW)	595.81	95.39	516.30	78.05
Brake Power (kW)	916.64	146.76	832.74	120.07
Volumetric flow rate (m^3/hr)	3113.11	498.43	2,697.64	2,625.84
Δ P (kPa)	689	689	689	107
NSPHA (m)	0.22	2.14	3.06	53.41
Head developed (m)	59.07	61.02	62.64	9.17
Efficiency	0.65	0.65	0.62	0.65
Net work required (kW)	916.64	146.76	832.74	120.07

Additionally, in order to improve column efficiency, the absorber was designed with two intercooling stages: one at the feed point of the semilean stream and one towards the top of the column. These were placed trying to divide the column in 3 even packing sections. This setup allowed the column to reach the required value for the rich solvent loading which is equivalent to a 90% CO_2 removal. However, as Figure 2 shows, temperatures in this system, at the intercooling points, are above 40^oC which has been established as a minimum cooling temperature using water. Furthermore, the determination of the semilean feed and intercooling point was carried out as a first approach and not optimized, thus the need to determine an optimum in order to maximize system performance.

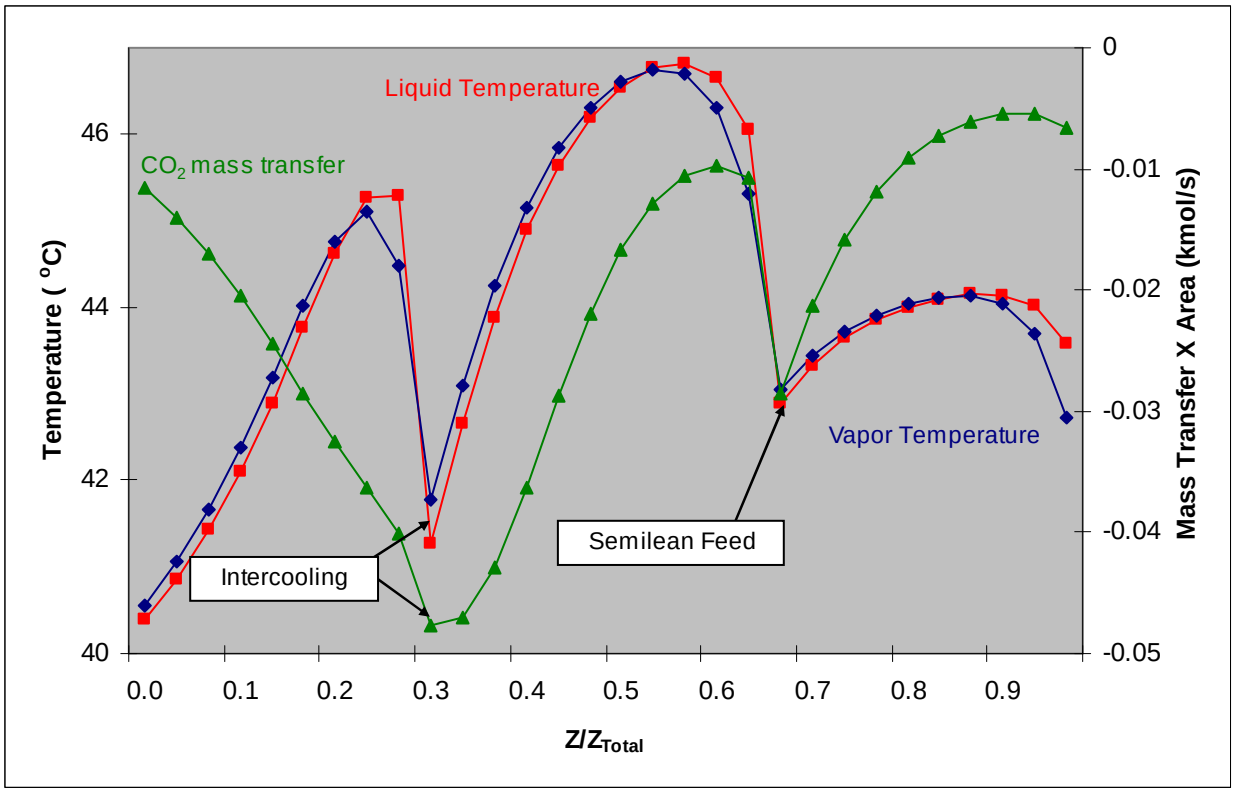

Figure 2: Temperature and CO_2 mass transfer profiles for absorber with semilean feed at 0.70 column height and intercooling at 0.33 column height. Solvent 4.5m K^+/4.5 m PZ. 0.5 kPa CO_2 Lean solvent. Not optimized.

For the optimization analysis the absorber was modeled independently. CO_2 removal was used as a criterion to determine equipment performance. Optimization was carried out using a simple one-dimensional analysis varying semilean position alone with no intercooling and later adding the second intercooling point. The following sections discuss this analysis.

Semilean feed position analysis

The semilean feed was introduced at different points of the column to observe variations in absorber performance based on the semilean feed position. Figure 3 shows the removal obtained by placing the semilean feed at different column locations.

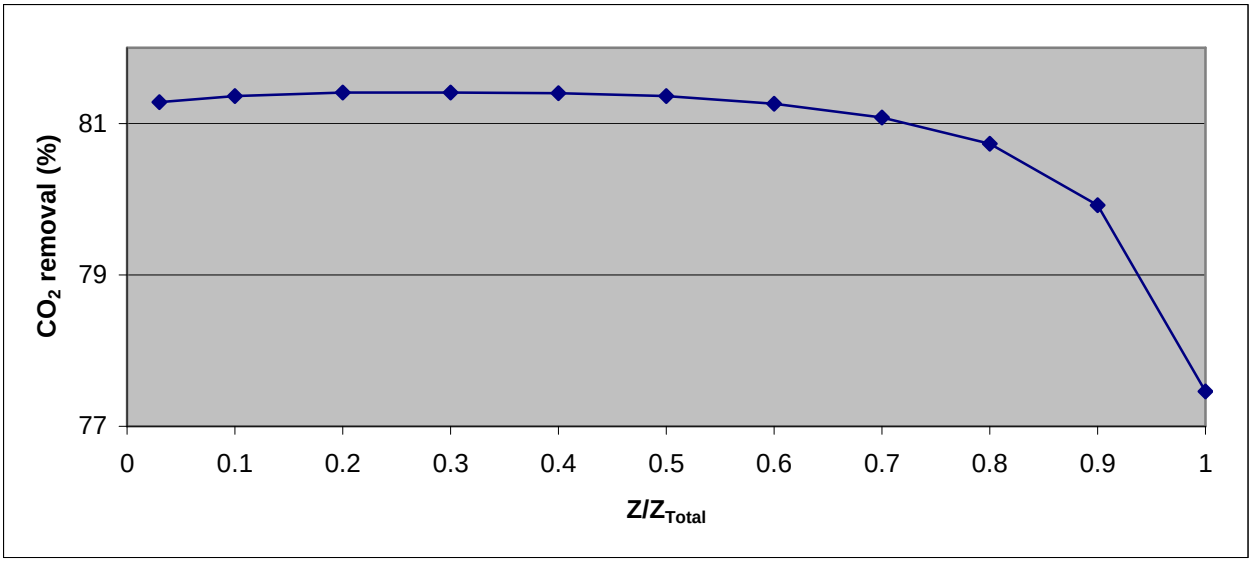

Figure 3: Change in CO_2 removal due to semilean feed position with no intercooling for the 4.5m/4.5 m K_2 CO_3/ PZ system. 0.5 kPa CO_2 Lean solvent.

It is possible to see that the change in the position of the semilean feed does not vary considerably the performance of the absorber. Efficiency remains around 81% removal and decreases as the feed is placed close to the extremes of the absorber. The optimum semilean feed position appears to be located around 1/3 the column height which is opposite to the configuration of the base case. It has been proposed that this optimum is probably due to the similarity between the semilean stream compositions and the compositions at that point in the column. However, further analysis is needed to determine which compositions or combinations of compositions may serve as matching criteria to determine semilean positioning. There is also the need to assess the effect of the intercooling in semilean positioning.

Intercooling

An additional option to improve absorber performance is to use intercooling (Freguia & Rochelle, 2003; Chang & Shih, 2005). Initially, intercooling was considered for the stage in which the semilean stream was fed into the column. The idea was to reduce the irreversibility generated by the difference in temperature between the semilean feed and the liquid at the point of entry. However, a plot of CO_2 mass transfer into the liquid showed that there was a pinch towards the bottom of the column (Figure 4), so additional intercooling was proposed to break the pinch. Additionally, the Aspen model run was set up to provide enough cooling for the stage to reach 40^{o}C.

The semilean feed was fixed at 0.30 of the column height and the additional intercooling position was moved from half the column height down evaluating removal performance in order to determine optimum intercooling placement. Figure 5 shows the results for this analysis. As with the semilean feed, cooling temperature at the intercooling point was set at 40^{o}C.

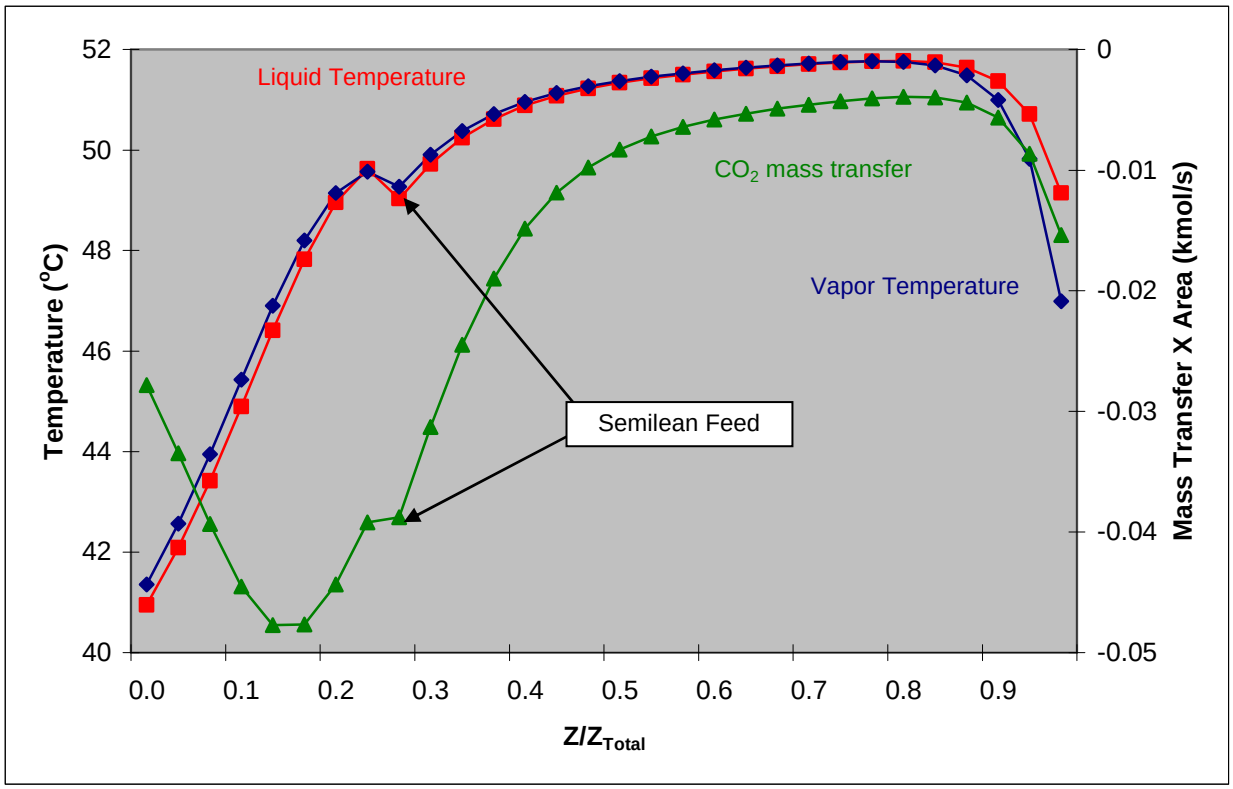

Figure 4: Temperature and CO_2 mass transfer profiles for absorber with semilean feed at 0.3 column ht no intercooling. Solvent 4.5m/4.5 m K_2CO_3/PZ. 0.5 kPa CO_2 Lean solvent.

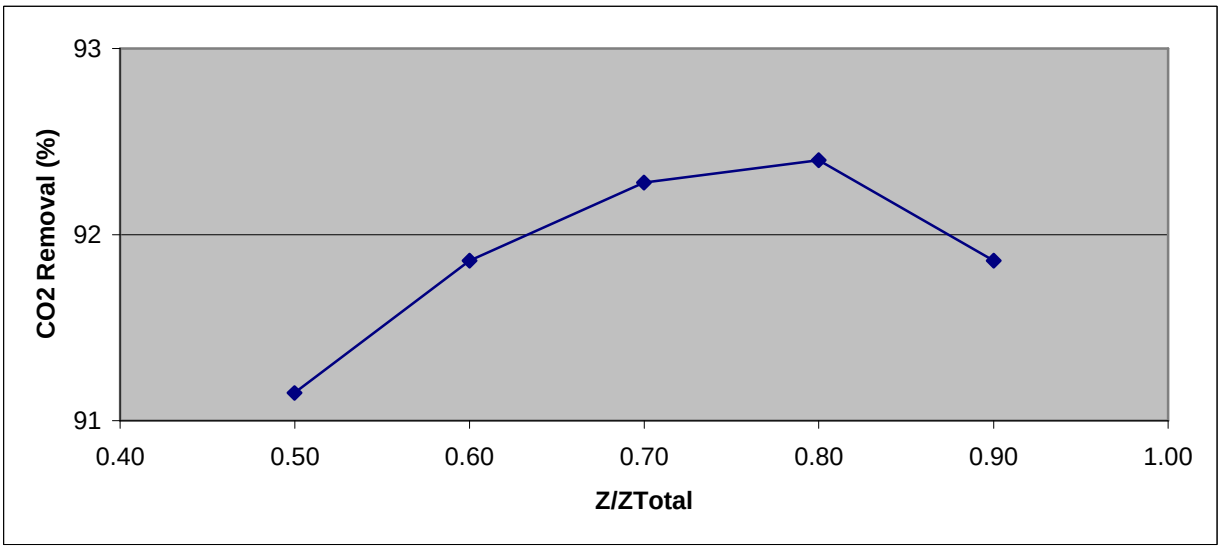

Figure 5: Change in CO_2 removal due to second intercooling positioning with fixed intercooled semilean feed at 0.30 of column height for the 4.5m/4.5 m K_2CO_3/PZ system. 0.5 kPa CO_2 Lean solvent.

Intercooling proves to be optimal if placed near the middle of the pinch, at approximately 0.80 of the column height. (Figures 5 and 6). In general CO_2 removal performance is increased by almost 14 %. Intercooling to reach 40 ^oC required removal of around 46,000 kW from the absorber.

An additional optimum was studied for the stripper. It provides a higher loading lean solvent corresponding to 0.7 kPa CO_2 partial pressure. The lean solvent loading is 0.4208, the semilean is 0.4743 and the split is at 0.1453. Using the optimized 4.5m/4.5 m K_2CO_3/PZ system configuration for the mentioned loading conditions a maximum removal of 83.7% is attained (Figure 7). Based on results for the 4.5m/4.5m K_2CO_3/PZ (see figures 3 and 5) an optimum setup for this system will be 1 to 2% above the current obtained removal value. These results are due to the higher CO_2 content in the solvent that renders lower absorber performance. Optimization of this system will be considered in the future although additional performance enhancing schemes are expected to be required (such as variation of liquid hold up values).

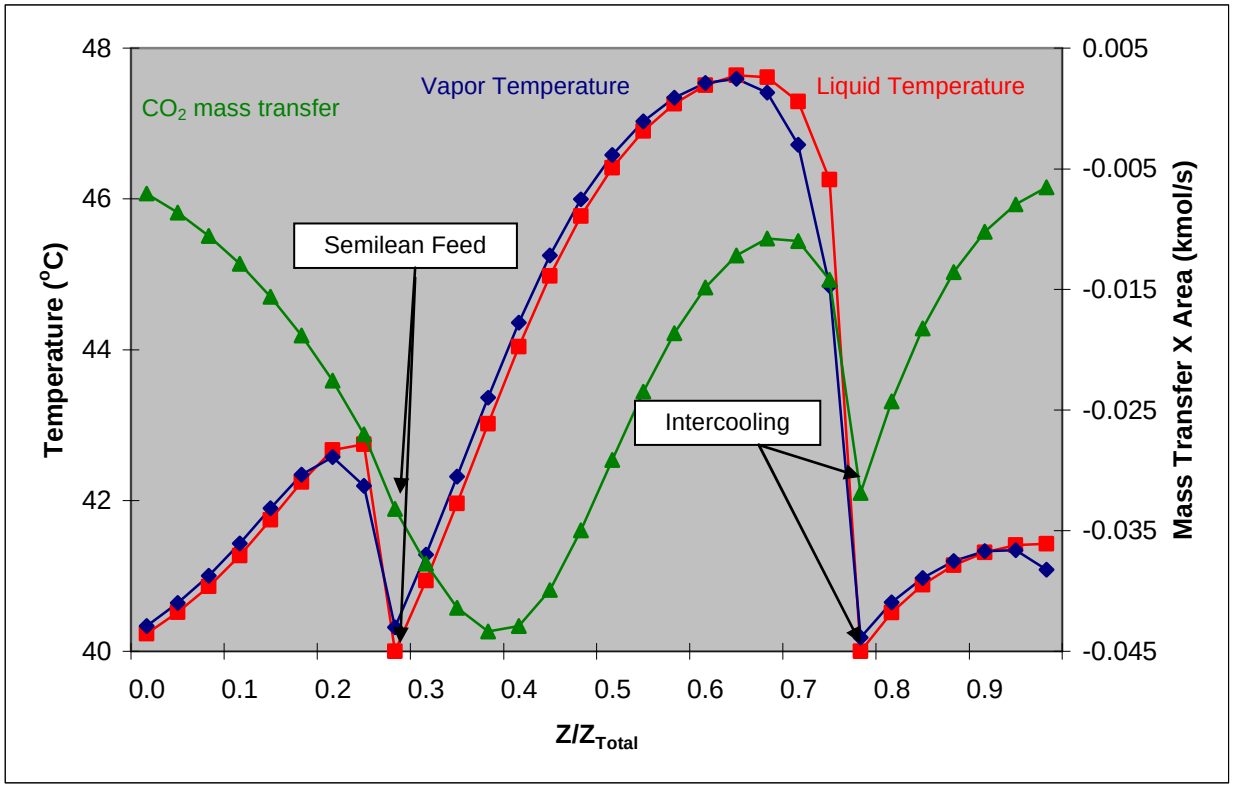

Figure 6: Temperature and CO_2 mass transfer profiles for absorber with semilean feed at 0.3 column height and intercooling at 0.8 column height for the 4.5m/4.5 m K_2CO_3/ PZ system optimized. 0.5 kPa CO_2 Lean solvent.

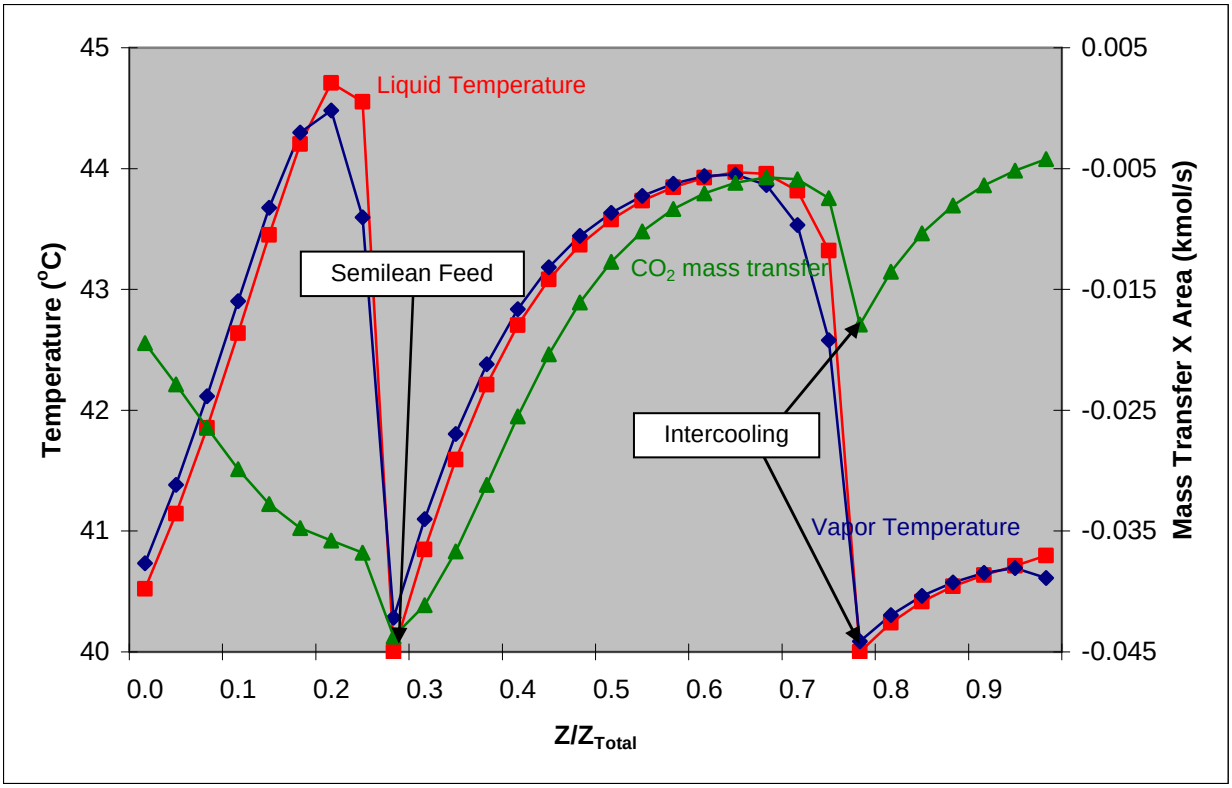

Figure 7: Temperature and CO_2 mass transfer profiles for absorber with semilean feed at 0.3 column height and intercooling at 0.8 column height for the 4.5m/4.5 m K_2CO_3/ PZ system. 0.7 kPa CO_2 Lean solvent.

Conclusions

Optimum semilean loading and intercooling increase absorber performance by a factor as high as 14%. The obtained CO_2 removal rates suggest that less packing height would give 90% removal for the 0.5 kPa lean loading case.

The initial case approach was capable of 90% removal even though the semilean feed was placed in the lower third of the column and intercooling temperatures did not reach 40°C (Figure 2). This shows that there might be multiple routes to achieve optimum column performance. Further analysis is required to define an adequate and efficient optimization scheme.

Results for the 0.7 kPa lean loading case show that supplementary operating schemes are required to reach desirable performance. It might be necessary to consider an additional intercooling stage and/or alternatives that provide higher liquid hold up thus providing higher reaction times.

Future Work

Additional work will be conducted to determine a feasible design and operating schemes using higher loading values for the lean and semilean feed streams. Although 0.7 kPa showed low removal, the use of loading higher than the corresponding to 0.5 kPa may still be feasible. The goal is to reduce stripper reboiler heat duties and thus operation costs. Two initial options

determined for future work are stage hold up and packing type. The latter is more focused towards reduction of pressure drop in the absorber.

Currently, feed and cooling points were determined using removal percentage as the optimization variable. Further work will be carried out to establish a more robust design parameter such as a relation to reduce irreversibilities in the system (Jimenez et al. 2004; Johannessen & Røjorde, 2007).

Finally, the stripper has been modeled under a different environment (see Task 1.8b) so work will be done to integrate both systems under the AspenPlus® platform. This will allow for global system optimization.

Subtask 1.8b – Predicted Stripper Performance with 4.5m K+/4.5m PZ

by David Van Wagener

(Supported by this contract and the TXU Carbon Management Program)

Introduction

The primary focus of this quarter was modeling a double matrix stripper using 4.5m K+/4.5m PZ. The stripper was modeled using several programs developed by previous work in this group. Once the model was operational, the combined duties of the stripper reboiler and vapor compressor were minimized. The simulation used a base case provided by Trimeric, who desired results of the absorber/stripper combination for this solvent for their SBIR contract.

Experimental

The first model that was used in this work was a VLE model written in Fortran which calculated the equilibrium partial pressure of CO_2, P^*_{CO2}, for a given temperature and composition (Cullinane, 2006). The model was fitted to extensive laboratory data, so the calculated values were expected to be as reliable as lab data. Second, a model was developed in Aspen Custom Modeler (ACM) which uses an equilibrium modeling approach to design and optimize the stripper section. Lastly, a separate Aspen simulation was developed to calculate the work in the compression section, which compresses the separated CO_2 to an adequate pressure for injecting into the Earth's crust.

Regression of VLE Data

The first goal was to develop a reasonable regression capable of predicting VLE data for the 4.5m K^+/4.5m PZ solvent system. A previously written Fortran model calculates the equilibrium CO_2 partial pressure for a given temperature, solvent concentration, and concentration of dissolved CO_2 (expressed as loading).

$$loading = \frac{mol\ CO_2}{mol\ Alkalinity} \qquad (1)$$

Using the specified solvent concentration of 4.5m K+/4.5m PZ, a range of temperature and CO_2 loading was run to calculate a regression to predict the equilibrium CO_2 partial pressure as a function of temperature and loading. The regression was a 7 term equation which was used for prior VLE models (Oyenekan, 2006). The form of the equation and the calculated constants are shown below:

$$\ln P^{*}_{CO_2} = a + b\,\gamma + \frac{c}{T} + d\,\frac{\gamma^2}{T^2} + e\,\frac{\gamma}{T^2} + f\,\frac{\gamma}{T} \qquad (2)$$

Table 6: Coefficients for VLE Progression

	Value	St. Error	% Error
a	7.21	1.44	19.9%
b	60.83	7.03	11.6%
c	-5116.22	656.84	12.8%
d	-4.71E+05	4.05E+05	86.0%
e	2.13E+06	8.17E+05	38.4%
f	-1.82E+04	4.73E+03	25.9%

The ratios between the regression predicted values and the model calculated values are between 0.8 and 1.2, indicating a maximum percent error of about 20%. However, the regression was calculated for a range in the variables larger than that of typical operating conditions. Considering that typical stripper operation uses temperatures between 90°C +/- 20°C and loadings between 0.45 +/- 0.0525, about 82% of the predicted values are within 5% of the model calculated values, demonstrated in Figure 8:

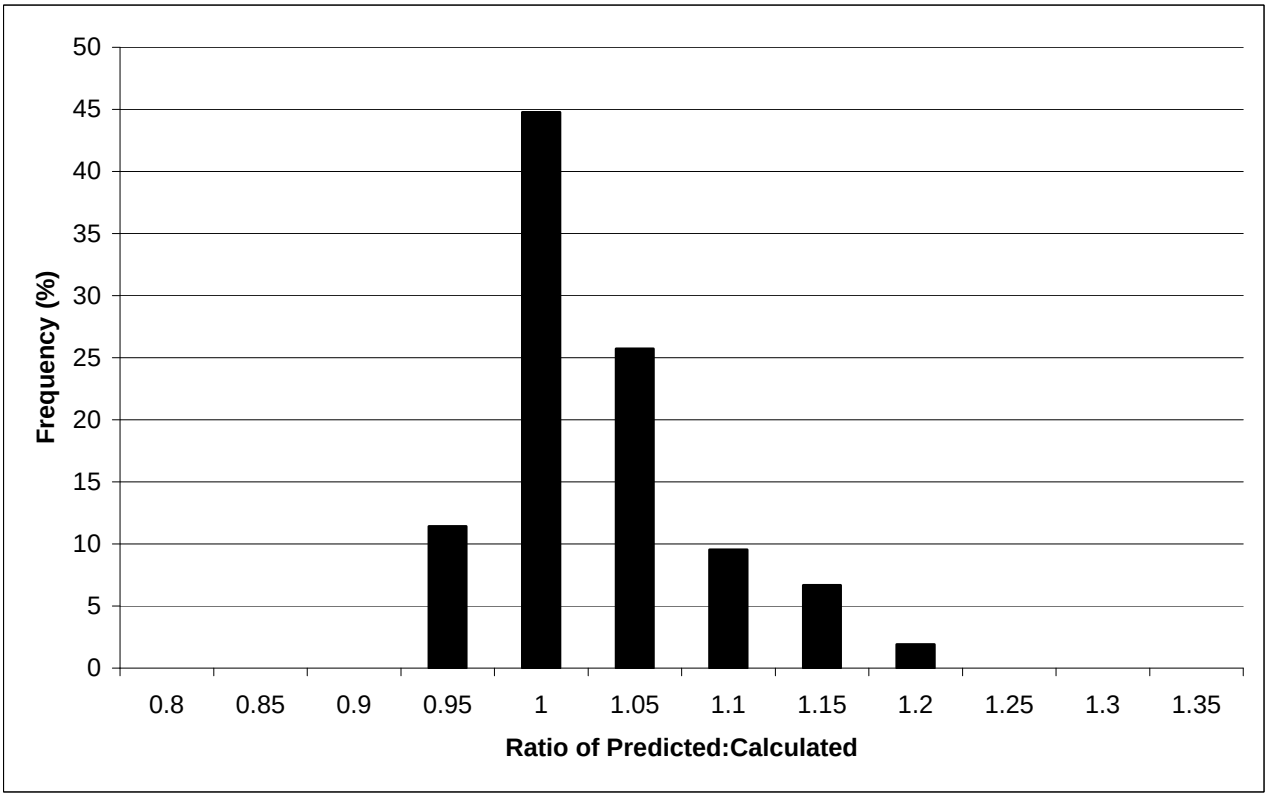

Figure 8: Accuracy of VLE Regression within Range of Typical Stripper Conditions

ACM Model

Following the development of the VLE regression, an equilibrium double matrix stripper model in Aspen Custom Modeler (ACM) written by Oyenekan (2006) was used to model the stripper section and optimize various operating conditions. The stripper model utilized the VLE regression to thermodynamically calculate the partitioning between vapor and liquid at each stage, and also to calculate the compositions in each phase. The code was modified by adding the regression coefficients listed above so that the model included the 4.5m K^+/4.5m PZ solvent as an option for the simulation. The configuration of the double matrix stripper is shown in Figure 9.

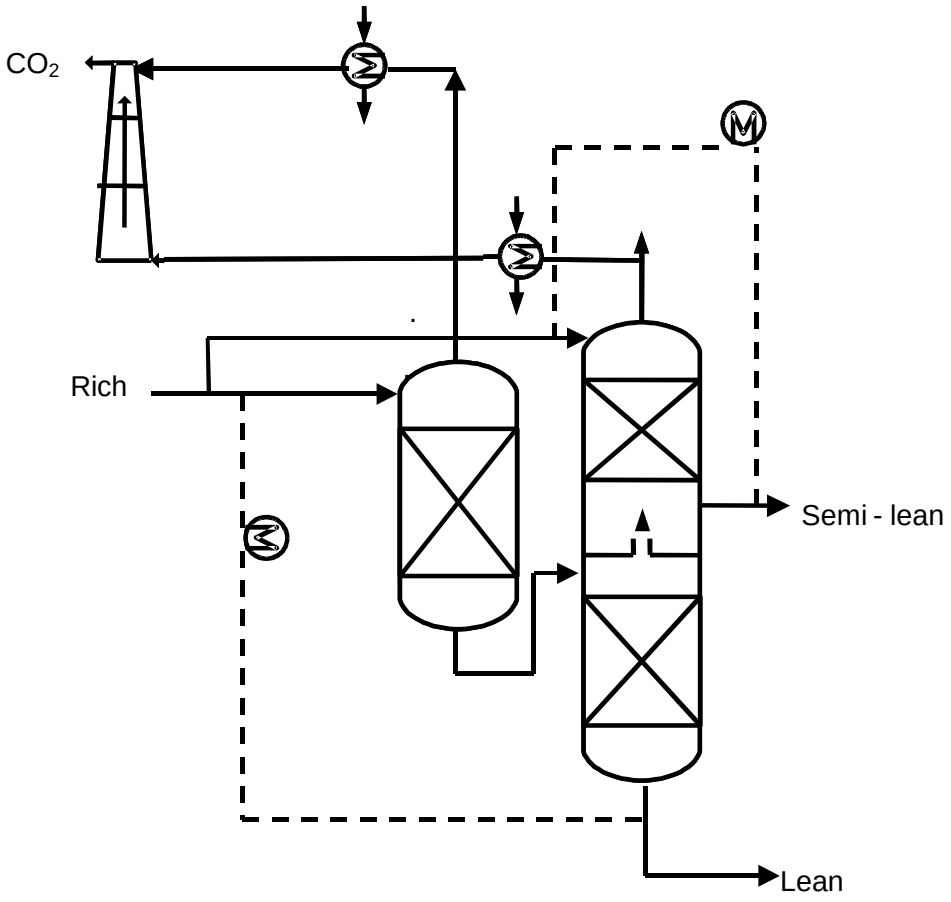

Figure 9: Double Matrix Stripper Design

In order to cooperate with the operating conditions of the absorber, a number of combinations of rich and lean loading were considered. The absorber was specified to run with CO_2 rich and lean loading to achieve a 90% removal of CO_2 in the flue gas, which also dictated an equivalent removal of CO_2 from the amine solution in the stripper. Running the stripper with higher loading resulted in a lower reboiler duty, so we initially considered running with rich and lean equilibrium partial pressures at 40^{o}C of 7 kPa and 0.7 kPa, respectively. However, the absorber model determined that the required height of the absorber would have been prohibitive, so a lower, more reasonable set of operating conditions of 5 kPa and 0.5 kPa was chosen. The

rich and lean compositions were determined by interpolation of the VLE data at 40°C to find the loadings which corresponded to 5 kPa and 0.5 kPa values of P^*_{CO2}.

Many of the variables in the stripper model were specified from previous stripper simulations using different solvents; including the stripper feed temperatures, the approach temperature, the pressure of each stripper, and the split. The split was defined as the ratio of the feeds to the two strippers:

$$Split = \frac{Feed_2}{Feed_1} \tag{3}$$

In addition to the values used from previous models, there were also values selected for this specific project. The rich and lean loadings were selected from desired equilibrium partial pressures, as described previously. The magnitude of flow rates were determined by the desired removal rate of CO_2, specified by Trimeric. The values used for the base case are listed in Table 7:

Table 7: Operating Conditions Used for Base Case

Feed Temperature 1	94℃
Feed Temperature 2	85℃
Approach Temperature, hot side	5℃
Stripper 1 Pressure	295 kPa
Stripper 2 Pressure	160 kPa
Split	0.4
Rich Loading	0.4960
Lean Loading	0.4012
Product CO_2 Flow	2258 kmol/hr

The results from ACM provided profiles of column temperature, composition, liquid flow rate, and vapor flow rate, and it calculated the equivalent work of each stripper. The equivalent work was the heat duty of the reboiler, expressed as the amount of work that could be reasonably extracted from the steam if were expanded in a turbine instead of being used in the boiler:

$$W_{eq,stripper} = 0.75 Q_{reb}\left(\frac{T_{reb} + 10°C - T_{cw}}{T_{reb} + 10°C}\right) \tag{4}$$

Additionally, the total equivalent work was normalized by the CO_2 flow in the vapor. It was desired to optimize the pressure of the first stripper as well as the split ratio.

Aspen Compression Model

In addition to the ACM model, a model was created in Aspen to simulate the vapor compression section which was not contained in the ACM model. It was important to include the compressors in order to optimize the stripper section more accurately. The compression section includes a cooler and compressor to increase the pressure of the vapor from the second stripper to the pressure of the vapor from the first stripper. Then the vapor streams are combined

and sent into a multistage compressor, which uses a four stage multistage compressor with interstate cooling to compress the CO_2 to its supercritical pressure. Water is also removed from each stage to maintain a pure vapor stream. The flow sheet is summarized in Figure 9:

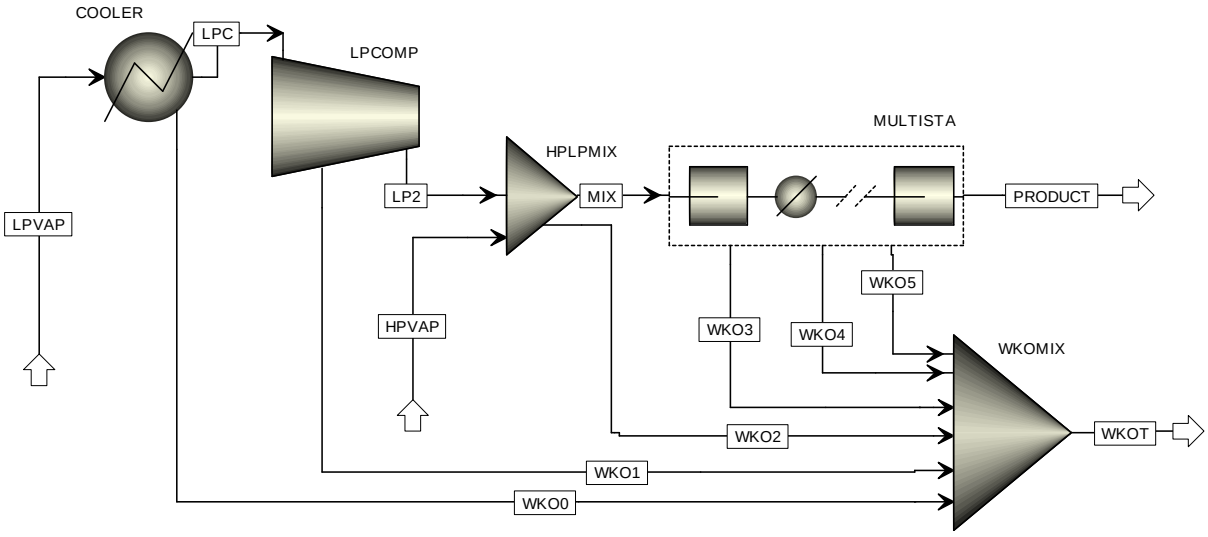

Figure 10: Compression Section Flow Diagram

The inputs for the compression section required results from the ACM model. The temperatures, pressures, molar flow rates, and compositions of the two input streams were found in the double matrix simulation. The only other specification was the final CO_2 pressure, which was chosen to be 1400 psi, approximately 10 MPa. The Aspen simulation calculated that the water knockout stream was pure water, and the product CO_2 stream was essentially pure CO_2, with only 0.3% water. The work for the compression section was the total of the work for the low-pressure compressor and the multistage compressor. Therefore, the total normalized equivalent work for the strippers and compression was:

$$W_{eq} = \frac{n_{CO_2,1} W_{eq,stripper1} + n_{CO_2,2} W_{eq,stripper2} + W_{LPCOMP} + W_{MULTISTAGE}}{n_{CO_2,product}} \qquad (5)$$

It was important to compare the total normalized equivalent work between operating conditions and configurations because it exemplifies the energy drain on a power plant per mole of CO_2 removed from the existing flue gas.

Optimization

The strippers and compressors were optimized where the objective function was the total normalized equivalent work. The variables used for optimization were the feed split ratio and the pressure of stripper 1. The optimization method was unilateral search with quadratic interpolation. The search started with initial operating conditions of 295 kPa and a split of 0.4, the operating conditions from the base case. While holding the pressure constant, the split was optimized by running various cases in ACM, using the outputs to run the Aspen compressor section, and then the total normalized equivalent work was calculated for each case. Next, the

pressure was optimized while holding the split constant at the value previously found. Six steps were required to locate the optimum operating conditions of 230 kPa and a split of 0.185, which resulted in an equivalent work of 31.79 kJ/mol. The compressor work made up 49% of the total equivalent work at the optimum. The performances of the two strippers are summarized in the following tables.

Table 8: Stripper 1 Profiles

Stage	Temperature (K)	Pressure (kPa)	Liquid (kmol/s)	Vapor (kmol/s)	Loading	Vapor CO2 Fraction
1	364.0	230	34587	490.0	0.4775	0.6854
2	371.9	230	34205	382.6	0.4417	0.5784

Table 9: Stripper 2 Profiles

Stage	Temperature (K)	Pressure (kPa)	Liquid (kmol/s)	Vapor (kmol/s)	Loading	Vapor CO2 Fraction
1	357.9	160	6417	453	0.4816	0.6429
2	360.2	160	6447	452	0.4736	0.6085
3	363.8	160	6496	482	0.4598	0.5514
4	368.2	160	34050	531	0.4253	0.4702
5	371.9	160	33674	376	0.4012	0.3939

Sensitivity

In addition to finding the exact optimum, the sensitivity of the system to slight variations in the decision variables from their optimum values was analyzed. Even though a definite optimum existed, the equivalent work did not change drastically when the variables changed. Overall, the split was varied from 0.1 to 0.45, and the stripper pressure was varied from 200 to 350 kPa. The greatest equivalent work encountered in the optimization search was when operating the first stripper with a pressure of 350 kPa and splitting the feed with a ratio of 0.2835. The equivalent work at these operating conditions was 33.38 kJ/mol, compared to the optimum of 31.79 kJ/mol. However, normal operating conditions would not be likely to change to such a drastic extent. Smaller changes in the operating conditions would have a very small impact on the equivalent work, demonstrated in Figures 11 and 12 below.

The optimum for this system was found to be considerably flat, demonstrated by the shallow slopes on the curves on the graphs. Considering only the smaller changes in conditions, the most significant impact would be a 1.2% increase in the equivalent work by a 15% change in the stripper pressure.

Integration with Absorber

Once optimized, the stripper system provided compositions, temperatures, and pressures of the inlet and outlet streams which recycled from and to the absorber.

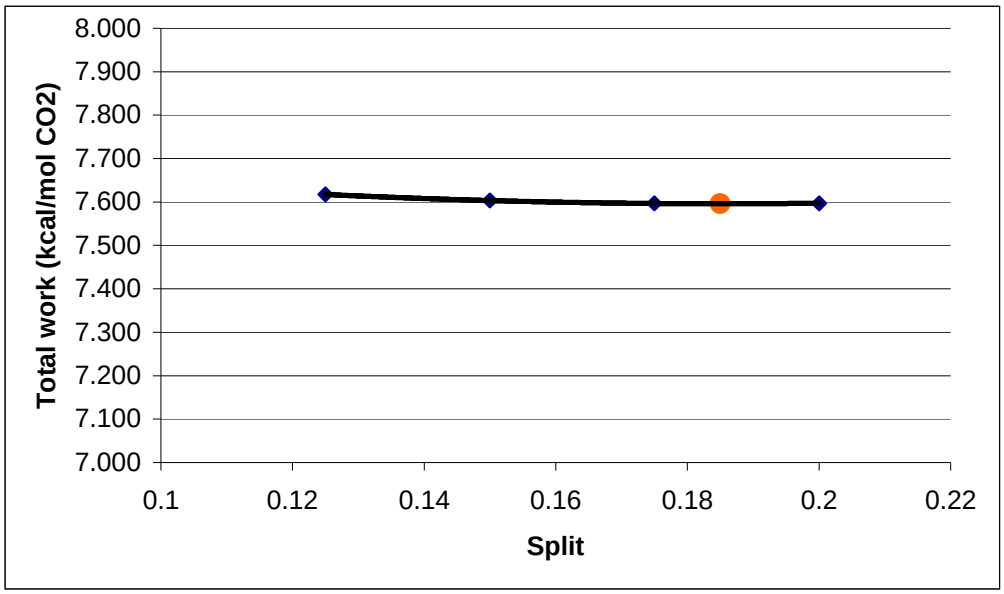

Figure 11: Variation of Total Equivalent Work with Split Ratio Variations

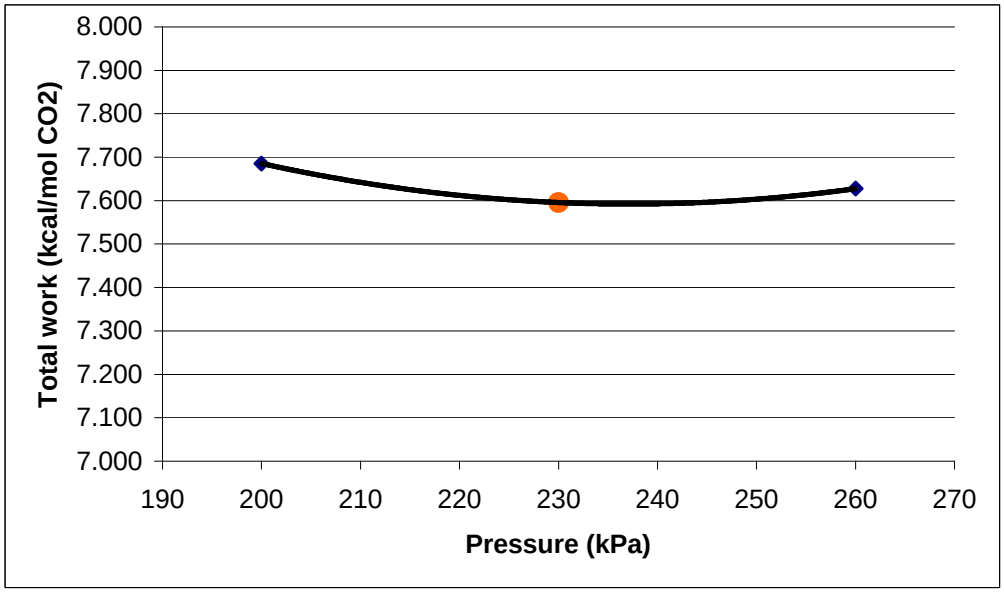

Figure 12: Variation of Total Equivalent Work With Stripper 1 Pressure Variations

Table 10: Stripper Inlet and Outlet Conditions

	Loading	Temperature (K)	Pressure (kPa)
Rich 1	0.4960	366.9	230
Rich 2	0.4960	358.8	160
Semi-lean	0.4598	363.8	160
Lean	0.4012	371.9	160

The absorber optimization took place alongside this project throughout the past quarter. Once the two processes were designed and optimized, the cross-exchange section was also designed to determine capital costs, pump duties, and heat duties for the heat exchanges and pumps, which make up the temperature and pressure differences between the absorber streams and the stripper streams.

Submission to Trimeric

Trimeric requested complete simulation results of the absorber and stripper sections. Trimeric provided the conditions of the inlet flue gas and expected feasible results for CO_2 removal. Most of the results from ACM consisted of user-defined variables, and many of the variables were only used for the calculations in the code. Therefore, the important variables from the simulation were picked out and emphasized. These variables are shown in Table 11.

Table 11: Important ACM Variable Output

B2.Pt(1)	Stripper 1 pressure	230	kPa
B1.Pt(1)	Stripper 2 pressure	160	kPa
B1.Lcf(0)	Stripper 2 molar feed	6418	kmol/s
B2.in_r.L	Stripper 1 molar feed	34695	kmol/s
	Split	0.185	-
B2.Qreboiler	Stripper 1 standardized reboiler duty	31.90	kcal/mol
B1.Qreboiler	Stripper 2 standardized reboiler duty	29.13	kcal/mol
B2.Weq2	Stripper 1 standardized equivalent work	4.309	kcal/mol
B1.Weq2	Stripper 2 standardized equivalent work	3.371	kcal/mol
B2.G(1)	Stripper 1 vapor molar flowrate	490.0	kmol/s
B2.yco2(1)	Stripper 1 vapor CO_2 composition	0.6854	-
B1.GCF(1)	Stripper 2 vapor molar flow rate	453.2	kmol/s
B1.yco2cf(1)	Stripper 2 vapor CO_2 composition	0.6429	-
B2.in_r.ldg	Rich loading	0.4960	-
B1.ldgcf(3)	Semilean loading	0.4598	-
B1.ldgout	Lean loading	0.4012	-
	Total equivalent work	7.595	kcal/mole CO2
	Total equivalent work	31.79	kJ/mole CO2

The output from Aspen from the compression section was a more familiar output for Trimeric, so the stream summaries for all the streams in the flowsheet were submitted. The four streams that connect with the absorber section (STR1RICH, STR2RICH, STRSLEAN, and STRLEAN) were also calculated and submitted in the absorber/cross-exchange section in this task, so the streams were not resubmitted with the stripper data. The stream summaries are displayed in Tables 12-15.

Table 12: Aspen Stream Summary Table 1

		STR1LEAN	HPVAP	LPVAP
From		STRIPPER 1	STRIPPER 1	STRIPPER 2
To		STRIPPER 2 MID	HPLPMIX	COOLER
Substream: MIXED				
Phase:		Mixed	Vapor	Vapor
Component Mole Flow				
H2O	KMOL/SEC	24.63	0.15	0.16
K2CO3	KMOL/SEC	0	0	0
KHCO3	KMOL/SEC	0	0	0
PZ	KMOL/SEC	0.08	0	0
K+	KMOL/SEC	2.06	0	0
H3O+	KMOL/SEC	0	0	0
CO2	KMOL/SEC	1.18	0.34	0.29
HCO3-	KMOL/SEC	0.63	0	0
OH-	KMOL/SEC	0	0	0
CO3--2	KMOL/SEC	0.02	0	0
PZH+	KMOL/SEC	1.38	0	0
PZCOO-	KMOL/SEC	0.11	0	0
PZCOO-2	KMOL/SEC	0.3	0	0
HPZCOO	KMOL/SEC	0.19	0	0
N2	KMOL/SEC	0	0	0
O2	KMOL/SEC	0	0	0
Component Mole Fraction				
H2O		0.81	0.31	0.36
K2CO3		0	0	0
KHCO3		0	0	0
PZ		0	0	0
K+		0.07	0	0
H3O+		0	0	0
CO2		0.04	0.69	0.64
HCO3-		0.02	0	0
OH-		0	0	0
CO3--2		0	0	0

PZH+		0.05	0	0
PZCOO-		0	0	0
PZCOO-2		0.01	0	0
HPZCOO		0.01	0	0
N2		0	0	0
O2		0	0	0
Component Mass Flow				
H2O	KG/SEC	443.74	2.78	2.92
K2CO3	KG/SEC	0	0	0
KHCO3	KG/SEC	0	0	0
PZ	KG/SEC	6.74	0	0
K+	KG/SEC	80.65	0	0
H3O+	KG/SEC	0	0	0
CO2	KG/SEC	51.93	14.78	12.83
HCO3-	KG/SEC	38.72	0	0
OH-	KG/SEC	0	0	0
CO3--2	KG/SEC	1.03	0	0
PZH+	KG/SEC	120.57	0	0
PZCOO-	KG/SEC	14.62	0	0
PZCOO-2	KG/SEC	51.76	0	0
HPZCOO	KG/SEC	24.35	0	0
N2	KG/SEC	0	0	0
O2	KG/SEC	0	0	0
Component Mass Fraction				
H2O		0.53	0.16	0.19
K2CO3		0	0	0
KHCO3		0	0	0
PZ		0.01	0	0
K+		0.1	0	0
H3O+		0	0	0
CO2		0.06	0.84	0.81
HCO3-		0.05	0	0
OH-		0	0	0
CO3--2		0	0	0

PZH+		0.14	0	0
PZCOO-		0.02	0	0
PZCOO-2		0.06	0	0
HPZCOO		0.03	0	0
N2		0	0	0
O2		0	0	0
Mole Flow	KMOL/SEC	30.59	0.49	0.45
Mass Flow	KG/SEC	834.1	17.56	15.74
Volume Flow	CUM/SEC	24.75	6.39	8.37
Temperature	K	371.94	363.99	357.85
Pressure	N/SQM	230000	230000	160000
Vapor Fraction		0.06	1	1
Liquid Fraction		0.94	0	0
Solid Fraction		0	0	0
Molar Enthalpy	J/KMOL	-288230300	-343666200	-337434900
Mass Enthalpy	J/KG	-10570110	-9590742	-9716657
Molar Entropy	J/KMOL-K	-167366.6	-6323.86	-5723.73
Mass Entropy	J/KG-K	-6137.74	-176.48	-164.82
Molar Density	KMOL/CUM	1.24	0.08	0.05
Mass Density	KG/CUM	33.71	2.75	1.88
Average Molecular Weight		27.27	35.83	34.73
CPMX	J/KG-K	4319.08	1072.98	1092.4

Table 13: Aspen Stream Summary Table 2

		LPC	LP2	MIX	PRODUCT
From		COOLER	LPCOMP	HPLPMIX	MULTISTA
To		LPCOMP	HPLPMIX	MULTISTA	
Substream: MIXED					
Phase:		Vapor	Vapor	Vapor	Vapor
Component Mole Flow					
WATER	KMOL/SEC	0	0	0.12	0
CO2	KMOL/SEC	0.29	0.29	0.63	0.63
Component Mole Fraction					
WATER		0	0	0.16	0

CO2		1	1	0.84	1
Component Mass Flow					
WATER	KG/SEC	0.01	0.01	2.14	0.03
CO2	KG/SEC	12.83	12.83	27.61	27.61
Component Mass Fraction					
WATER		0	0	0.07	0
CO2		1	1	0.93	1
Mole Flow	KMOL/SEC	0.29	0.29	0.75	0.63
Mass Flow	KG/SEC	12.83	12.83	29.75	27.64
Volume Flow	CUM/SEC	4.71	3.64	8.03	0.05
Temperature	K	313.15	347.44	384.99	313.15
Pressure	N/SQM	160000	230000	295000	9652660
Vapor Fraction		1	1	1	1
Liquid Fraction		0	0	0	0
Solid Fraction		0	0	0	0
Molar Enthalpy	J/KMOL	-392805900	-391488200	-366106000	-400871200
Mass Enthalpy	J/KG	-8932415	-8902450	-9182548	-9124349
Enthalpy Flow	WATT	-114622600	-114238100	-273165300	-252200900
Molar Entropy	J/KMOL-K	820.86	1818.33	-244.63	-55297.42
Mass Entropy	J/KG-K	18.67	41.35	-6.14	-1258.64
Molar Density	KMOL/CUM	0.06	0.08	0.09	12.35
Mass Density	KG/CUM	2.72	3.53	3.71	542.68
Average Molecular Weight		43.98	43.98	39.87	43.93
CPMX	J/KG-K	871.24	908.29	1013.19	6715.72

Table 14: Aspen Stream Summary Table 3

		WKO0	WKO1	WKO2	WKO3
From		COOLER	LPCOMP	HPLPMIX	MULTISTA
To		WKOMIX	WKOMIX	WKOMIX	WKOMIX
Substream: MIXED					
Phase:		Liquid	Missing	Liquid	Liquid
Component Mole Flow					
WATER	KMOL/SEC	0.16	0	0.04	0.11
CO2	KMOL/SEC	0	0	0	0

Component Mole Fraction					
WATER		1	0	1	1
CO2		0	0	0	0
Component Mass Flow					
WATER	KG/SEC	2.91	0	0.64	2.01
CO2	KG/SEC	0	0	0	0
Component Mass Fraction					
WATER		1		1	1
CO2		0		0	0
Mole Flow	KMOL/SEC	0.16	0	0.04	0.11
Mass Flow	KG/SEC	2.91	0	0.64	2.01
Volume Flow	CUM/SEC	0	0	0	0
Temperature	K	313.15		384.99	313.15
Pressure	N/SQM	160000	230000	295000	671706.1
Vapor Fraction		0		0	0
Liquid Fraction		1		1	1
Solid Fraction		0		0	0
Molar Enthalpy	J/KMOL	-284694300		-279269100	-284686100
Mass Enthalpy	J/KG	-15802930		-15501790	-15802480
Enthalpy Flow	WATT	-45970490		-9967576	-31706700
Molar Entropy	J/KMOL-K	-159453.1		-143867.6	-159459.1
Mass Entropy	J/KG-K	-8851		-7985.87	-8851.33
Molar Density	KMOL/CUM	55.08		52.7	55.09
Mass Density	KG/CUM	992.32		949.35	992.55
Average Molecular Weight		18.02		18.02	18.02
CPMX	J/KG-K	4172.2		4224.93	4170.93

Table 15: Aspen Stream Summary Table 4

		WKO4	WKO5	WKOT
From		MULTISTA	MULTISTA	WKOMIX
To		WKOMIX	WKOMIX	
Substream: MIXED				
Phase:		Liquid	Liquid	Liquid

Component Mole Flow				
WATER	KMOL/SEC	0	0	0.31
CO2	KMOL/SEC	0	0	0
Component Mole Fraction				
WATER		1	1	1
CO2		0	0	0
Component Mass Flow				
WATER	KG/SEC	0.07	0.03	5.66
CO2	KG/SEC	0	0	0
Component Mass Fraction				
WATER		1	1	1
CO2		0	0	0
Mole Flow	KMOL/SEC	0	0	0.31
Mass Flow	KG/SEC	0.07	0.03	5.66
Volume Flow	CUM/SEC	0	0	0.01
Temperature	K	313.15	313.15	343.05
Pressure	N/SQM	1656001	4012235	101325
Vapor Fraction		0	0	0
Liquid Fraction		1	1	1
Solid Fraction		0	0	0
Molar Enthalpy	J/KMOL	-284670400	-284632900	-284074400
Mass Enthalpy	J/KG	-15801610	-15799530	-15768530
Enthalpy Flow	WATT	-1172034	-430837.2	-89247630
Molar Entropy	J/KMOL-K	-159467.6	-159485.7	-156456.5
Mass Entropy	J/KG-K	-8851.8	-8852.8	-8684.66
Molar Density	KMOL/CUM	55.12	55.18	52.71
Mass Density	KG/CUM	992.98	994.01	949.52
Average Molecular Weight		18.02	18.02	18.02
CPMX	J/KG-K	4168.49	4162.71	4545.28

Conclusions and Future Work

The VLE regression that was calculated for this work was accurate compared to the model calculated values. The work done to adapt a previous double matrix equilibrium model to simulate 4.5m K^+/4.5m PZ was successful, and optimum operating conditions were determined

so that the system would require the minimum total equivalent work. The minimum equivalent work was 31.79 kJ/mol with a pressure in the first stripper of 230 kPa and a feed ratio of 0.185. The stripper results, along with the absorber and cross-exchange results, were sent to Trimeric for further analysis.

In the future a similar stripper model will be developed in Aspen using the same equilibrium calculations as the absorber. If a double matrix system can be developed to yield similar results, the strippers can be directly linked to the compressor section as well as the absorber and cross-exchange section, and the optimization process will be much more straightforward. More aggressive optimization techniques could be attempted in which more variables would be used, and a more economic optimum could be found.

Task 3 – Solvent Losses

Subtask 3.2 – Oxidative Degradation

by Andrew Sexton

(Supported by this contract and the TXU Carbon Management Program)

Introduction

This effort is an extension of work by George Goff on the oxidative degradation of MEA. Goff showed that oxidative degradation, under high catalyst conditions, is mass-transfer limited by the physical absorption of O_2 into the amine and not by reaction kinetics. Goff also theorized that the oxidative degradation of MEA produced volatile ammonia as well as a host of other proposed degradation products. The major degradation products among these include the heat stable salts of carboxylic acids, nitrite, and nitrate.

The oxygen stoichiometry necessary to produce these degradation products varies for each individual component; overall, it varies anywhere from 0.5 to 2.5 (Goff, 2004). It is believed that the particular degradation products are specific to certain metal catalysts present in the absorption/stripping system – specifically iron and copper. For example, the following balanced reactions illustrate the differences in oxygen consumption based upon the end products:

$$\text{MEA} + 1.5\ O_2 \rightarrow 2\ \text{Formate} + \text{Ammonia}$$

$$\text{MEA} + 3.5\ O_2 \rightarrow 2\ \text{Formate} + \text{Nitrate} + \text{Water}$$

$$\text{MEA} + O_2 \rightarrow \text{Glycolate} + \text{Ammonia}$$

Goff's work on MEA degradation was limited to analyzing MEA degradation rates via the evolution of NH_3. The ammonia evolution rates were measured using a Fourier Transform Infrared (FT-IR) analyzer. This effort extends Goff's gas-phase analysis by applying various methods of liquid-phase analysis, specifically ion chromatography. These analytical methods will be used to quantify the rate of amine degradation as well as the rate of degradation product formation for amine systems.

Since most gas treating processes using alkanolamines for CO_2 removal are performed in the absence of oxygen, oxidative degradation is a source of solvent degradation that has not been

properly quantified. Oxidative degradation is important because it can impact the environment, process economics, and decrease equipment life due to corrosion.

The environmental effects refer to the degradation products themselves: what is being produced, how much of it is being produced, and how can it be disposed of without doing significant damage to the environment. Process economics being impacted are the solvent make-up rate and design of the reclaiming operation. If amine is continually being degraded, then fresh amine must be continually added to the process at a significant cost. In addition, CO_2 loaded amine solutions corrode carbon steel equipment, which catalyzes oxidative degradation even further. It is imperative to quantify how much of this solvent make-up rate is due to oxidative degradation.

Experimental

As stated in prior reports, ion chromatography is the most extensively used liquid-phase analytical method. Anion chromatography utilizes an AS15 (a low-capacity column designed to separate low-molecular weight anions, specifically acetate, glycolate, and formate) IonPac column and an ASRS 4-mm self regenerating suppressor made by Dionex, while cation analysis uses a CS17 and a CSRS 4-mm self-regenerating suppressor. Anion analysis employs a linear gradient of NaOH eluent, while cation analysis uses a constant concentration methanesulfonic acid (MSA) eluent. Refer to the June 2006 quarterly report for a detailed explanation of the analytical methods.

During the most recent quarter, three other analytical methods were examined: high pressure liquid chromatography coupled with mass spectrometry (HPLC-MS), acid-base titration for total amine concentration, and pH measurements (to construct pH profiles for the degradation experiments).

HPLC-MS was carried out by the Mass Spectrometry Facility (MSF) of the Department of Chemistry and Biochemistry/Institute for Cellular and Molecular Biology at the University of Texas at Austin, which is directed by Dr. Mehdi Moini. HPLC-MS is an analytical tool used to separate and identify molecular compounds.

HPLC is a general class of analytical techniques under which the subset of ion chromatography falls. A sample, containing the analytes of importance, is carried by the mobile phase into the column, known as the stationary phase. As the mobile phase is continually passed through the column, any nonpolar analytes contained within the sample are retained on the column. Based on each substance's affinity for the resin, each analyte will be retained for a particular length of time (Waters, 2007).

HPLC-MS combines the separation power of HPLC with the detection power of mass spectrometry. Mass spectrometry is designed to separate gas phase ions according to their m/z (mass to charge ratio) value. The MS analyzer uses electrical and/or magnetic fields to move the ions from the region where they are produced to a detector where they produce an amplified signal. Since the motion and separation of ions is based on electrical and magnetic fields, it is the mass to charge ratio, not just the mass, which is of importance. The analyzer is operated under high vacuum, so that the ions can travel to the detector with a sufficient yield.

Interfacing an HPLC system with a mass spectrometer is not trivial. The difficulty is to transform a solute into a gas phase ion. The challenge is to get rid of the solvent while maintaining adequate vacuum level in the mass spectrometer, and to generate the gas phase ions.

The Mass Spectrometry Facility at UT uses electrospray ionization (ESI) to achieve this function. In electrospray ionization, the HPLC line is connected to the electrospray probe, which consists of a metallic capillary surrounded with nitrogen flow. A voltage is applied between the probe tip and the sampling cone. The voltage is applied on the capillary, while the sampling cone is held at low voltage (Waters, 2007).

At the tip of the capillary in the electrical field, the surface of the droplets containing the ionized compound will get charged either positively or negatively, depending on the voltage polarity. Due to solvent evaporation, the size of the droplet reduces, and the density of charges at the droplet surface increases. The repulsion forces between the charges increase until there is an explosion of the droplet. This process repeats until analyte ions evaporate from the droplet, and are ready for MS analysis.

Acid-base titration analysis is utilized to determine the total base concentration of a solution. Marcus Hilliard, another graduate researcher at the University of Texas at Austin, has developed a titration method specifically for MEA/PZ amine solutions. Approximately 0.5g of amine solution is diluted with 60g of distilled, deionized water in a 200mL beaker. A pH probe is inserted into the diluted solution to monitor pH in situ. The titration is carried out using the 835 Titrando manufactured by Metrohm. 0.2 N sulfuric acid is continually added from a reservoir in 0.1mL increments, while a magnetic stirrer keeps the solution well mixed, until the pH of the solution reaches 2.0 (Hilliard, 2007).

Two equivalence points are visible for a loaded amine solution using H_2SO_4 acid titration. The first equivalence point, reached around a pH of 7, signifies that all the CO_2 has been liberated from the amine solution. The second equivalence point, reached at pH 4.5, is the point at which all the base in the solution has been neutralized by the acid. From this equivalence point, the total base concentration can be calculated (MEA + 2*PZ, since piperazine is diprotonated).

The acidic solution is transferred to a hot plate, where the solution is brought to a slow boil for approximately 30 seconds. This ensures that any CO_2 remaining in the solution after acid titration is boiled off. The beaker is then taken off the hot plate and placed in an ambient temperature water bath and allowed to cool. Once the solution is at ambient temperature, it can be back-titrated with 0.1 N sodium hydroxide. Using the 835 Titrando, the 0.1 N NaOH is continuously added in 0.1mL increments until the pH of the solution is raised to 9.5.

Two equivalence points are reached as well for the base titration. The first equivalence point (@ pH 4.5) gives the amount of NaOH needed to titrate the total amine concentration (MEA + PZ). The second equivalence point (@ pH 7) gives the amount of NaOH needed to neutralize all base in the solution (MEA + 2*PZ). The difference in the two equivalence points gives the total piperazine concentration in mol/kg solution. Once the total piperazine concentration is known, the MEA concentration can be determined from the total base concentration determined from the acid titration (Hilliard, 2007).

The final analytical "technique" instituted this quarter was determining pH profiles of the low gas flow degradation experiments using a Cole Parmer pH/^{o}C/mV analyzer with a Cole Parmer pH probe. A calibration curve was constructed by inserting the probe into buffer solutions ranging from pH 2 to 11 and recording the measured value. A plot of the actual buffer value versus the measured value was constructed and an equation correlating the two was formulated. For each low gas flow experiment, 0.5g of each sample (includes initial and final

samples as well as all intermediate samples) was diluted with 60g of water. The probe was inserted into each diluted experimental sample and a pH value was recorded. Then, using the correlated equation, the actual pH of each diluted solution was determined.

Two experimental apparatuses were utilized in this quarter to provide samples for analysis: the low gas flow degradation apparatus and the hydrogen peroxide apparatus. As stated in previous reports, amine solutions in the low gas flow degradation apparatus are oxidized for 12 to 14 days in a low-gas flow jacketed reactor at 55^{o}C. The solutions are agitated at 1400 RPM to produce a high level of gas/liquid mass transfer by vortexing. 98% O_2/2% CO_2 at 100 ml/min is introduced across the vortexed surface of 350 ml of aqueous amine. Samples were taken from the reactor at regular intervals in order to determine how degradation products formed over the course of the experiment. Prior quarterly reports provide a detailed explanation of the low gas flow degradation apparatus.

Two low gas flow apparatuses are now operating in parallel. One system operates via the original configuration, which uses an inlet gas of 98% O_2/2% CO_2 premixed in a cylinder provided by Matheson Tri-Gas. A Cole-Parmer rotameter is used to control the flowrate at 100 mL/min. The second apparatus is set up for the modified configuration, which operates with two separate cylinders provided by Matheson Tri-Gas – a pure oxygen cylinder and a pure CO_2 cylinder. The 98% O_2/2% CO_2 mixture is achieved using a 4 channel Brose box made by Brooks and two model 5850E mass flow controllers also manufactured by Brooks. Oxygen flowrate is controlled by a 100cc flow controller, while carbon dioxide is controlled by a 20cc flow controller. The control box displays a digital readout corresponding to the % open of the valve on the mass flow controller. The valve % open corresponds to a gas flowrate, which is determined from the calibration curve constructed for each flowmeter.

The hydrogen peroxide experimental apparatus was derived from previous hydrogen experiments performed by Masters' students Susan Chi and Terraun Jones. 100mL of a loaded amine solution is placed into a 250mL Erlenmeyer flask and capped with rubber stopper. A hole is cut into the rubber stopper so that a plastic funnel can be placed inside the hole. The amine solution is kept at a constant temperature of 55^{o}C using a Lauda E100 heat bath filled with water. Using a 50% by weight hydrogen peroxide solution, 10mL of a 2M H_2O_2 solution is made and poured into a 10mL burette. H_2O_2 is an excellent free radical initiator and produces dissolved oxygen when it breaks down. The dissolved O_2 is the oxygen source used to degrade the amine. The H_2O_2 is delivered dropwise into the flask via the burette over a 2 hour time period. The degraded amine solution is then analyzed via ion chromatography (Mellin, 2007).

Results

Using the analytical methods for the AS15 and CS17 columns, analysis was completed on low gas flow experiments conducted during the prior quarters:

1. November 2006 PZ experiment (Oxidative degradation of 2.5m PZ/5m $KHCO_3$, 55^{o}C, 1400 rpm, 500 ppm V, 98%O_2/2%CO_2).
2. December 2006 PZ experiment (Oxidative degradation of 2.5m PZ, 55^{o}C, 1400 rpm, 100 mM "A", 500 ppm V, 98%O_2/2%CO_2).
3. September 2006 MEA experiment (Oxidative degradation of 35 wt % MEA, 55^{o}C, 1400 rpm, 5 ppm Fe, 0.4 moles CO_2/mol MEA, 98%O_2/2%CO_2).
4. September 2006 MEA/PZ experiment (Oxidative degradation of 7m MEA / 2m PZ, 55^{o}C, 1400 rpm, 5 ppm Fe, 250 ppm Cu, 98%O_2/2%CO_2).

Currently, the following experiment is being conducted on the low gas flow apparatus (analysis will be carried out during the next quarter):

5. March 2007 AMP experiment (Oxidative degradation of 3M AMP, 55°C, 1400 rpm, 50 ppm Fe, 0.55 moles CO_2/mol MEA, 98%O_2/2%CO_2).

Figures 13 through 17 show the degradation product formation rates for low gas flow experiments 1 through 4 (two figures are included for experiment 4). Figure 13 illustrates the degradation product concentrations for the PZ/V/K experiment. Figure 14 details the degradation products for the PZ/V/A experiment, while Figure 15 shows a revised figure (from the previous quarter) for the 35 wt % MEA experiment. The 35 wt % MEA experiment represents an uninhibited commercial system in which iron is continually removed from the absorber/stripper system. The MEA/PZ experiment (Figures 16 and 17) represents a commercial system in which Cu is added as a corrosion inhibitor. Figure 16 illustrates rates for all degradation products, while Figure 17 provides an enlarged view for the degradation products at lower concentrations.

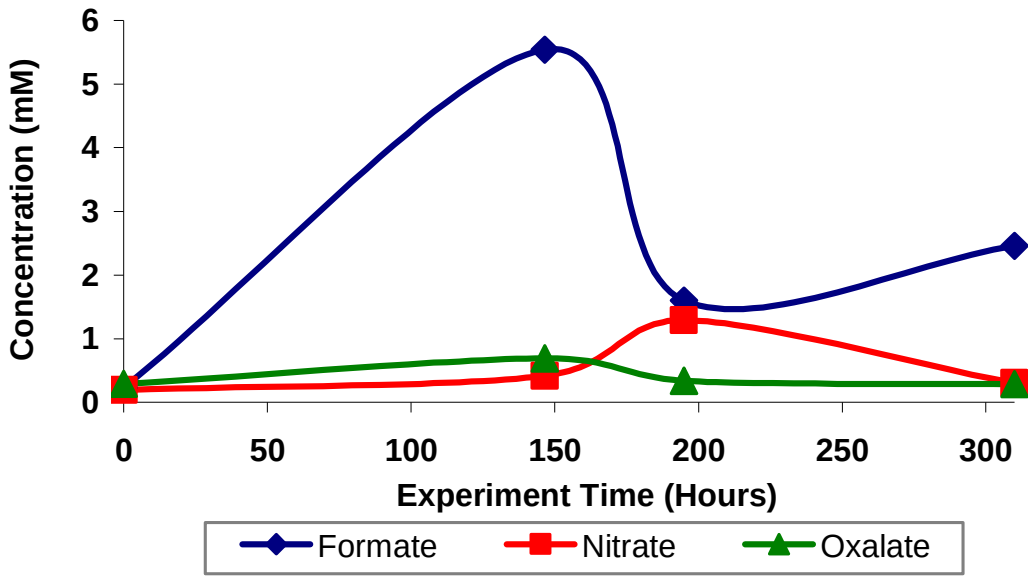

Figure 13: November 2006 PZ experiment (Oxidative degradation of 2.5m PZ/5m $KHCO_3$, 55 °C, 1400 rpm, 500 ppm V, 98% O_2/2% CO_2)

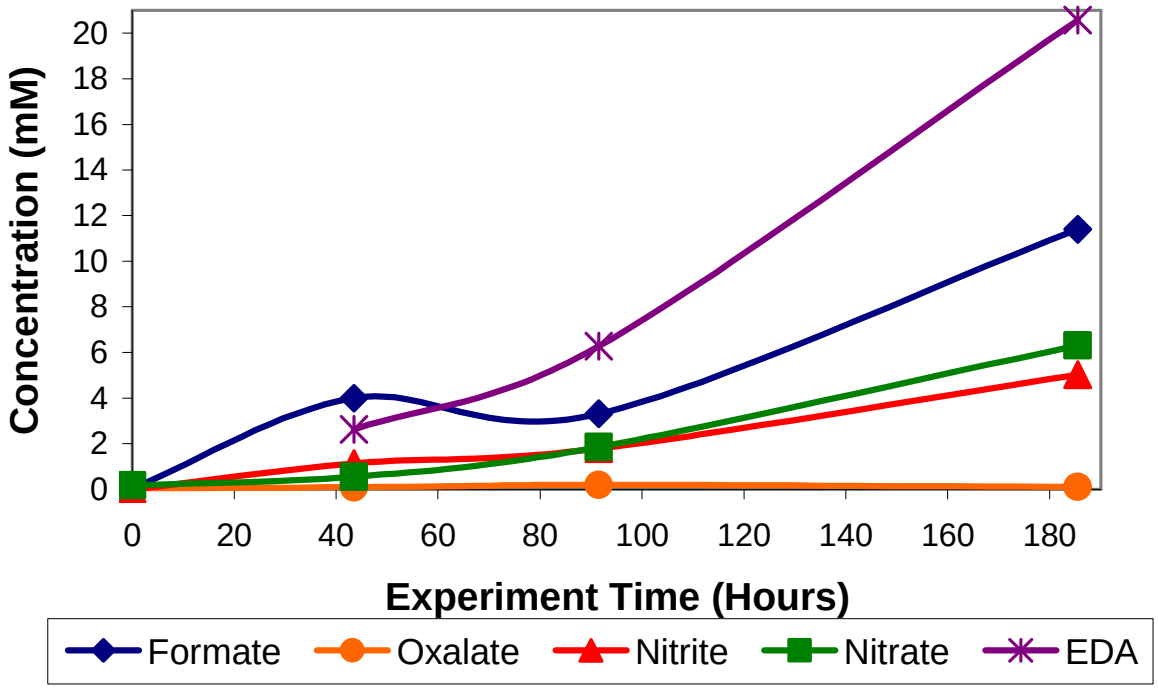

Figure 14: December 2006 PZ experiment (Oxidative degradation of 2.5m PZ, 55 °C, 1400 rpm, 100 mM "A", 500 ppm V, 98% O_2/2% CO_2)

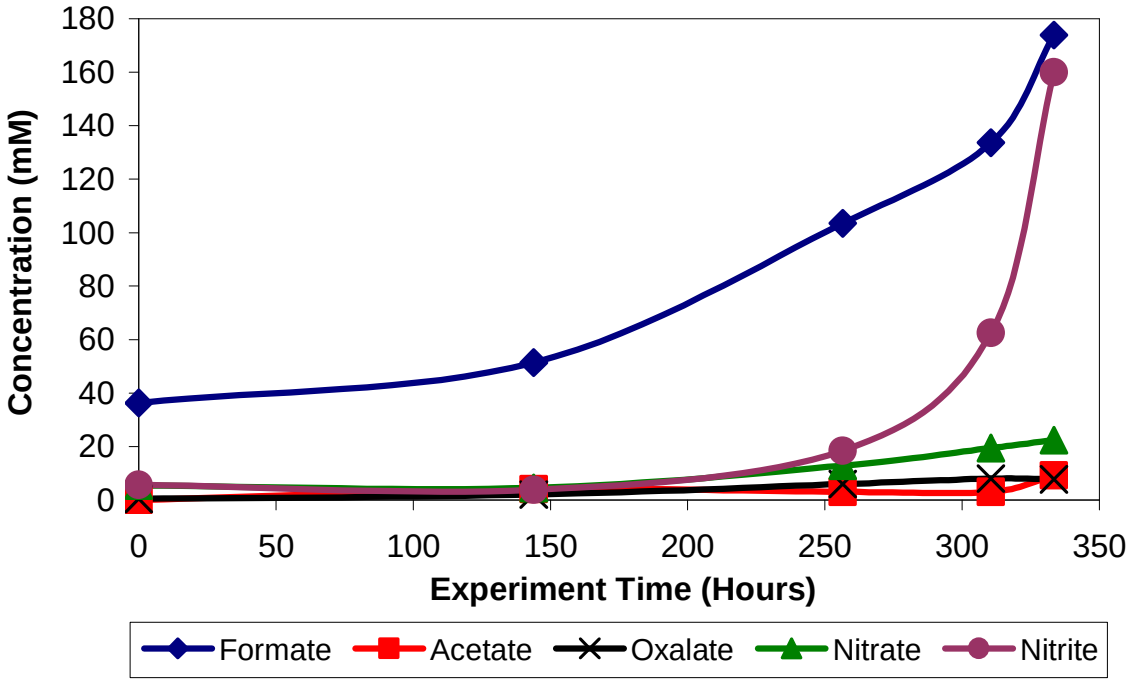

Figure 15: September 2006 MEA experiment (Oxidative degradation of 35 wt % MEA, 55°C, 1400 rpm, 5 ppm Fe, 0.4 moles CO_2/mol MEA, 98% O_2/2% CO_2)

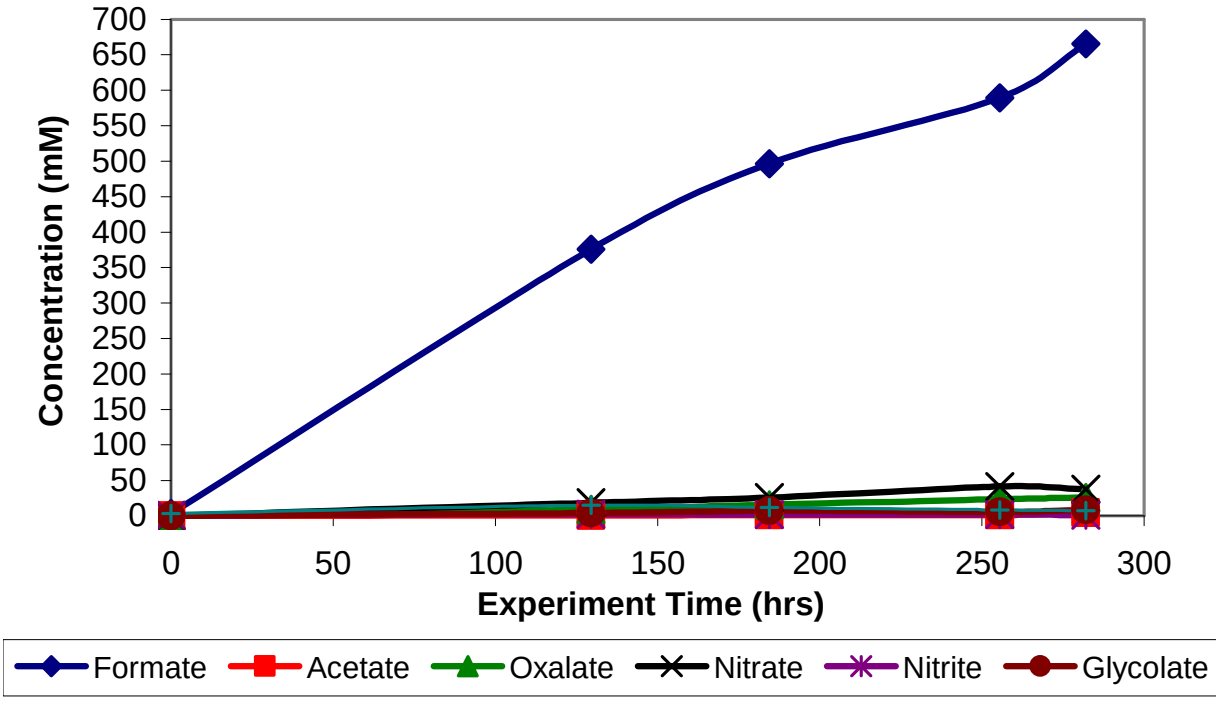

Figure 16: September 2006 MEA/PZ experiment (Oxidative degradation of 7 m MEA/2 m PZ, 55 °C, 1400 rpm, 5 ppm Fe, 250 ppm Cu, 98% O_2/2% CO_2)

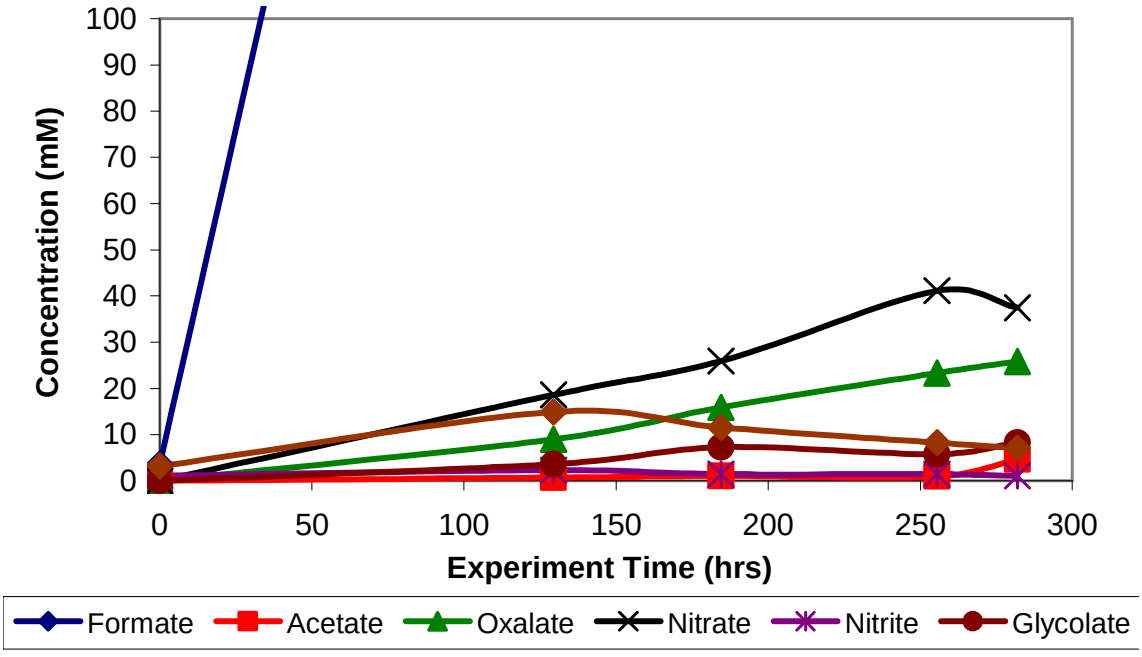

Figure 17: September 2006 MEA/PZ experiment (Oxidative degradation of 7 m MEA/2 m PZ, 55 °C, 1400 rpm, 5 ppm Fe, 250 ppm Cu, 98% O_2/2% CO_2) – Expanded View

According to Figure 13, only formate, nitrate, and oxalate are present, all in quantities of less than 3 mM at the end of the two week experiment. This information agrees with data obtained from the prior PZ/K/V experiment. EDA and formate are the most abundant degradation products in the PZ/V/A experiment. However, product concentrations do not exceed 20 mM.

The 35% MEA degradation experiment (Figure 15) experienced some type of enhanced degradation over the final two days of the experiment. The formate rate doubled, while the nitrite concentration increased by a factor of 8, although other product formation rates remained linear over that time. The 7m MEA/2m PZ solution experienced a large amount of degradation (Figure 16). The final formate concentration at the end of the experiment was 0.7M, almost 20 times the concentration of any of the other degradation products. Concentrations of that magnitude have never been seen before in the low gas flow degradation apparatus.

Tables 16 and 17 provide degradation product formation rates in mM/hr. Table 16 displays product formation rates for the 4 experiments listed in the figures above. Table 17 compares the rates from experiments 2 (PZ/V/A) and 4 (MEA/PZ/Fe/Cu). Experiment 2 is compared to a prior piperazine degradation experiment (2.5m piperazine with 500 ppm V, but no "A"), while experiment 4 is compared to 7m MEA with high copper concentration (250 ppm Cu).

A brief glance reveals that formate is the most abundant identifiable degradation product (another degradation product of similar peak area in the raw scans still has not be properly identified) for all the experiments – with the exception of the 35% MEA experiment, where nitrite formation increased exponentially at the end of the experiment. The formate production rate in the MEA/PZ was 2.35 mM/hr, which is an order of magnitude higher than seen in past experiments. K^+ appears to be an effective degradation inhibitor for piperazine solutions. Degradation product formation rates are less than 0.01 mM/hr, which confirms the results from the prior PZ/K/V experiment from April 2006.

Table 16: Degradation Product Formation Rates (mM/hr)

Distinguishing Conditions	35 wt % MEA, 5 ppm Fe	7 m MEA/2 m PZ, 5 ppm Fe, 250 ppm Cu	2.5m PZ, 100mM A, 500 ppm V	2.5m PZ/5m K, 500 ppm V
Formate	0.413	2.347	0.061	0.007
Acetate	0.028	0.017		0.002
Oxalate	0.022	0.091	0.0003	
Glycolate		0.029		
Nitrate	0.051	0.133	0.033	0.0004
Nitrite	0.462		0.027	
EDA		0.025	0.111	0.001

Table 17: Comparing Degradation Rates with Prior Experiments (mM/hr)

Distinguishing Conditions	7 m MEA, 250 ppm Cu	7 m MEA/2 m PZ, 5 ppm Fe, 250 ppm Cu	2.5m PZ/100mM A, 500 ppm V	2.5m PZ, 500 ppm V
Formate	0.39	2.35	0.06	0.18
Acetate	0.01	0.02		
Oxalate	0.04	0.09	0.00	0.00
Glycolate	0.10	0.03		
Nitrate	0.15	0.13	0.03	0.19
Nitrite	0.31		0.03	0.00
EDA	-	0.03	0.11	0.09

Information from Table 17 demonstrates that "A" appears to be an effective degradation inhibitor for PZ as well as MEA. While EDA rates are similar, both formate and nitrate concentrations are reduced by factor of 3 to 6. It represents an overall reduction in degradation by about 50%. Comparing the first two columns shows that high copper catalyst concentration leads to sufficient degradation of the amine solution. Acetate, oxalate, glycolate, and nitrate degradation rates are similar for the 7 m MEA and the 7 m MEA/2 m PZ solutions. The glaring differences involve nitrite and formate. No nitrite is present in the degraded MEA/PZ sample, while the formate rate is 6 times the rate from the MEA only experiment. It appears that some mechanism takes place in the MEA/PZ solutions that does not favor nitrite production.

Three amine solutions (3 M AMP, 7 m MEA, and 2.5 m PZ) were oxidized by hydrogen peroxide. The 3 M AMP, 7 m MEA, and 2.5 m PZ were loaded to 0.55, 0.40, and 0.60 mol CO_2 per mol of amine, respectively. These are believed to be typical loadings that would be found in an industrial application. Next, 1mM of iron (50 ppm Fe) in the form of ferrous sulfate heptahydrate was dissolved in 100 mL of each amine solution. Then, each loaded amine/iron solution was oxidized by 10 mL of a 2M solution of hydrogen peroxide added over the course of two hours via a burette (Mellin, 2007).

Anion IC analysis revealed the presence of formate, nitrite, nitrate, and oxalate in the degraded samples of each of the amines. Cation IC analysis confirmed the PZ degradation with the presence of ethylenediamine (EDA); however, cation IC analysis has yet to be performed for the degraded MEA and AMP samples. Table 18 lists degradation product concentrations (in mM) for each of the degraded samples. Formate is the most concentrated degradation product, as seen in the low gas flow degradation experiments. AMP degrades less than the MEA and PZ, which appear to have similar degradation product concentrations. However, in the MEA formate and nitrite appear in similar concentrations, while in PZ there is less nitrite and more formate.

Table 18: H_2O_2 Experiments – Degradation Product Concentrations (Mellin, 2007)

Distinguishing Conditions	3M AMP, 50 ppm Fe	7m MEA, 50 ppm Fe	2.5m PZ, 50 ppm Fe
Formate	2.63	6.58	10.81
Nitrite	0.77	6.97	0.61
Oxalate	1.37	3.09	3.18
Nitrate	0.12	1.17	0.75
EDA	-	-	4.23

As stated in the experimental section of this report, acid-base titration was investigated this quarter as a means to determine total amine concentration in experimentally degraded samples. Initial (if one was preserved) and final samples from every low and high gas flow experiment run since May 2004 were diluted and titrated for total base concentration as well as specific amine concentration.

Figures 17 and 18 are titration curves for the initial sample of a 7 m MEA/2 m PZ high gas flow experiment performed on 5/18/06. Figure 17 illustrates the first titration with 0.2 N sulfuric acid. From the graph you can see the two equivalence points: the first one (unmarked) occurs at a pH of 7 when the CO_2 is liberated, and the second one is at pH 4.5 (designated with the purple square) when all the base has been neutralized. Figure 18 shows the titration with 0.1 N sodium hydroxide. The two equivalence points are marked with a purple square (when all the amine, MEA + PZ, has been titrated) and a yellow triangle (when all the base, MEA + 2*PZ, has been titrated).

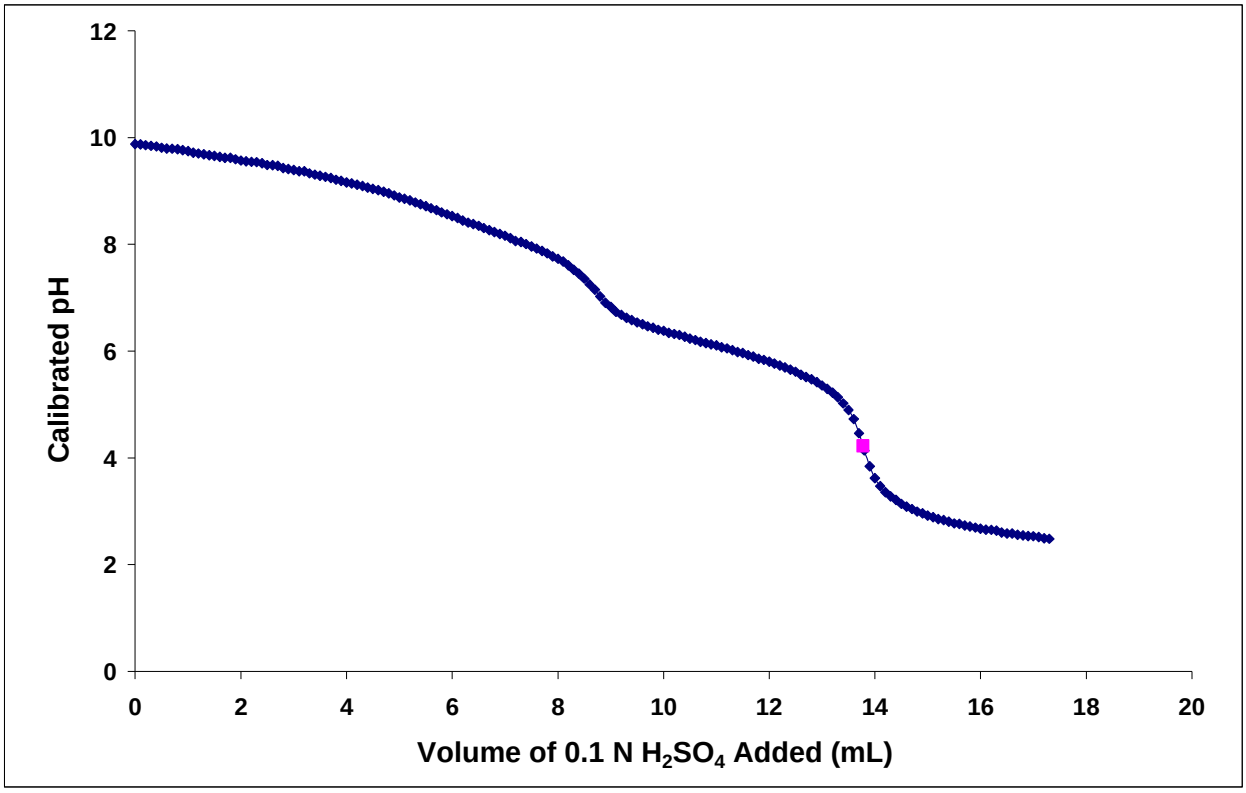

Figure 18: Acid Titration Curve for 7 m MEA/2m PZ Initial Sample

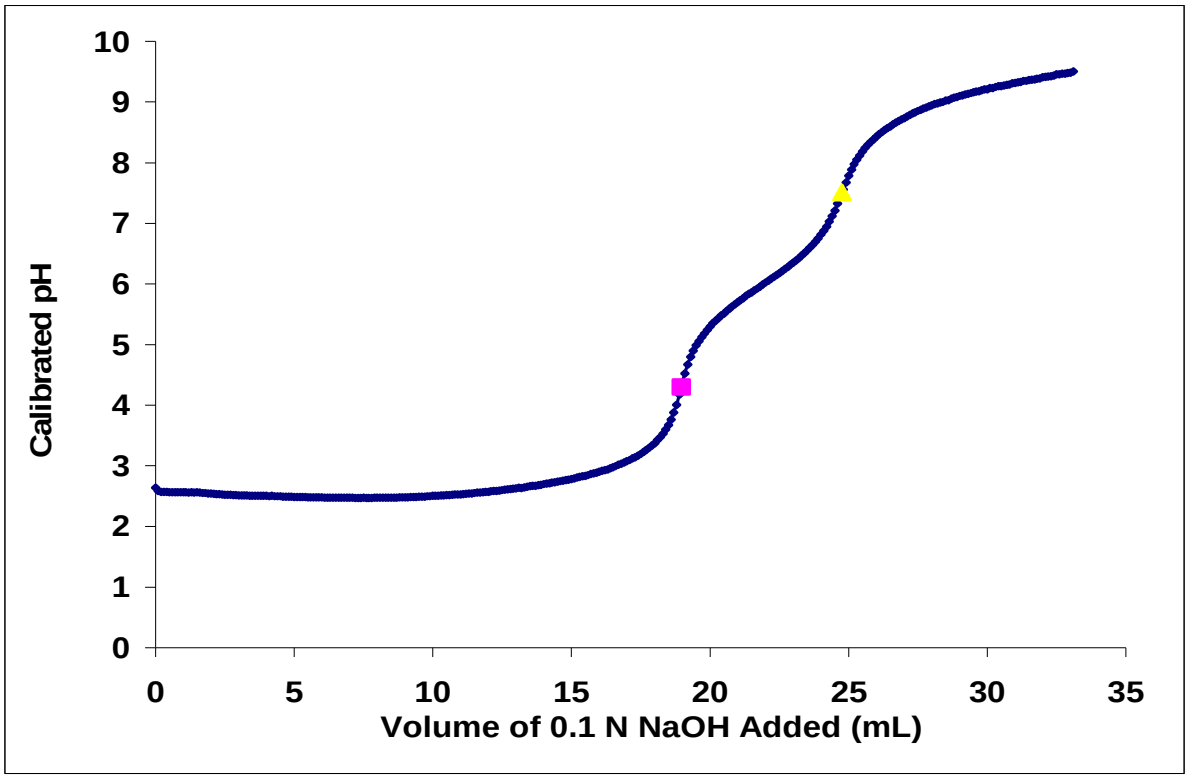

Figure 19: Base Titration Curve for 7 m MEA/2m PZ Initial Sample

Every sample containing MEA was acid titrated for total base concentration; for these samples it was assumed that all the base present in the sample was MEA. Every sample containing a mixture of MEA and PZ was titrated with sulfuric acid, then back titrated with sodium hydroxide to determine MEA and PZ concentrations (in mol/kg solution). In addition to the titration method, all of these samples were diluted and analyzed for amine concentration using the cation IC.

Tables 19, 20, and 21 tabulate the results of the titration and cation IC analysis. Table 19 lists three key pieces of information for all the samples from the high gas flow experiments: the MEA and PZ molalities (if applicable) as determined from titration analysis, MEA and PZ molalities as determined from cation IC analysis, and the calculated absolute error between the two analyses. Table 20 gives the same information for all samples from the low gas flow experiments. Table 21 tabulates the MEA and PZ degraded during experiments where the final and initial samples are available.

Everything highlighted in blue in Table 19 represents an experiment in which inhibitor D was added initially or at some point during the experiment. The analysis method developed by Hilliard did not take the presence of "D" into account. NaOH titration curves show that "D" appears to be neutralized along with the MEA. Therefore, it is impossible to separated "D" concentration from MEA concentration. The numbers in blue represent a combined MEA/"D" concentration. Anything highlighted in red represents cation IC analysis I believe is incorrect. In the middle of the cation IC analysis, piperazine results became very inconsistent. The large amount of consecutive piperazine injections seemed to plug the column. All piperazine concentrations highlighted in red were analyzed when this began to occur.

If all data in red and blue is discarded, the error in MEA concentration between the two analysis methods ranged from 1.6% to 33.0%, while the error in piperazine concentration ranged from 25.8% to 52.9%.

Table 19: Total Amine Concentration of Samples from High Gas Flow Experiments

Experimental Conditions	Titration		IC		Analysis	
High Gas Flow	MEA Concentration (molality)	PZ concentration (molality)	MEA Concentration (molality)	PZ concentration (molality)	% MEA Difference	% PZ Difference
5/3/05, 7m MEA, 4 mM Cu, 200 mM "A", a=0.15	6.00		5.90		1.6	
5/9/05, 7m MEA, 4 mM Cu, 0.2 mM Fe, 200 mM "A", a=0.15	5.85		5.61		4.1	
5/16/05, 7m MEA, 4 mM Cu, 0.2 mM Fe, 200 mM "A"	4.42		5.88		33.0	
5/16/06 (Pre-D), 35% MEA, 5 ppm Fe	6.93		5.87		15.3	
5/16/06 (Post-D), 35% MEA, 2% D	7.01		6.27		10.6	
5/18/06 (Initial), 25% MEA, 8% PZ, 5 ppm Fe	4.44	1.61	4.83	0.13	8.7	
5/18/06 (Final), 25% MEA, 8% PZ, 5 ppm Fe	3.63	1.54	3.53	1.14	2.6	25.8
6/6/06, 7m MEA, 5 ppm Fe	5.17		4.58		11.3	
6/7/06, 7m MEA, 2m PZ, 5 ppm Fe	4.10	1.67	3.72	1.17	9.2	30.1
7/24/06, 35% MEA	8.39		7.49		10.8	
7/26/06, 35% MEA, 5% D	16.21		7.22		55.4	
7/27/06, 35% MEA, 5% PZ, 2% D	6.97	1.17	5.69	0.96	18.4	18.0
8/9/06, 35% MEA, 5% PZ	9.24	1.82	6.42	0.86	30.5	52.9
9/27/06, 7m MEA, 50 ppm Fe	5.90		5.34		9.5	
9/28/06 (Initial), 7m MEA, 5 ppm Fe, 250 ppm Cu	6.22		6.58		5.8	
9/28/06 (Final), 7m MEA, 5 ppm Fe, 250 ppm Cu	5.00		3.88		22.4	
9/29/06, 7m MEA, 2m PZ, 5 ppm Fe, 250 ppm Cu	3.91	1.66	3.54	1.03	9.4	37.9

Anything highlighted in blue from Table 20 (low gas flow experimental results) represents concentrations generated from titration analysis that I believe is incorrect. In the case of the 9/10 MEA/PZ experiment, the initial concentration of the sample is reported as 3.57m MEA, when it should be 7m MEA. It is believable that some degradation has occurred from sample storage, but 50% degradation is too much. The 5/06 MEA/PZ and 1/06 MEA/Cu/Fe/"A" experiments were called into question because the analysis concluded that the final MEA concentration was greater that the initial concentration. Surprisingly, cation IC analysis confirmed this observation. A logical explanation is that a significant amount of water evaporated from these samples during the course of the experiment, thereby increasing the concentration of the amines (while the amount remained the same). All piperazine concentrations highlighted in red are samples that were run in which piperazine analysis became wildly inconsistent. When the statistical anomalies are discarded, the difference in the two methods in calculating MEA concentration varies from 6.1% to 19.5%.

Table 20: Total Amine Concentration of Samples from Low Gas Flow Experiments

Experimental Conditions	Titration		IC		Analysis	
Low Gas Flow	MEA Concentration (molality)	PZ concentration (molality)	MEA Concentration (molality)	PZ concentration (molality)	% MEA Difference	% PZ Difference
12/06 (Initial), 2.5m PZ, 500 ppm V, 100 mM "A"		2.49		0.15		
12/06 (Final), 2.5m PZ, 500 ppm V, 100 mM "A"		1.94		0.08		
11-12/06 (Initial), 2.5m PZ, 5m K, 500 ppm V		2.53		4.87		
11-12/06 (Final), 2.5m PZ, 5m K, 500 ppm V		2.34		0.30		
9-10/06 (Initial), 7m MEA, 2m PZ, 0.1 mM Fe, 4 mM Cu	3.57	2.26	6.56	0.11	83.7	
9-10/06 (Final), 7m MEA, 2m PZ, 0.1 mM Fe, 4 mM Cu	0.69	1.18	3.36	0.10	387.2	
8/06 (Initial), 35% MEA	7.72		7.25		6.1	
8/06 (Final), 35% MEA	5.70		6.46		13.3	
5/06 (Initial), 7m MEA, 2m PZ, 5 ppm Fe	4.07	2.63	5.84	0.04	43.5	
5/06 (Final), 7m MEA, 2m PZ, 5 ppm Fe	6.98	4.55	7.42	0.04	6.3	
3-4/06 (Initial), 2.5m PZ, 5m K, 500 ppm V		2.50				
3-4/06 (Final), 2.5m PZ, 5m K, 500 ppm V		0.63				
3/06 (Initial), 7m MEA, 0.2 mM Fe	6.21		5.94		4.3	
3/06 (Final), 7m MEA, 0.2 mM Fe	5.95		4.79		19.5	
1/06 (Initial), 7m MEA, 0.2 mM Fe, 0.2 mM Cu, 100 mM "A"	5.80		6.77		16.7	
1/06 (Final), 7m MEA, 0.2 mM Fe, 0.2 mM Cu, 100 mM "A"	8.33		8.76		5.1	
10/05 (Initial), 2.5m PZ, 500 ppm V		2.88				
10/05 (Final), 2.5m PZ, 500 ppm V		6.96		0.06		
8/05 (Initial), 7m MEA, 0.2 mM Fe, 0.2 mM Cu	4.60		5.49		19.3	
8/05 (Final), 7m MEA, 0.2 mM Fe, 0.2 mM Cu	1.51		2.63		74.1	
12/04 (Initial), 7m MEA, 0.2 mM Cu	5.18		5.97		15.2	
12/04 (Final), 7m MEA, 0.2 mM Cu	4.61		5.68		23.3	

Table 21: Total Amine Losses From Degradation

Experimental Conditions	Titration		Analysis	
High Gas Flow	**MEA Concentration (molality)**	**PZ concentration (molality)**	**% MEA Degradation**	**% PZ Degradation**
5/18/06 (Initial), 25% MEA, 8% PZ, 5 ppm Fe	4.44	1.61		
5/18/06 (Final), 25% MEA, 8% PZ, 5 ppm Fe	3.63	1.54	18.24	4.35
9/28/06 (Initial), 7m MEA, 5 ppm Fe, 250 ppm Cu	6.22			
9/28/06 (Final), 7m MEA, 5 ppm Fe, 250 ppm Cu	5.00		19.61	
Low Gas Flow	**MEA Concentration (molality)**	**PZ concentration (molality)**	**% MEA Degradation**	**% PZ Degradation**
12/06 (Initial), 2.5m PZ, 500 ppm V, 100 mM "A"		2.49		
12/06 (Final), 2.5m PZ, 500 ppm V, 100 mM "A"		1.94		22.09
11-12/06 (Initial), 2.5m PZ, 5m K, 500 ppm V		2.53		
11-12/06 (Final), 2.5m PZ, 5m K, 500 ppm V		2.34		7.51
8/06 (Initial), 35% MEA	7.72			
8/06 (Final), 35% MEA	5.70		26.17	
3-4/06 (Initial), 2.5m PZ, 5m K, 500 ppm V		2.50		
3-4/06 (Final), 2.5m PZ, 5m K, 500 ppm V		0.63		74.80
3/06 (Initial), 7m MEA, 0.2 mM Fe	6.21			
3/06 (Final), 7m MEA, 0.2 mM Fe	5.95		4.19	
8/05 (Initial), 7m MEA, 0.2 mM Fe, 0.2 mM Cu	4.60			
8/05 (Final), 7m MEA, 0.2 mM Fe, 0.2 mM Cu	1.51		67.17	
12/04 (Initial), 7m MEA, 0.2 mM Cu	5.18			
12/04 (Final), 7m MEA, 0.2 mM Cu	4.61		11.00	

Where the appropriate data was available, a percent MEA and percent PZ loss due to degradation were calculated for two of the high gas flow experiments and six of the low gas flow experiments. Even for the initial samples, it is very clear that some degradation has occurred from the samples aging. Therefore, in the future, it will be imperative to perform this type of quantitative analysis shortly after the samples have been collected. In the high gas flow apparatus, MEA losses were 18 to 19 percent, while piperazine losses were 4.4%. In the low gas flow apparatus, MEA losses ranged from 4 to 67%, while piperazine losses ranged from 7 to 75%.

Figure 20 details pH profiles for several of the low gas flow experiments that have been run since December 2004: 5 MEA experiments, 1 PZ experiment, and 1 MEA/PZ experiment. All of the initial diluted samples have a pH level in the range of 9.0 to 9.5 (undiluted samples would be in the range of 11.0 to 11.5). The pH level of all the end samples range from 8.7 to 9.2 (10.7 to 11.2). These results are logical because the pure amine solutions are highly basic, and become slightly more acidic as degradation products accumulate as the solution degrades.

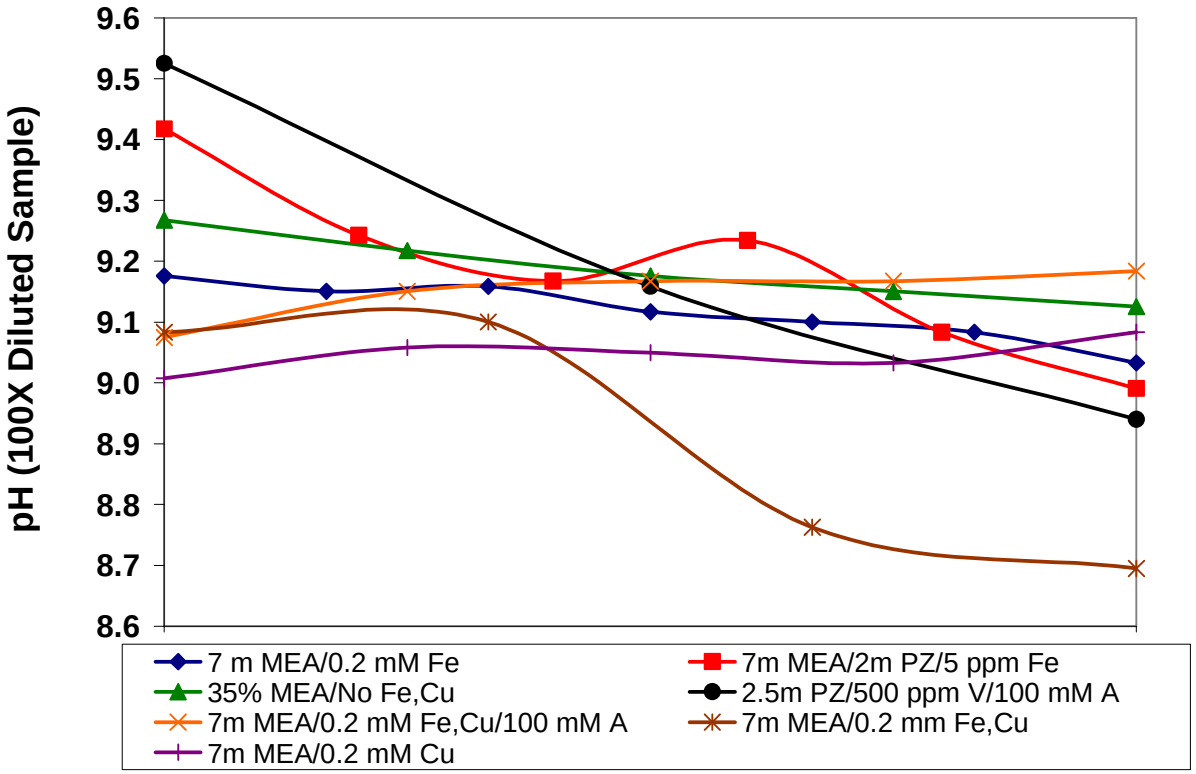

Figure 20: pH Profiles of Low Gas Flow Experiments

Figures 21, 22, and 23 display some preliminary HPLC-MS analysis. Figure 21 is a blank that was run before the amine samples were injected onto the column. It shows peaks of mass to charge ratio (m/z) 242 (retention time of 17 minutes) and an m/z of 353 (retention time of 19 minutes); these peaks are impurities that are contaminating the HPLC system. Figure 22 is an HPLC-MS scan of the control sample – unloaded 7 m MEA with 1mM Fe added. It shows a broad peak of m/z 62 at two minutes (MEA) as well as the two impurities in the system. Figure 23 depicts an HPLC-MS scan of an experimentally degraded sample of 7 m MEA. In addition to the peaks revealed in the control sample, two unknown peaks of molecular weights 303 and 362 are present.

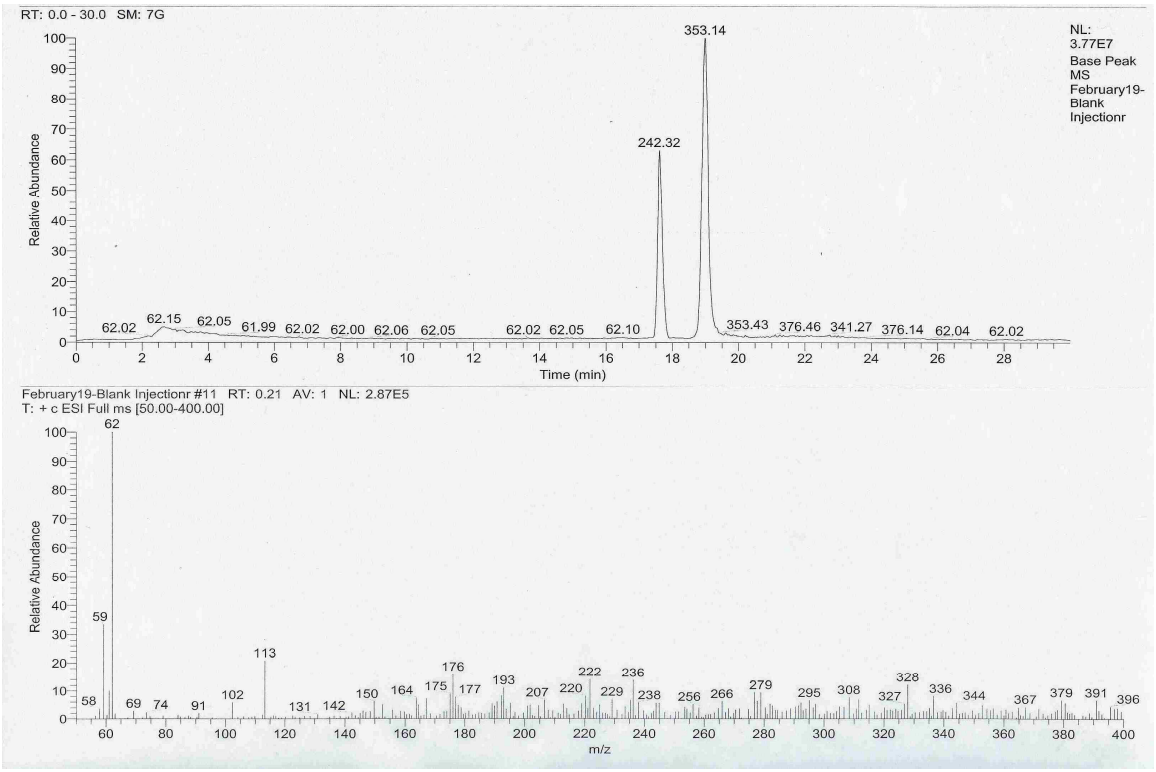

Figure 21: Blank HPLC-MS Sample (Water)

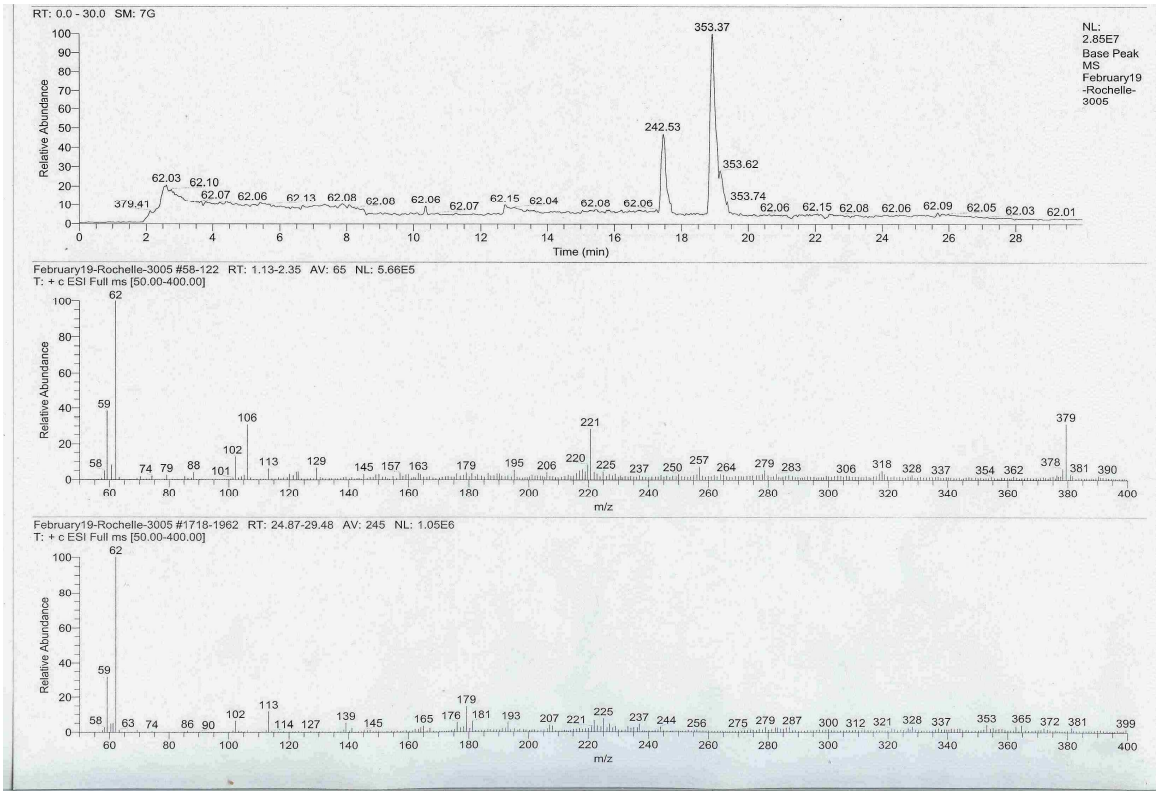

Figure 22: Control HPLC Sample (Unloaded 7 m MEA, 1 mM Fe)

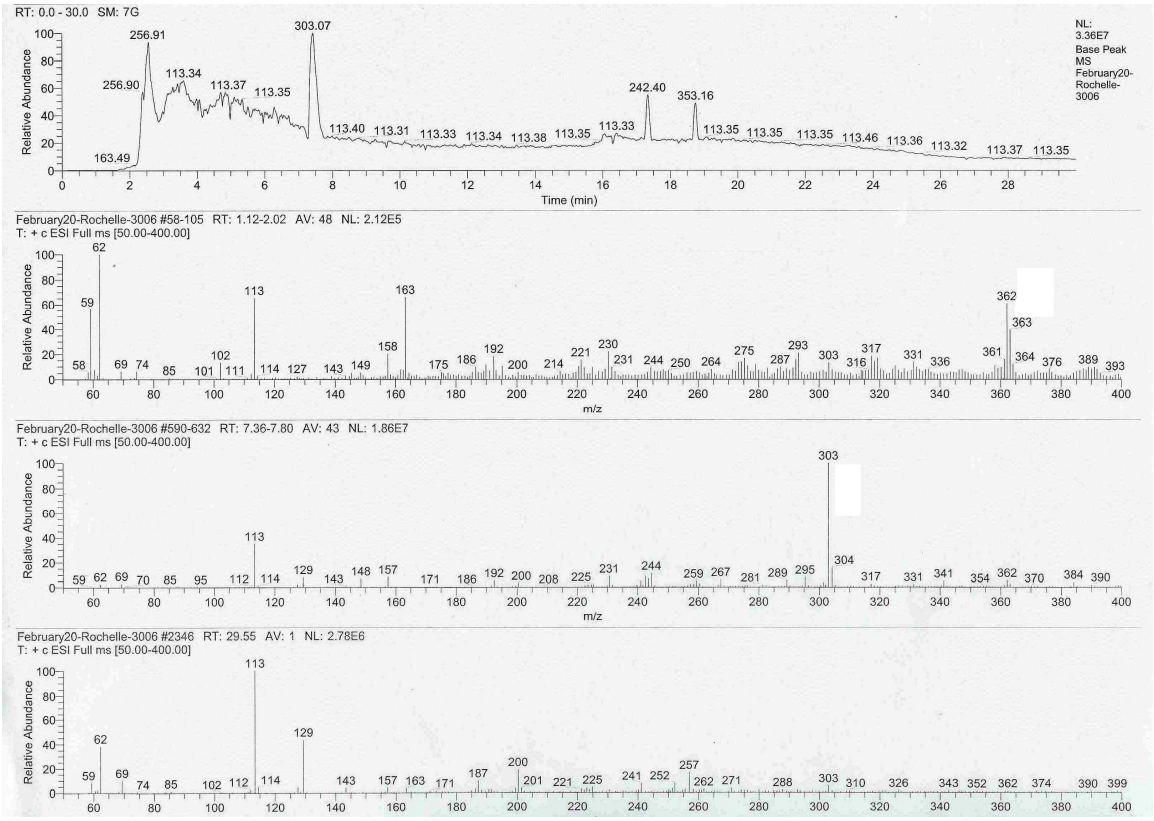

Figure 23: Experimental HPLC Sample (7 m MEA, 250 ppm Cu, α = 0.4)

Conclusions and Future Work

During this past quarter, anion chromatography analysis revealed some significant information regarding piperazine degradation. A second piperazine/potassium carbonate degradation experiment supported the earlier conclusion that the addition of 5 molal potassium carbonate to a 2.5 molal piperazine solution (with 500 ppm vanadium) does an excellent job on inhibiting amine oxidative degradation. Degradation products do exist (showing that degradation of the amine solvent is being detected), but the formation rate of all detected products are less than 0.01 mmol*L/hr. This phenomenon occurs because the high concentration of potassium ion in the solution greatly reduces the oxygen solubility in the amine solution.

The oxygen scavenger, inhibitor "A", also proved to be an excellent oxidative degradation inhibitor for a 2.5m piperazine solution containing 500 ppm V. The addition of 100 mM of inhibitor "A" reduced the formation of detectable ionic degradation products by 50%. While the effectiveness of "A" was not as great as it was for a solution of 7 m MEA with copper and iron added (a 70% reduction in oxidative degradation product formation), it is still significant. However, if ethylenediamine (which is not formed from MEA degradation) is removed from the analysis, then the overall reduction in degradation product formation is approximately 70%. It may be pure coincidence, but it is possible that inhibitor A's mechanism for degradation inhibition has no effect on ethylenediamine production, but reduces the formation of the carboxylic acids and nitrite/nitrate.

Re-evaluation of the 7 m MEA/2m PZ experiment (with 0.1 mM iron and 5 mM copper added) shows that the addition of piperazine to MEA solutions does not have a positive impact on degradation. In fact, it appears that the addition of piperazine to MEA may actually accelerate the degradation product formation rate, which was not expected. A comparison of the 7 m MEA/2m PZ solution to a 7 m MEA solution, both at high copper concentration (5 mM), reveals that with the exception of formate, all degradation product formation rates are similar. If formate followed this trend as well, it would be reasonable to conclude that the MEA was protecting the piperazine from degrading. However, the formate production rate for the 7 m MEA/2 m PZ solution is almost 6X the formate rate for 7 m MEA. From this striking discrepancy, I theorize that MEA/PZ blends degrade just as fast, if not faster, than MEA solutions.

Preliminary work from the H_2O_2 experiments indicates that hydrogen peroxide does indeed oxidize amines to create degradation products similar to those from a low gas flow apparatus. In the presence of 1 mM iron, AMP does degrade, but at a lower rate than MEA and PZ (both of which have similar rates from H_2O_2 degradation). However, the product concentrations observed in the H_2O_2 experiment do not match product concentrations from the gas flow apparatus, in terms of both overall concentration and product mixes. In order to increase the mass transfer of H_2O_2 (and hence dissolved oxygen) into the amine solution, it may be advisable to add the hydrogen peroxide over a longer period of time (1-2 days) at a much slower rate in a lightly stirred reactor (Mellin, 2007).

Total amine concentration analysis yielded inconclusive results. Cation IC analysis for piperazine did not yield positive results because about halfway through the sample batch, piperazine stopped appearing on the IC scans. Cross-contamination during sample preparation may have occurred, or piperazine became bound to the column and stopped eluting properly. I am unsure as to which of the two is to blame.

Titration analysis was not completely flawless either. Hilliard designed the titration analysis methods for undegraded amine MEA, PZ, or MEA/PZ solutions. Samples that contained inhibitor D and potassium ion interfered with the analysis. Furthermore, some titration curves revealed that the amine concentration actually went up as the solution degraded. Unless a large amount of water evaporated during the experiment, this is physically impossible.

On removing all of the data that were suspected to be incorrect, an absolute error between the two analytical methods was calculated. For all of the high gas flow experiments, the difference in MEA concentration ranged from 1.6% to 33.0%, while piperazine absolute error ranged from 18.0% to 52.9%. With respect to the low gas flow experiments, MEA concentrations differed from 5.1% to 19.5%, while PZ error could not be calculated. Where data were believed to be correct, and initial and final samples had been preserved, amine degradation percentages were calculated using the titration analysis numbers. In 5 of the 6 cases, MEA degradation ranged from 4% to 20% of the total MEA; in 3 of the 4 cases for PZ, degradation ranged from 4% to 23%.

Two things need to be stated with regards to this analysis:

- It is not known how the presence of degradation products affects the titration curves.
- Most of the samples were over 6 months old. It is impossible to know how much of the total amine degradation was from the experiment and how much of the degradation was from sample aging.

The two other analytical techniques introduced during this quarter yielded limited results. The pH analysis on the degraded samples revealed that as the oxidative degradation experiment progresses, the pH of the solution decreases by half a unit from beginning to end. This is due to the formation of acidic degradation products in solution. This trend held true for MEA, PZ, and MEA/PZ solutions. HPLC-MS analysis of a degraded 7 m MEA sample showed that two products, one with a molecular weight of 304 and one with a molecular weight of 362, may be present in solution.

I intend to continue work in all of the mentioned analytical areas covered during this report. In the low gas flow apparatus, an AMP oxidative degradation experiment is currently running (3 M AMP, $\alpha = 0.55$, 1 mM Fe). If it is found that AMP does degrade, its oxidative degradation products will be identified, and the effects of other catalysts and inhibitors will be examined.

Several other solvent compositions will be examined in the near future. These include:

- 7 m MEA/2 m PZ in the absence of copper and/or with the addition of inhibitor A
- Higher weight percentage MEA solutions (40%)
- Highly concentrated piperazine solutions (5 molal)
- Higher loadings for 7m MEA solutions ($\alpha = 0.6$)

Furthermore, the high gas flow apparatus will be at my disposal this quarter now that equilibrium studies have been completed using this apparatus. 7 day experiments will be conducted on MEA, PZ, and AMP solutions in an effort to collect simultaneous gas-phase and liquid-phase product analysis.

Titration analysis will be conducted from now on for all degraded amine samples immediately after the samples are withdrawn – to prevent the effects of sample aging. Furthermore, titration analysis will be conducted again on all the samples reported in this report to confirm the findings. HPLC-MS analysis will be suspended at the MSF lab until Jason Davis comes up with a suitable method for thermally degraded amines. Once he develops a robust HPLC method for degraded amines, I will apply it for oxidatively degraded amines.

Subtask 3.3 – Thermal Degradation

by Jason Davis

(Supported by this contract and the TXU Carbon Management Program)

Introduction

This subtask will be used to define future work for the development of a kinetic model for MEA thermal degradation by carbamate polymerization. While the initial products of thermal degradation have been identified, the kinetics of the thermal degradation pathways have not been clearly defined. Currently, MEA concentrations are capped at 30 wt % to minimize thermal degradation and prevent corrosion in industrial applications; however, with a better understanding of degradation kinetics, this number can be optimized. This work will also allow us to better understand solvent losses by thermal degradation.

Theory

Polderman, Dillon and Steele describe the mechanism for thermal degradation by carbamate polymerization. In CO_2 capture, MEA associates with CO_2 in the absorber to form MEA carbamate as illustrated below.

This reaction is normally reversed in the stripper, but in some cases the MEA carbamate will polymerize to form 2-oxazolidone, which is also a reversible reaction, as shown below.

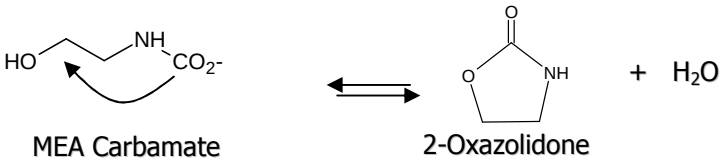

MEA carbamate can also irreversibly dehydrolize to form N,N'-di(2-hydroxyethyl)urea.

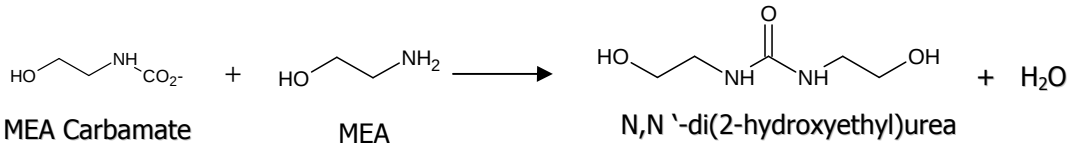

The former product, 2-Oxazolidone, can then react with another molecule of MEA to form 1-(2-hydroxyethyl)-2-imidazolidone which is sometimes referred to as HEIA.

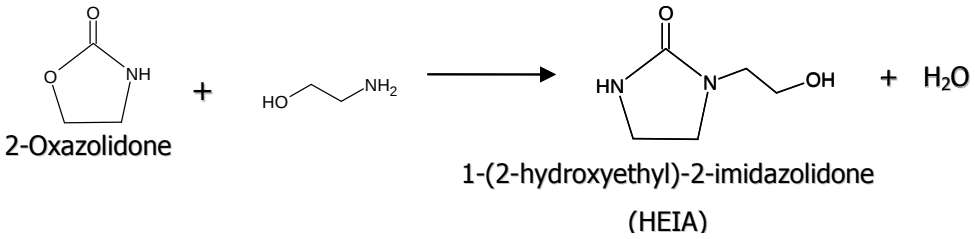

HEIA can then be hydrolyzed to form N-(2-hydroxyethyl)-ethylenediamine or HEEDA.

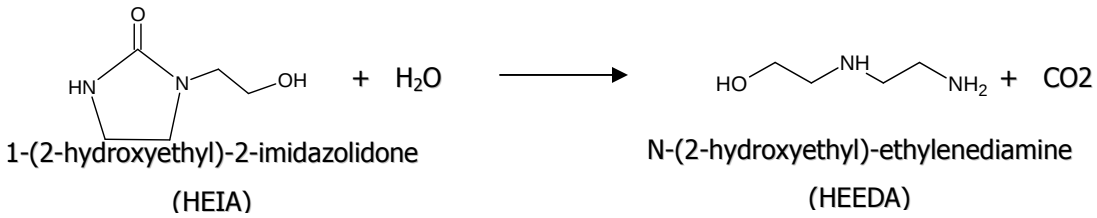

These four species (2-oxazolidone, dihydroxyethylurea, HEIA and HEEDA) are believed to be the main products of thermal degradation. The rate of formation of these products is a function of temperature (faster kinetics), CO_2 loading (more carbamate present) and MEA concentration.

Methods

High Temperature Experiment with Polar Column

A set of 5-2ml sample bombs were constructed using 316L SS tubing and Swagelok fittings. These bombs were filled with an amine solution and placed in a Stabil-Therm constant temperature cabinet made by Blue M for temperature control. The temperature was monitored periodically with a thermometer.

7 m MEA solutions were made using Huntsman MEA and deionized water and were loaded to 0.4 mol CO_2/mol amine. 2mL of this solution were placed in each of the five sample bombs and placed in the Stabil-Therm oven and held at 150^{o}C. Samples were removed over the course of several weeks, diluted, and injected onto the GC for analysis.

Full Range Temperature Experiments with New GC Column

A set of sample bombs were constructed similar to the high temperature experiments. This time a matrix of MEA concentrations and loadings were used. Solutions of 3.5m, 7m, and 11 m MEA were loaded to 0.2, 0.4 and 0.5 moles CO_2 per mole amine and loaded into a Stabil-Therm oven held at 100^{o}C, 120^{o}C and 135^{o}C. Samples were pulled at 1, 2, 4, 6, and 8 weeks and diluted 5:1 by weight with DI water before being injected on the HP-5 GC column.

New sample bombs were created made of ½" tubing and Swagelok end-caps. The new sample bombs contained 10ml of sample instead of the previous 2ml sample bombs. New ovens were ordered to accommodate the scale-up in operation and were used for the 135 ^{o}C data. These new ovens are forced convection Imperial V ovens from Barnstead Labs with closed loop temperature control and digital read-out.

GC Methods

An HP5890 gas chromatograph was acquired and reconditioned complete with a 7673A automatic sampler and equipped with FID and TCD detectors. Based on a paper by Dawodu and Meisen[3] and another paper by Supap et al[4], a polar column was selected for the method development which follows the standard practice of polarity matching of the column to the analyte of interest. Initially, an HP-Innowax column (30m x 0.25mm ID x 25um film thickness) was selected for the high-temperature experiments. The inlet and FID detector were maintained at 250^{o}C and the oven temperature was increased from 80^{o}C to 240^{o}C at a rate of 7^{o}C/min and held at the maximum temperature for 10 minutes. The carrier gas was helium and was used to maintain the pressure in the column at 25psig with a split ratio of 30:1. The split flow was determined by using a bubbler attached to the purge flow and measuring the column flow by injecting a nonretained organic solvent (hexane) and dividing the known column volume by the retention time.

A second column and method was used for all the other experiments. The Agilent HP-5 column (30m x 0.53mm x 1.50um film thickness) was selected and the temperature profile was modified to start at 80^{o}C and increase to 250^{o}C at a rate of 10^{o}C /min. The column pressure was maintained at 20psig and all other parameters were held constant as compared to the previous method.

HPLC Methods

A Thermo Finnigan HPLC-MS system was used to develop a HPLC method for the separation of amines from their degradation products. Two methods are currently being

evaluated. The first is a reverse-phased separation using a Waters T3 C18 column, and the second uses a HILIC separation using a carbohydrate column from Agilent. The results from this work will be discussed in future reports.

Results and Discussion

High Temperature Experiments

The high temperature experiments were only run at one MEA concentration and loading. Figure 24 shows a sample GC chromatogram from the 150°C MEA degradation experiments.

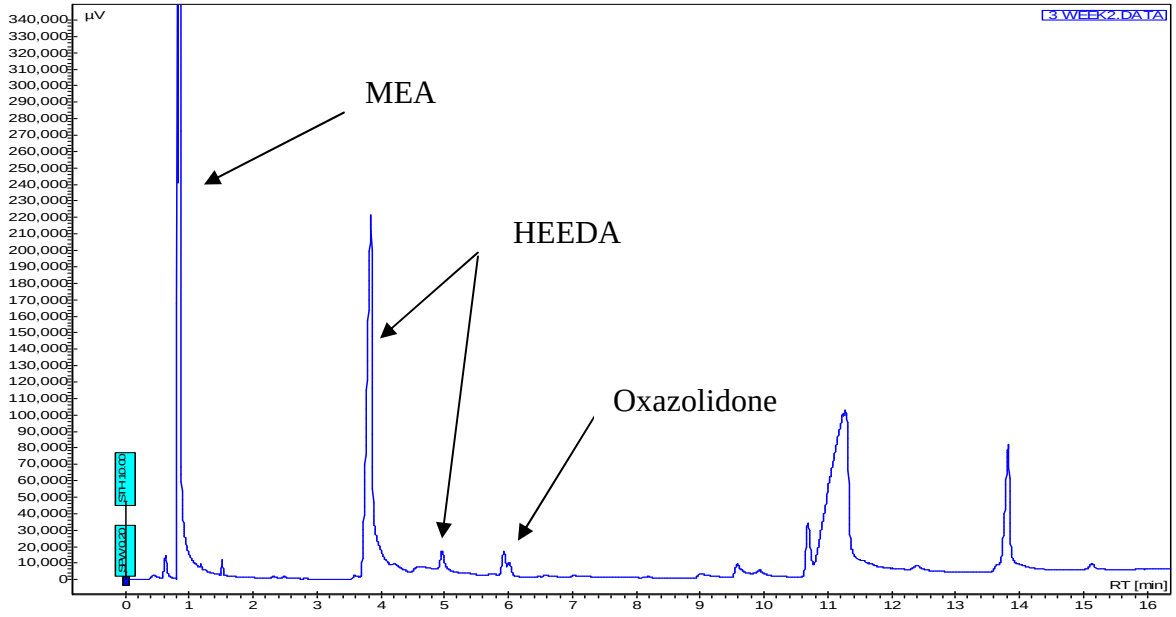

Figure 24: MEA degraded at 150°C for 3 weeks on HP-5 GC column

The MEA, HEEDA and oxazolidone have clear baseline resolution with good separation. Additional unidentified impurity peaks are present at longer retention times. The one problem with this method, is that the MEA elutes at roughly column dead time. This means that any nonretained species will coelute with the MEA making it difficult to say with certainty that the MEA peak is not masking potential impurities.

MEA losses were estimated based on the total MEA peak area counts for the time 0, 2, 3, 5, and 8 week samples. Figure 25 shows the total MEA area counts over time.

As is clear from Figure 25, the loss mechanism is an exponential decay with 75% degradation after just 3 weeks at 150°C. The amount of oxazolidone and HEEDA increased from the week 1 to week 3 samples, but actually decreased in the 5 and 8 week samples. Since the oxazolidone is in equilibrium with the amount of MEA carbamate present, it would decrease as the amount of available MEA decreased. The HEEDA would also decrease since it would further polymerize to higher molecular weight components and would be formed at a slower rate due to the disappearance of oxazolidone.

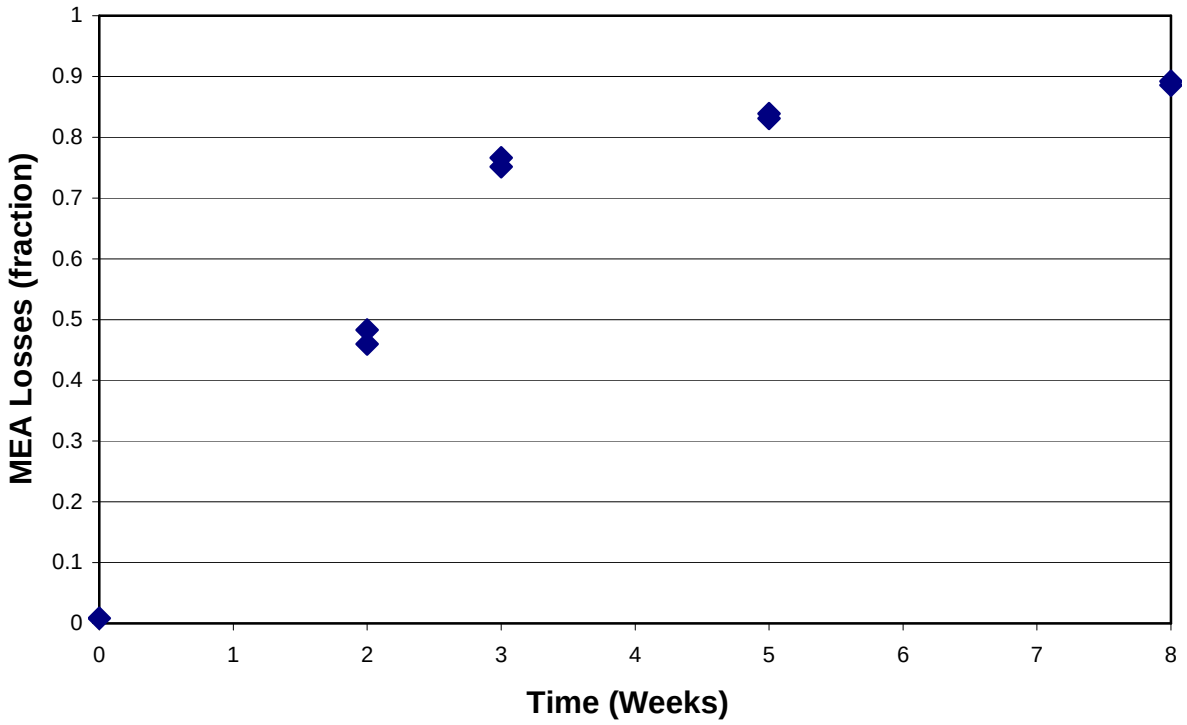

Figure 25: MEA losses at 150°C over an 8 week period

The total chromatogram area counts decreased with time indicating that some high boiling point compounds were not being vaporized properly indicating that some high molecular weight polymerization products were being formed.

Full Temperature Range Experiments

A set of 45 2ml sample bombs were constructed and placed in an oven at various amine concentrations and loadings and placed in an oven at 100°C for varying amounts of time. A set of the bombs were removed at 1, 2, 4, 6, and 8 weeks. Little degradation occurred over the entire time span used. Using the HP-5 column the total degradation fell within the standard error for the experiment.

A set of 90 10ml sample bombs were constructed and placed in an oven at the same amine concentrations and loadings as the 100°C experiments. For this report we have data for weeks 1-4 of the 120°C experiments. Figure 26 shows the amount of MEA remaining over the 8 week time span for the 2 temperature ranges.

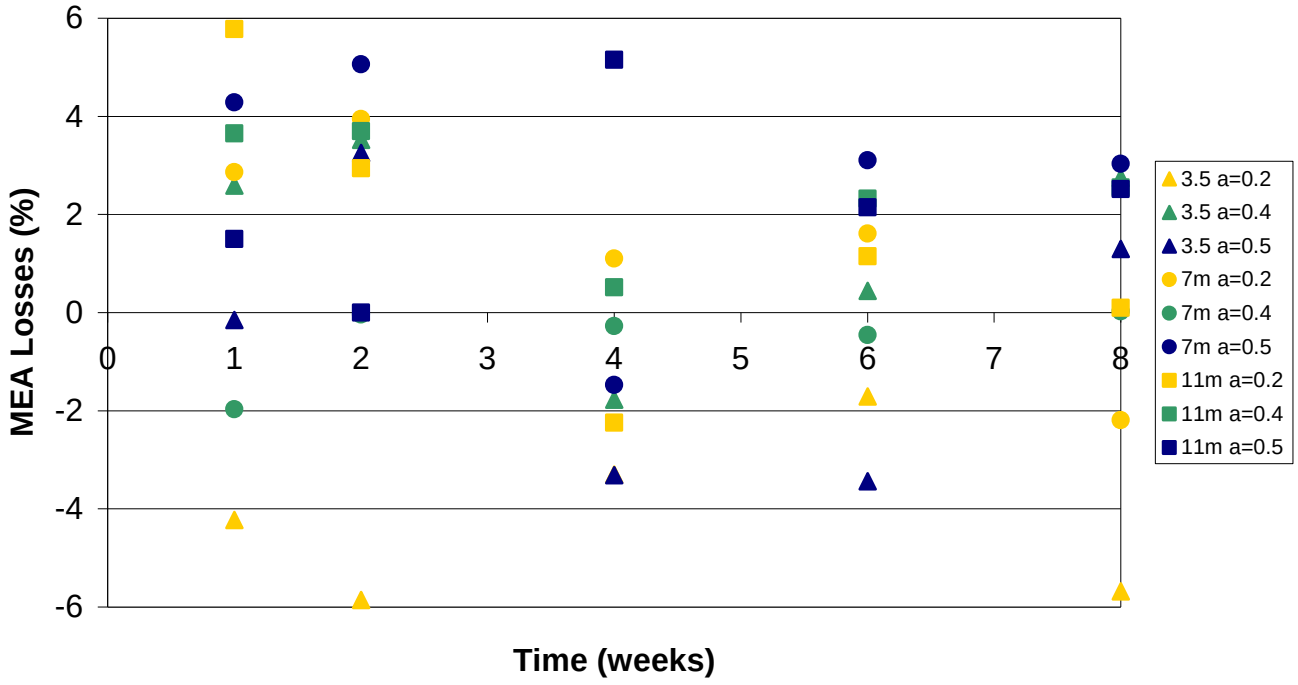

Figure 26: MEA Losses over an 8 week period at 100°C

MEA degraded very little if any at 100°C based on the data shown in Figure 26. The data was all within 6% of the original solution. Averaging the 6 and 8 week samples across all loadings and concentrations, there was a slight direct correlation between loading and MEA loss as well as MEA concentration and MEA loss as shown in Tables 22 and 23 below.

Table 22: MEA losses at 100°C as a function of MEA concentration

MEA Concentration (m)	MEA Losses (%)
3.5	-1.1
7	0.9
11	1.8

Table 23: MEA losses at 100°C as a function of CO_2 loading

CO_2 Loading	MEA Losses (%)
0.2	-1.1
0.4	1.3
0.5	1.4

The data for the 120°C experiments are still underway, but data for weeks 1-4 are currently available. Figure 27 below shows the data for MEA losses over this time span.

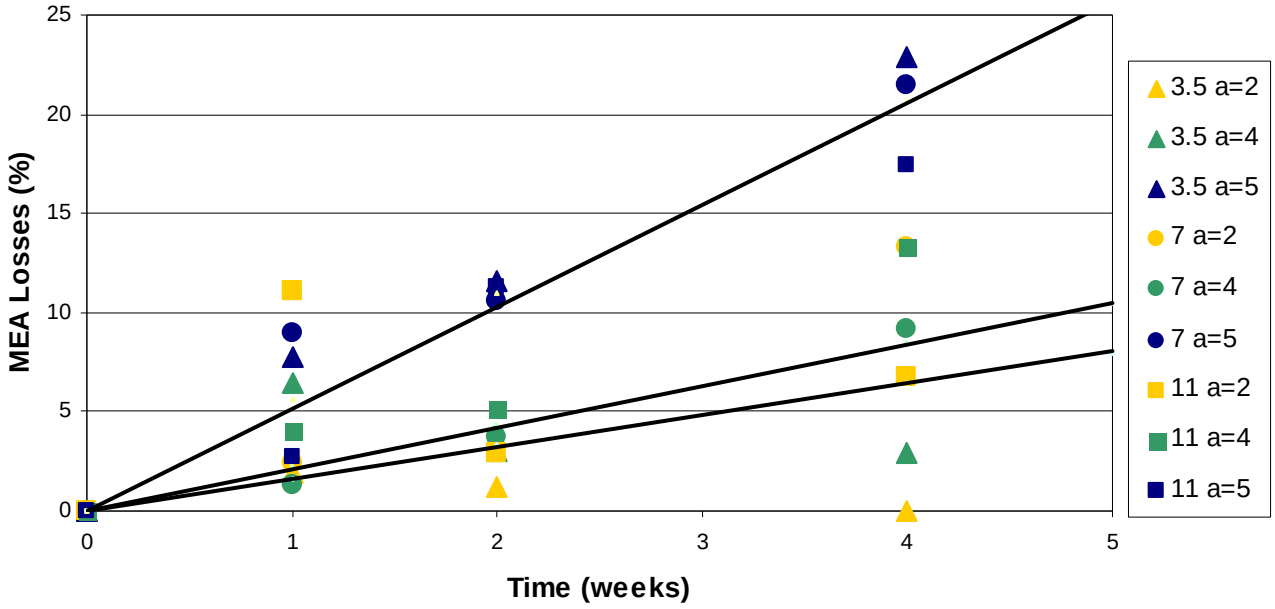

Figure 27: MEA losses at 120°C over a 4 week period

From the 120°C data it can be seen that MEA thermal degradation seems to be a strong function of CO_2 loading. The 4-week data points show groupings based on loading with the highest loadings showing the largest percent losses. This data also seems to suggest that thermal degradation is 1st order with respect to MEA concentration. A proposed rate expression is given below.

$$C = C_o e^{-k_1 t} \qquad (6)$$

Where C is the concentration of MEA at time t, C_o is the initial MEA concentration, and k_1 is the rate constant that would be dependent on temperature and loading. Using this rate equation given above, the data for k_1 is given in Table 24.

Table 24: Values of the rate constant k_1 for thermal MEA losses at 120°C

Loading	k_1 at 120°C (week^{-1})
0.2	1.7×10^{-2}
0.4	2.2×10^{-2}
0.5	5.8×10^{-2}

These values should be further refined once the 6- and 8-week samples are included in the data set, but they show a direct correlation between loading and MEA loss.

Table 25 shows tabulated data for all of the MEA thermal degradation experiments performed to date. From this table can be seen the large increase in thermal degradation that occurs from the 100°C to 120°C experiments and again from the 120°C experiments to the 150°C experiments.

Table 25: MEA Losses (%) over an 8-week time span at varying MEA concentrations, CO2 loadings and temperatures

MEA Molality	CO2 Loading	Temperature (°C)	1 week	2 weeks	4 weeks	6 weeks	8 weeks
3.5	0.2	100	-4.2	-5.9	-3.3	-1.7	-5.7
3.5	0.4	100	2.6	3.5	-1.8	0.4	2.7
3.5	0.5	100	-0.2	3.3	-3.3	-3.4	1.3
7	0.2	100	2.9	3.9	1.1	1.6	-2.2
7	0.4	100	-2.0	0.0	-0.3	-0.5	0.0
7	0.5	100	4.3	5.1	-1.5	3.1	3.0
11	0.2	100	5.8	2.9	-2.2	1.1	0.1
11	0.4	100	3.7	3.7	0.5	2.3	2.5
11	0.5	100	1.5	0.0	5.2	2.1	2.5
3.5	0.2	120	2.0	1.2	0.0	-	-
3.5	0.4	120	6.5	3.0	3.0	-	-
3.5	0.5	120	7.8	11.6	22.8	-	-
7	0.2	120	2.4	-	13.3	-	-
7	0.4	120	1.3	3.7	9.2	-	-
7	0.5	120	8.9	10.6	21.4	-	-
11	0.2	120	11.1	3.0	6.7	-	-
11	0.4	120	4.1	5.2	13.3	-	-
11	0.5	120	2.7	11.3	17.4	-	-
7	0.4	150	-	47.1	75.9*	83.5*	88.9

* The 150°C experiments were collected at weeks 1, 2, 3, 5, and 8.

Future Work

The 120°C data set for MEA will be completed in the next two weeks and a full data set for MEA at 135°C will be completed over the next 8 weeks. A long term 100°C data set will also be pursued in order to get some useful rate data from the current data set. A HPLC method is also being pursued in order to help identify higher boiling point degradation products that will not be seen by the current GC method. This method development is currently underway and should be included in the next report.

Subtask 3.4 – Amine Volatility

by Marcus Hilliard

(Supported by the TXU Carbon Management Program)

Reagents

The chemicals employed, carbon dioxide (CO_2) (Matheson Tri-Gas, ≥ 99.99% pure), nitrogen (N_2) (Cryogenics Laboratory at the University of Texas at Austin, ≥ 99.0% pure), ethanolamine (MEA) (Acros Organics, 99% pure), piperazine (PZ) (Fluka Chemie GmbH, ≥ 98.0% pure), potassium carbonate (K_2CO_3) (Fluka Chemie GmbH, ≥ 99.0% pure), potassium bicarbonate ($KHCO_3$) (Sigma-Aldrich Inc., ≥ 99.5% pure), were used without any further purification. The amine solutions were prepared from deionized water by weight.

Experimental Methods

Tests were conducted in the stirred reactor system documented in a previous report, using N_2 dilution as shown in Figure . The apparatus was designed to operate at atmospheric pressure and temperatures up to 70°C.

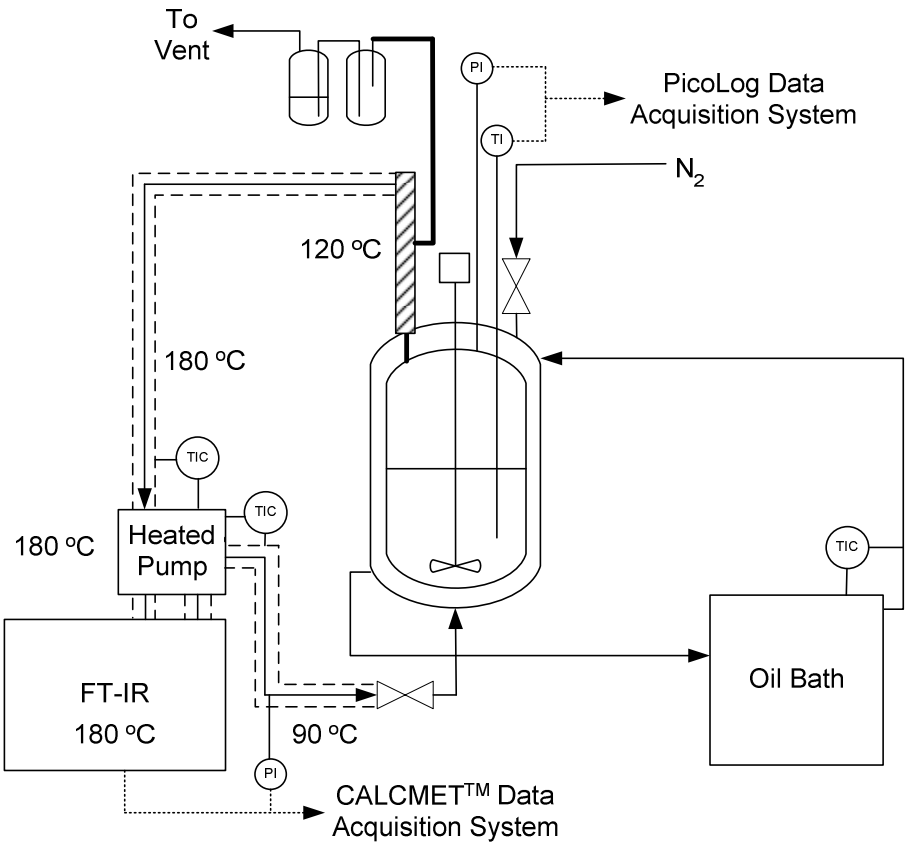

Figure 28: Process Flow Diagram for Vapor Phase Speciation Experiments

Tabulated Results

The following tabulated results serve to document vapor-liquid equilibrium measurements at the University of Texas at Austin.

Binary Systems: Overall Sample Concentrations

Table 26: Batch solutions of ethanolamine-water

Solution	MEA/gm	H_2O/gm	MEA/m	x_{MEA}	x_{H2O}
1	99.3	464.9	3.50	5.930E-02	9.407E-01
2	88.2	412.7	3.50	5.930E-02	9.407E-01
1[a]	531.5	2486.2	3.50	5.931E-02	9.407E-01
3[a]	529.2	2476.7	3.50	5.929E-02	9.407E-01
3	150.3	351.6	7.00	1.120E-01	8.880E-01
4	150.3	351.6	7.00	1.120E-01	8.880E-01
5	150.3	351.6	7.00	1.120E-01	8.880E-01
10[a]	901.8	2109.2	7.00	1.120E-01	8.880E-01
12[a]	904.9	2116.8	7.00	1.120E-01	8.880E-01
2[a]	1212.3	1804.3	11.0	1.654E-01	8.346E-01
3[a]	1212.3	1804.8	11.0	1.654E-01	8.346E-01
2	298.8	205.6	23.8	3.000E-01	7.000E-01

a: Sample part of MEA-CO_2-H_2O data set

Table 27: Batch solutions of piperazine-water

Solution	PZ/gm	H_2O/gm	PZ/m	x_{PZ}	x_{H2O}
1	36.0	464.2	0.90	1.595E-02	9.841E-01
2	36.0	468.5	0.89	1.581E-02	9.842E-01
1[a]	216.0	2785.2	0.90	1.595E-02	9.841E-01
3[a]	216.2	2785.4	0.90	1.596E-02	9.840E-01

a: Sample part of PZ-CO_2-H_2O data set

Table 28: Batch solutions of piperazine-water, continued

Solution	PZ/gm	H_2O/gm	PZ/m	x_{PZ}	x_{H2O}
1	67.4	434.6	1.80	3.139E-02	9.686E-01
2	67.6	435.7	1.80	3.141E-02	9.686E-01
1[a]	443.4	2571.9	2.00	3.478E-02	9.652E-01
4[a]	444.1	2576.0	2.00	3.478E-02	9.652E-01
2	89.2	415.2	2.49	4.297E-02	9.570E-01
3	89.3	414.3	2.50	4.311E-02	9.569E-01
1[a]	535.7	2486.0	2.50	4.309E-02	9.569E-01
3[a]	536.1	2487.9	2.50	4.309E-02	9.569E-01
1	119.8	386.2	3.60	6.088E-02	9.391E-01
2	120.1	387.3	3.60	6.086E-02	9.391E-01
1[a]	719.1	2317.8	3.60	6.089E-02	9.391E-01
3[a]	725.7	2338.6	3.60	6.090E-02	9.391E-01
1	153.3	355.7	5.00	8.263E-02	9.174E-01
1[a]	919.6	2133.7	5.00	8.263E-02	9.174E-01
3[a]	919.6	2133.7	5.00	8.263E-02	9.174E-01

a: Sample part of PZ-CO_2-H_2O data set

Binary Systems: Tabulated Experimental Data

Table 29: Experimental results for solutions of ethanolamine-water

MEA/m	Date	T/°C	Soln	P_{MEA}/kPa	P_{H2O}/kPa	y_{MEA}	y_{H2O}
3.50	03/15/06	45.952	1-1	0.00588	8.69	6.755E-04	9.993E-01
	03/15/06	51.210	1-2	0.00800	11.8	6.763E-04	9.993E-01
	03/15/06	58.875	1-3	0.0135	16.6	8.119E-04	9.992E-01
	03/15/06	65.294	1-4	0.0190	21.0	9.054E-04	9.991E-01
3.50	03/21/06	42.698	2-1	0.00451	6.85	6.580E-04	9.993E-01
	03/21/06	49.400	2-2	0.00729	9.76	7.465E-04	9.993E-01
	03/21/06	56.312	2-3	0.0112	13.6	8.192E-04	9.992E-01
	03/21/06	65.471	2-4	0.0182	19.9	9.158E-04	9.991E-01
3.50	10/31/06	59.950	1[a]	0.0132	17.1	7.705E-04	9.992E-01
3.50	11/06/06	39.969	3[a]	0.00419	6.94	6.042E-04	9.994E-01

a: Sample part of MEA-CO_2-H_2O data set

Table 30: Experimental results for solutions of ethanolamine-water, continued

MEA/m	Date	T/°C	Soln	P_{MEA}/kPa	P_{H2O}/kPa	y_{MEA}	y_{H2O}
7.00	03/10/06	72.656	3-5	0.0790	29.1	2.710E-03	9.973E-01
7.00	03/14/06	64.734	4-5	0.0336	20.6	1.628E-03	9.984E-01
7.00	03/22/06	42.114	5-1	0.0106	6.60	1.605E-03	9.984E-01
	03/22/06	49.250	5-2	0.0156	9.29	1.680E-03	9.983E-01
	03/22/06	52.797	5-3	0.0205	11.0	1.853E-03	9.981E-01
	03/22/06	56.752	5-4	0.0210	13.1	1.605E-03	9.984E-01
	03/22/06	61.433	5-5	0.0283	15.4	1.842E-03	9.982E-01
7.00	09/22/06	39.800	10[a]	0.0100	7.50	1.330E-03	9.987E-01
7.00	10/02/06	59.945	12[a]	0.0271	18.3	1.481E-03	9.985E-01
11.00	10/03/06	60.026	3[a]	0.0402	15.3	2.621E-03	9.974E-01
11.00	10/09/06	39.993	2[a]	0.0120	6.17	1.942E-03	9.981E-01
23.80	03/23/06	42.768	2-1	0.0243	4.86	4.978E-03	9.950E-01
	03/23/06	49.948	2-2	0.0447	6.70	6.633E-03	9.934E-01
	03/23/06	53.872	2-3	0.0611	8.26	7.338E-03	9.927E-01
	03/23/06	61.686	2-4	0.141	12.1	1.146E-02	9.885E-01

a: Sample part of MEA-CO_2-H_2O data set

Table 31: Experimental results for solutions of piperazine-water

PZ/m	Date	T/°C	Soln	P_{PZ}/kPa	P_{H2O}/kPa	y_{PZ}	y_{H2O}
0.90	04/03/06	35.949	1-1	0.00049	6.06	8.079E-05	9.999E-01
	04/03/06	44.290	1-2	0.00129	9.51	1.355E-04	9.999E-01
	04/03/06	52.768	1-3	0.00216	14.0	1.541E-04	9.998E-01
	04/03/06	63.411	1-4	0.00544	22.2	2.448E-04	9.998E-01
0.89	05/01/06	35.467	2-1	0.00056	6.01	9.300E-05	9.999E-01
	05/01/06	44.040	2-2	0.00125	9.37	1.332E-04	9.999E-01
	05/01/06	52.474	2-3	0.00267	13.7	1.943E-04	9.998E-01
	05/01/06	61.592	2-4	0.00517	19.7	2.624E-04	9.997E-01
0.90	11/08/06	40.012	1[a]	0.00104	7.23	1.438E-04	9.999E-01
0.90	11/14/06	59.994	3[a]	0.00375	18.1	2.072E-04	9.998E-01

a: Sample part of PZ-CO_2-H_2O data set

Table 32: Experimental results for solutions of piperazine-water, continued

PZ/m	Date	T/°C	Soln	P_{PZ}/kPa	P_{H2O}/kPa	y_{PZ}	y_{H2O}
1.80	04/05/06	36.180	1-1	0.00150	5.93	2.531E-04	9.997E-01
	04/05/06	44.427	1-2	0.00211	9.08	2.321E-04	9.998E-01
	04/05/06	52.833	1-3	0.00434	13.6	3.196E-04	9.997E-01
	04/05/06	60.405	1-4	0.00759	19.4	3.907E-04	9.996E-01
1.80	05/02/06	35.553	2-1	0.00149	5.87	2.534E-04	9.997E-01
	05/02/06	43.857	2-2	0.00208	9.16	2.267E-04	9.998E-01
	05/02/06	52.210	2-3	0.00458	13.6	3.358E-04	9.997E-01
	05/02/06	60.725	2-4	0.00680	19.4	3.499E-04	9.997E-01
2.00	11/17/06	60.026	1[a]	0.00678	17.6	3.842E-04	9.996E-01
2.00	11/29/06	40.019	4[a]	0.00217	7.06	3.078E-04	9.997E-01
2.49	04/06/06	32.722	2-1	0.00160	6.17	2.600E-04	9.997E-01
	04/06/06	39.704	2-2	0.00299	9.13	3.277E-04	9.997E-01
	04/06/06	52.920	2-3	0.00720	16.6	4.332E-04	9.996E-01
	04/06/06	61.006	2-4	0.0124	23.1	5.349E-04	9.995E-01
2.50	05/03/06	35.610	3-1	0.00140	5.78	2.415E-04	9.998E-01
	05/03/06	44.035	3-2	0.00302	9.03	3.346E-04	9.997E-01
	05/03/06	52.255	3-3	0.00526	13.4	3.920E-04	9.996E-01
	05/03/06	60.393	3-4	0.0101	19.2	5.236E-04	9.995E-01
2.50	12/04/06	40.006	1[a]	0.00267	7.15	3.728E-04	9.996E-01
2.50	12/07/06	59.976	3[a]	0.00763	17.9	4.269E-04	9.996E-01
3.60	04/07/06	34.655	1-1	0.00194	5.70	3.400E-04	9.997E-01
	04/07/06	45.083	1-2	0.00471	9.97	4.725E-04	9.995E-01
	04/07/06	53.218	1-3	0.00885	14.6	6.061E-04	9.994E-01
	04/07/06	61.156	1-4	0.0156	20.8	7.493E-04	9.993E-01
3.60	05/04/06	35.122	2-1	0.00201	5.66	3.544E-04	9.996E-01
	05/04/06	43.804	2-2	0.00422	8.73	4.828E-04	9.995E-01
	05/04/06	52.513	2-3	0.00685	13.1	5.230E-04	9.995E-01
	05/04/06	60.376	2-4	0.0114	18.6	6.101E-04	9.994E-01
3.60	12/13/06	39.995	3[a]	0.00374	6.99	5.351E-04	9.995E-01
3.60	12/11/06	60.001	1[a]	0.0116	17.7	6.533E-04	9.993E-01
5.00	05/05/06	40.558	1-1	0.00430	6.70	6.420E-04	9.994E-01
	05/05/06	44.713	1-2	0.00540	8.45	6.384E-04	9.994E-01
	05/05/06	53.317	1-3	0.0108	12.8	8.487E-04	9.992E-01
	05/05/06	60.970	1-4	0.0238	18.3	1.296E-03	9.987E-01
5.00	02/06/07	40.013	1[a]	0.00512	6.77	7.555E-04	9.992E-01
5.00	02/08/07	60.006	3[a]	0.0172	17.1	1.003E-03	9.990E-01

a: Sample part of PZ-CO_2-H_2O data set

Ternary Systems: Overall Sample Concentrations

Table 33: Batch solutions of ethanolamine-carbon dioxide-water

Solution(s)	MEA/gm	H_2O/gm	MEA/m	x_{MEA}	x_{H2O}
1-2	531.5	2486.2	3.50	5.931E-02	9.407E-01
3-4	529.2	2476.7	3.50	5.929E-02	9.407E-01
6	901.8	2109.2	7.00	1.120E-01	8.880E-01
7	901.8	2109.2	7.00	1.120E-01	8.880E-01
8	901.8	2109.2	7.00	1.120E-01	8.880E-01
9	901.8	2109.2	7.00	1.120E-01	8.880E-01
10-11	901.8	2109.2	7.00	1.120E-01	8.880E-01
12-13	904.9	2116.8	7.00	1.120E-01	8.880E-01
1-2	1212.3	1804.3	11.0	1.654E-01	8.346E-01
3-4	1212.3	1804.8	11.0	1.654E-01	8.346E-01

Table 34: Batch solutions of piperazine-carbon dioxide-water

Solution(s)	MEA/gm	H_2O/gm	MEA/m	x_{MEA}	x_{H2O}
1-2	531.5	2486.2	3.50	5.931E-02	9.407E-01
3-4	529.2	2476.7	3.50	5.929E-02	9.407E-01
6	901.8	2109.2	7.00	1.120E-01	8.880E-01
7	901.8	2109.2	7.00	1.120E-01	8.880E-01
8	901.8	2109.2	7.00	1.120E-01	8.880E-01
9	901.8	2109.2	7.00	1.120E-01	8.880E-01
10-11	901.8	2109.2	7.00	1.120E-01	8.880E-01
12-13	904.9	2116.8	7.00	1.120E-01	8.880E-01
1-2	1212.3	1804.3	11.0	1.654E-01	8.346E-01
3-4	1212.3	1804.8	11.0	1.654E-01	8.346E-01

Table 35: Experimental results for solutions of ethanolamine-carbon dioxide-water

MEA/m	Date	T/°C	Soln	α^a	P_{CO2}/kPa	P_{MEA}/kPa	P_{H2O}/kPa	x_{CO2}	x_{MEA}	x_{H2O}	y_{CO2}	y_{MEA}	y_{H2O}
3.57	11/01/06	59.948	2-1	0.159	0.0212	0.0110	17.57	9.520E-03	5.985E-02	9.306E-01	1.206E-03	6.231E-04	9.982E-01
3.63	11/01/06	60.057	2-2	0.219	0.0780	0.00926	17.63	1.326E-02	6.060E-02	9.261E-01	4.401E-03	5.226E-04	9.951E-01
3.53	11/01/06	60.039	2-3	0.307	0.244	0.00720	17.64	1.803E-02	5.874E-02	9.232E-01	1.363E-02	4.025E-04	9.860E-01
3.57	11/01/06	60.018	2-4	0.380	0.794	0.00508	17.62	2.246E-02	5.907E-02	9.185E-01	4.313E-02	2.758E-04	9.566E-01
3.55	11/02/06	59.944	2-5	0.477	4.32	0.00323	17.70	2.783E-02	5.839E-02	9.138E-01	1.961E-01	1.468E-04	8.037E-01
3.54	11/02/06	60.005	2-6	0.504	14.8	0.00219	18.01	2.934E-02	5.824E-02	9.124E-01	4.514E-01	6.664E-05	5.486E-01
3.53	11/06/06	39.979	4-1	0.121	0.00555	0.00391	6.880	7.167E-03	5.943E-02	9.334E-01	8.061E-04	5.679E-04	9.986E-01
3.46	11/06/06	40.023	4-2	0.212	0.0140	0.00341	6.971	1.226E-02	5.791E-02	9.298E-01	2.005E-03	4.880E-04	9.975E-01
3.51	11/07/06	39.938	4-3	0.300	0.0362	0.00281	6.980	1.749E-02	5.836E-02	9.242E-01	5.165E-03	4.001E-04	9.944E-01
3.54	11/07/06	40.079	4-4	0.369	0.116	0.00224	7.024	2.167E-02	5.871E-02	9.196E-01	1.624E-02	3.139E-04	9.834E-01
3.57	11/07/06	40.003	4-5	0.467	0.879	0.00168	7.058	2.746E-02	5.881E-02	9.137E-01	1.107E-01	2.119E-04	8.891E-01
3.49	11/08/06	39.969	4-6	0.552	8.56	0.00098	7.128	3.160E-02	5.725E-02	9.111E-01	5.455E-01	6.270E-05	4.545E-01
6.88	09/05/06	39.987	6-1	0.153	0.00570	0.00658	6.60	1.657E-02	1.085E-01	8.749E-01	8.622E-04	9.948E-04	9.981E-01
6.98	09/05/06	39.985	6-2	0.170	0.00721	0.00636	6.65	1.867E-02	1.096E-01	8.717E-01	1.082E-03	9.543E-04	9.980E-01
6.95	09/05/06	40.058	6-3	0.163	0.00664	0.00636	6.69	1.778E-02	1.093E-01	8.729E-01	9.907E-04	9.485E-04	9.981E-01
6.85	09/07/06	40.034	6-4	0.194	0.00985	0.00645	6.71	2.090E-02	1.075E-01	8.716E-01	1.464E-03	9.593E-04	9.976E-01
6.97	09/07/06	40.144	6-5	0.191	0.00995	0.00623	6.61	2.081E-02	1.092E-01	8.700E-01	1.500E-03	9.405E-04	9.976E-01
6.93	09/07/06	40.353	6-6	0.272	0.0224	0.00511	6.65	2.925E-02	1.077E-01	8.630E-01	3.350E-03	7.654E-04	9.959E-01
7.06	09/11/06	40.034	7-1	0.232	0.0146	0.00563	6.63	2.548E-02	1.100E-01	8.645E-01	2.191E-03	8.461E-04	9.970E-01
7.08	09/11/06	40.120	7-2	0.246	0.0191	0.00553	6.65	2.703E-02	1.100E-01	8.630E-01	2.864E-03	8.283E-04	9.963E-01
7.10	09/11/06	39.968	7-3	0.269	0.0231	0.00516	6.63	2.962E-02	1.100E-01	8.604E-01	3.471E-03	7.757E-04	9.958E-01
7.12	09/12/06	39.870	7-4	0.360	0.0966	0.00355	6.75	3.936E-02	1.092E-01	8.514E-01	1.409E-02	5.186E-04	9.854E-01
7.05	09/12/06	39.990	7-5	0.350	0.0721	0.00423	6.75	3.794E-02	1.084E-01	8.537E-01	1.057E-02	6.193E-04	9.888E-01
7.06	09/12/06	39.880	7-6	0.386	0.120	0.00362	6.66	4.170E-02	1.081E-01	8.502E-01	1.775E-02	5.340E-04	9.817E-01
7.05	09/18/06	39.850	8-1	0.389	0.113	0.00338	6.59	4.205E-02	1.080E-01	8.500E-01	1.692E-02	5.039E-04	9.826E-01
7.05	09/18/06	40.000	8-2	0.400	0.128	0.00350	6.71	4.316E-02	1.078E-01	8.490E-01	1.867E-02	5.123E-04	9.808E-01
7.58	09/19/06	40.050	8-3	0.382	0.131	0.00332	6.72	4.388E-02	1.149E-01	8.412E-01	1.907E-02	4.846E-04	9.804E-01
7.00	09/19/06	39.930	8-4	0.466	0.574	0.00270	6.75	4.957E-02	1.065E-01	8.440E-01	7.835E-02	3.691E-04	9.213E-01
7.11	09/19/06	40.000	8-5	0.591	28.3	0.00146	6.72	6.286E-02	1.064E-01	8.308E-01	8.081E-01	4.164E-05	1.919E-01
7.06	09/19/06	39.990	8-6	0.481	0.883	0.00247	6.73	5.149E-02	1.071E-01	8.414E-01	1.160E-01	3.251E-04	8.837E-01
7.17	09/22/06	40.019	9-1	0.464	0.750	0.00266	6.67	5.038E-02	1.086E-01	8.410E-01	1.010E-01	3.578E-04	8.986E-01
7.06	09/22/06	40.018	9-2	0.501	1.87	0.00199	6.80	5.355E-02	1.068E-01	8.396E-01	2.155E-01	2.296E-04	7.843E-01
7.11	09/25/06	39.878	9-3	0.491	1.10	0.00193	6.68	5.284E-02	1.076E-01	8.396E-01	1.413E-01	2.475E-04	8.584E-01
7.06	09/25/06	39.997	9-4	0.518	3.03	0.00172	6.80	5.515E-02	1.066E-01	8.383E-01	3.083E-01	1.751E-04	6.915E-01
7.06	09/25/06	39.866	9-5	0.326	0.0485	0.00458	6.60	3.544E-02	1.088E-01	8.557E-01	7.290E-03	6.879E-04	9.920E-01
7.04	09/26/06	39.879	9-6	0.348	0.0662	0.00423	6.60	3.774E-02	1.083E-01	8.540E-01	9.921E-03	6.332E-04	9.894E-01
7.00	10/03/06	59.868	11-1	0.114	0.0194	0.0215	16.6	1.259E-02	1.106E-01	8.768E-01	1.168E-03	1.297E-03	9.975E-01
7.08	10/03/06	59.964	11-2	0.191	0.0589	0.0186	16.7	2.118E-02	1.107E-01	8.681E-01	3.510E-03	1.108E-03	9.954E-01
7.07	10/03/06	59.960	11-3	0.291	0.209	0.0141	16.6	3.182E-02	1.094E-01	8.587E-01	1.238E-02	8.377E-04	9.868E-01
7.03	10/04/06	59.884	11-4	0.386	0.763	0.0100	16.7	4.161E-02	1.077E-01	8.507E-01	4.360E-02	5.728E-04	9.558E-01
7.14	10/04/06	59.771	11-5	0.485	4.86	0.00494	16.8	5.234E-02	1.080E-01	8.397E-01	2.246E-01	2.284E-04	7.751E-01
7.17	10/04/06	60.106	11-6	0.544	25.8	0.00316	16.8	5.760E-02	1.078E-01	8.346E-01	6.054E-01	7.420E-05	3.946E-01
7.38	10/31/06	59.945	13	0.565	50.2	0.00288	18.0	5.931E-02	1.104E-01	8.303E-01	7.356E-01	4.227E-05	2.643E-01
11.00	10/09/06	39.989	1-1	0.115	0.00505	0.0104	6.09	1.871E-02	1.622E-01	8.190E-01	8.283E-04	1.712E-03	9.975E-01
10.75	10/11/06	40.021	1-2	0.201	0.0108	0.00842	6.12	3.162E-02	1.571E-01	8.113E-01	1.765E-03	1.373E-03	9.969E-01
10.90	10/12/06	39.938	1-3	0.298	0.0295	0.00603	6.14	4.665E-02	1.565E-01	7.968E-01	4.770E-03	9.760E-04	9.943E-01
11.28	10/12/06	40.108	1-4	0.373	0.104	0.00439	6.18	5.932E-02	1.589E-01	7.818E-01	1.655E-02	6.983E-04	9.828E-01
11.06	10/13/06	39.996	1-5	0.485	1.62	0.00198	6.29	7.461E-02	1.538E-01	7.716E-01	2.048E-01	2.499E-04	7.950E-01
11.12	10/13/06	39.967	1-6	0.545	22.3	0.00095	6.59	8.336E-02	1.530E-01	7.636E-01	7.715E-01	3.302E-05	2.284E-01
11.21	10/03/06	59.996	4-1	0.136	0.0155	0.03609	15.4	2.239E-02	1.643E-01	8.133E-01	1.003E-03	2.333E-03	9.967E-01
11.17	10/03/06	60.043	4-2	0.225	0.0731	0.02838	15.5	3.634E-02	1.614E-01	8.023E-01	4.678E-03	1.816E-03	9.935E-01
11.12	10/04/06	59.986	4-3	0.291	0.199	0.02252	15.5	4.627E-02	1.591E-01	7.946E-01	1.268E-02	1.436E-03	9.859E-01
11.36	10/04/06	60.041	4-4	0.415	0.847	0.0143	15.5	6.592E-02	1.587E-01	7.754E-01	5.188E-02	8.750E-04	9.472E-01
11.32	10/04/06	59.931	4-5	0.464	6.98	0.00655	15.8	7.282E-02	1.570E-01	7.702E-01	3.063E-01	2.874E-04	6.934E-01
10.98	10/02/06	60.003	4-6	0.502	26.5	0.00416	16.3	7.651E-02	1.525E-01	7.709E-01	6.190E-01	9.716E-05	3.809E-01

a: α = loading = mole CO_2/mol MEA

Table 36: Experimental results for solutions of piperazine carbon-dioxide water

PZ/m	Date	T/°C	Soln	α[a]	P_{CO2}/kPa	P_{PZ}/kPa	P_{H2O}/kPa	x_{CO2}	x_{PZ}	x_{H2O}	y_{CO2}	y_{PZ}	y_{H2O}
0.89	11/09/06	39.977	2-1	0.208	0.0440	0.00083	7.29	6.547E-03	1.572E-02	9.777E-01	5.992E-03	1.129E-04	9.939E-01
0.91	11/09/06	40.089	2-2	0.217	0.0705	0.00089	7.33	6.963E-03	1.602E-02	9.770E-01	9.535E-03	1.199E-04	9.903E-01
0.93	11/09/06	39.987	2-3	0.241	0.103	0.00085	7.37	7.868E-03	1.632E-02	9.758E-01	1.373E-02	1.137E-04	9.862E-01
0.91	11/13/06	40.000	2-4	0.284	0.234	0.00072	7.22	9.044E-03	1.595E-02	9.750E-01	3.134E-02	9.659E-05	9.686E-01
0.91	11/13/06	40.012	2-5	0.344	0.987	0.00066	7.39	1.095E-02	1.594E-02	9.731E-01	1.178E-01	7.913E-05	8.821E-01
0.90	11/13/06	40.024	2-6	0.418	4.85	0.00053	7.46	1.314E-02	1.570E-02	9.712E-01	3.938E-01	4.320E-05	6.062E-01
0.91	11/14/06	60.051	4-1	0.111	0.0290	0.00325	18.5	3.574E-03	1.611E-02	9.803E-01	1.564E-03	1.753E-04	9.983E-01
0.91	11/14/06	60.001	4-2	0.217	0.299	0.00197	18.6	6.933E-03	1.599E-02	9.771E-01	1.582E-02	1.043E-04	9.841E-01
0.91	11/14/06	60.016	4-3	0.242	0.841	0.00157	18.6	7.714E-03	1.594E-02	9.763E-01	4.325E-02	8.058E-05	9.567E-01
0.89	11/15/06	60.003	4-4	0.325	1.93	0.00108	18.3	1.020E-02	1.566E-02	9.741E-01	9.544E-02	5.326E-05	9.045E-01
0.89	11/15/06	60.032	4-5	0.370	8.29	0.00085	18.5	1.157E-02	1.565E-02	9.728E-01	3.089E-01	3.168E-05	6.910E-01
0.91	11/16/06	59.948	4-6	0.383	14.7	0.00080	18.6	1.225E-02	1.597E-02	9.718E-01	4.415E-01	2.402E-05	5.584E-01
2.03	11/17/06	60.058	2-1	0.132	0.0924	0.00555	18.0	9.237E-03	3.501E-02	9.558E-01	5.115E-03	3.069E-04	9.946E-01
2.02	11/17/06	60.039	2-2	0.193	0.296	0.00480	18.1	1.340E-02	3.464E-02	9.520E-01	1.608E-02	2.610E-04	9.837E-01
2.03	11/18/06	59.999	2-3	0.275	1.40	0.00293	17.9	1.905E-02	3.467E-02	9.463E-01	7.238E-02	1.515E-04	9.275E-01
2.02	11/18/06	59.998	2-4	0.330	3.95	0.00224	18.1	2.263E-02	3.430E-02	9.431E-01	1.795E-01	1.018E-04	8.204E-01
2.02	11/18/06	60.037	2-5	0.370	9.91	0.00177	18.2	2.533E-02	3.419E-02	9.405E-01	3.525E-01	6.278E-05	6.474E-01
2.00	11/19/06	59.951	2-6	0.412	24.7	0.00128	18.5	2.787E-02	3.385E-02	9.383E-01	5.723E-01	2.966E-05	4.276E-01
1.90	11/28/06	59.945	3-1	0.169	0.142	0.00513	17.9	1.110E-02	3.278E-02	9.561E-01	7.873E-03	2.849E-04	9.918E-01
2.07	11/28/06	59.965	3-2	0.383	13.7	0.00187	18.3	2.682E-02	3.505E-02	9.381E-01	4.280E-01	5.851E-05	5.720E-01
2.03	11/29/06	40.050	5-1	0.146	0.0215	0.00212	7.13	1.017E-02	3.485E-02	9.550E-01	3.006E-03	2.960E-04	9.967E-01
2.08	11/29/06	40.013	5-2	0.227	0.106	0.00180	7.21	1.617E-02	3.556E-02	9.483E-01	1.452E-02	2.468E-04	9.852E-01
2.02	11/29/06	40.072	5-3	0.257	0.184	0.00168	7.20	1.775E-02	3.448E-02	9.478E-01	2.493E-02	2.281E-04	9.748E-01
2.05	11/30/06	40.007	5-4	0.309	0.526	0.00149	7.07	2.156E-02	3.487E-02	9.436E-01	6.926E-02	1.960E-04	9.305E-01
2.03	11/30/06	40.090	5-5	0.372	1.95	0.00138	7.18	2.560E-02	3.443E-02	9.400E-01	2.139E-01	1.517E-04	7.860E-01
1.99	11/30/06	40.058	5-6	0.431	10.1	0.00109	7.51	2.896E-02	3.362E-02	9.374E-01	5.735E-01	6.176E-05	4.264E-01
2.57	12/04/06	40.007	2-1	0.166	0.0317	0.00229	7.16	1.450E-02	4.362E-02	9.419E-01	4.412E-03	3.187E-04	9.953E-01
2.50	12/05/06	39.969	2-2	0.228	0.0884	0.00208	7.13	1.924E-02	4.226E-02	9.385E-01	1.224E-02	2.876E-04	9.875E-01
2.49	12/05/06	39.975	2-3	0.278	0.247	0.00184	7.23	2.334E-02	4.196E-02	9.347E-01	3.305E-02	2.461E-04	9.667E-01
2.50	12/06/06	39.966	2-4	0.328	0.662	0.00152	7.27	2.749E-02	4.191E-02	9.306E-01	8.345E-02	1.912E-04	9.164E-01
2.49	12/06/06	40.014	2-5	0.423	7.51	0.00125	7.53	3.502E-02	4.142E-02	9.236E-01	4.993E-01	8.306E-05	5.006E-01
2.48	12/06/06	40.011	2-6	0.437	10.6	0.00115	7.57	3.599E-02	4.122E-02	9.228E-01	5.826E-01	6.368E-05	4.173E-01
2.51	12/07/06	59.974	4-1	0.164	0.141	0.00618	18.1	1.400E-02	4.259E-02	9.434E-01	7.770E-03	3.392E-04	9.919E-01
2.50	12/07/06	60.029	4-2	0.196	0.263	0.00527	18.0	1.662E-02	4.243E-02	9.409E-01	1.437E-02	2.880E-04	9.853E-01
2.53	12/08/06	59.980	4-3	0.251	0.725	0.00456	18.0	2.134E-02	4.260E-02	9.361E-01	3.874E-02	2.436E-04	9.610E-01
2.52	12/08/06	60.018	4-4	0.341	3.96	0.00311	18.2	2.878E-02	4.215E-02	9.291E-01	1.790E-01	1.407E-04	8.208E-01
2.53	12/08/06	60.028	4-5	0.400	16.9	0.00245	18.5	3.372E-02	4.213E-02	9.242E-01	4.781E-01	6.922E-05	5.218E-01
2.45	12/08/06	60.021	4-6	0.443	27.4	0.00224	18.6	3.612E-02	4.075E-02	9.231E-01	5.952E-01	4.868E-05	4.047E-01
3.63	12/11/06	59.991	2-1	0.158	0.129	0.00747	17.7	1.906E-02	6.015E-02	9.208E-01	7.255E-03	4.186E-04	9.923E-01
3.58	12/11/06	60.016	2-2	0.217	0.431	0.00642	17.7	2.562E-02	5.903E-02	9.154E-01	2.375E-02	3.539E-04	9.759E-01
3.58	12/11/06	60.013	2-3	0.277	1.05	0.00493	17.8	3.245E-02	5.857E-02	9.090E-01	5.581E-02	2.618E-04	9.439E-01
3.60	12/12/06	60.009	2-4	0.338	3.49	0.00382	17.8	3.952E-02	5.850E-02	9.020E-01	1.643E-01	1.797E-04	8.356E-01
3.67	12/12/06	60.006	2-5	0.385	13.6	0.00309	17.9	4.553E-02	5.913E-02	8.953E-01	4.303E-01	9.798E-05	5.696E-01
3.66	12/12/06	60.128	2-6	0.400	19.3	0.00277	18.1	4.720E-02	5.897E-02	8.938E-01	5.154E-01	7.402E-05	4.845E-01
3.63	12/13/06	40.031	4-1	0.146	0.0211	0.00331	7.10	1.765E-02	6.029E-02	9.221E-01	2.957E-03	4.647E-04	9.966E-01
3.59	12/13/06	40.017	4-2	0.217	0.0628	0.00251	7.02	2.569E-02	5.915E-02	9.152E-01	8.865E-03	3.544E-04	9.908E-01
3.65	12/13/06	40.009	4-3	0.272	0.211	0.00212	7.08	3.247E-02	5.971E-02	9.078E-01	2.889E-02	2.914E-04	9.708E-01
3.61	12/14/06	39.995	4-4	0.318	0.687	0.00183	7.02	3.734E-02	5.878E-02	9.039E-01	8.918E-02	2.380E-04	9.106E-01
3.65	12/14/06	40.043	4-5	0.384	4.37	0.00144	7.11	4.521E-02	5.893E-02	8.959E-01	3.806E-01	1.254E-04	6.193E-01
3.58	12/14/06	40.024	4-6	0.412	8.42	0.00141	7.27	4.754E-02	5.764E-02	8.948E-01	5.366E-01	8.974E-05	4.634E-01
5.09	02/06/07	40.028	2-1	0.172	0.0287	0.00312	6.83	2.814E-02	8.169E-02	8.902E-01	4.187E-03	4.550E-04	9.954E-01
4.83	02/06/07	40.049	2-2	0.220	0.0605	0.00288	6.92	3.402E-02	7.730E-02	8.887E-01	8.661E-03	4.121E-04	9.909E-01
5.07	02/06/07	40.029	2-3	0.274	0.211	0.00220	6.86	4.382E-02	8.007E-02	8.761E-01	2.980E-02	3.116E-04	9.699E-01
4.97	02/06/07	39.997	2-4	0.339	0.798	0.00103	6.83	5.276E-02	7.783E-02	8.694E-01	1.047E-01	1.349E-04	8.951E-01
4.96	02/06/07	40.029	2-5	0.409	5.71	0.00082	6.94	6.276E-02	7.682E-02	8.604E-01	4.513E-01	6.476E-05	5.487E-01
5.02	02/06/07	40.051	2-6	0.413	6.99	0.00086	6.99	6.414E-02	7.761E-02	8.582E-01	5.000E-01	6.130E-05	5.000E-01
5.18	02/08/07	60.023	4-1	0.164	0.137	0.0102	17.3	2.717E-02	8.302E-02	8.898E-01	7.884E-03	5.821E-04	9.915E-01
5.05	02/08/07	60.020	4-2	0.226	0.365	0.00745	17.3	3.626E-02	8.034E-02	8.834E-01	2.066E-02	4.221E-04	9.789E-01
5.08	02/08/07	60.042	4-3	0.296	1.29	0.00559	17.6	4.733E-02	7.991E-02	8.728E-01	6.841E-02	2.959E-04	9.313E-01
5.05	02/08/07	60.075	4-4	0.330	3.31	0.00486	17.4	5.216E-02	7.899E-02	8.688E-01	1.602E-01	2.350E-04	8.395E-01
5.02	02/08/07	60.046	4-5	0.386	18.3	0.00286	17.6	6.015E-02	7.791E-02	8.619E-01	5.088E-01	7.954E-05	4.911E-01
4.96	02/08/07	60.061	4-6	0.417	51.4	0.00223	18.5	6.400E-02	7.674E-02	8.593E-01	7.357E-01	3.201E-05	2.643E-01

a: α = loading = mole CO_2/mol 2·PZ

Task 4 – Solvent Reclaiming

Subtask 4.1a – Reclaiming by crystallization – potassium sulfate

by Qing Xu

(Supported by this contract and by the TXU Carbon Management Program)

Introduction

One side reaction in CO_2 capture when using MEA is the generation of sulfate from SO_2. This sulfate has to be removed so that the MEA solution can be reused for CO_2 capture. Potassium compounds are often used in the removal of sulfate. In order to determine how best to accomplish this, the solubility of potassium sulfate was measured in with variable MEA concentration and with CO_2 loading.

Experimental

Method 1

The first experimental method was used by a group of undergraduate students as a special project in a senior laboratory course in summer 2006. (Sachde and Sivaram, 2006)

MEA solutions were gravimetrically prepared 3, 7, 11.4, and 15 m (moles amine/kg water). Then 10ml of MEA solutions was mixed with 1.5g K_2SO_4 and agitated in a water bath for about 48 hours. Four temperatures (25, 40, 60, and 80^oC) were chosen within the operating of the absorption-stripping system. Undissolved solids were collected using vacuum filtration, dried, and weighed with a balance. The solids dissolved in the solution sample were also dried and weighed to determine residual K_2SO_4 to reduce error. The filtration process was performed quickly to prevent the filtrate from cooling down so that no K_2SO_4 would precipitate out of solution.

Method 2

The second experimental method was used by a group of undergraduate students as a special project in a senior laboratory course in fall 2006. (Abesamis et al., 2006)

7 m MEA was prepared gravimetrically as a stock solution. 100g of this solution was agitated with stir bar. Solid K_2SO_4 was added to the system in 0.1g increments. The conductivity of the solution was measured with each addition. Additions were continued until the solution was saturated. Then an excess of K_2SO_4 was added to the solution and the final conductivity was measured. A correlation of conductivity and K_2SO_4 concentration was developed from the data collected before saturation and the concentration at saturation was calculated with the correlation from the final measured conductivity. In modifications of this procedure, KOH or H_2SO_4 was added to the solution before the additions of K_2SO_4. A water bath was used to conduct these experiments at 45ºC and 60ºC.

Method 3, CO_2 loaded

This method was used to measure loaded solutions.

A bubbler was used to add CO_2 to stock amine solutions (7m MEA, 11m MEA, 7m MEA/2m PZ, and 4m PZ). The amounts of CO_2 added into the solutions were weighed with a balance. In these experiments, CO_2 was added to form specific molal CO_2 solutions. Another way to prepare CO_2 loading solution is by adding $KHCO_3$ to form specific molal $KHCO_3$

solutions. 50g of the loaded solution was agitated by a stir bar during the following process. 0.1-0.4g K_2SO_4 was sequentially added to the system and conductivity was measured with each addition until the solution was saturated. Then an excess of K_2SO_4 was added to the solution and the final conductivity was recorded. Conductivity was correlated with K_2SO_4 concentration and extrapolated to obtain the K_2SO_4 saturation concentration. In modifications of this procedure, KOH or H_2SO_4 was added to the solution before the additions of K_2SO_4. These experiments were carried out at room temperature and at 40°C. A water bath was used to conduct the experiments at 40ºC.

Examples

Following are experimental graph examples. The intersections of the curves are the saturation points, and the solubility of K_2SO_4 is calculated from the two equations of the curves.

With an increasing solubility after the saturation point:

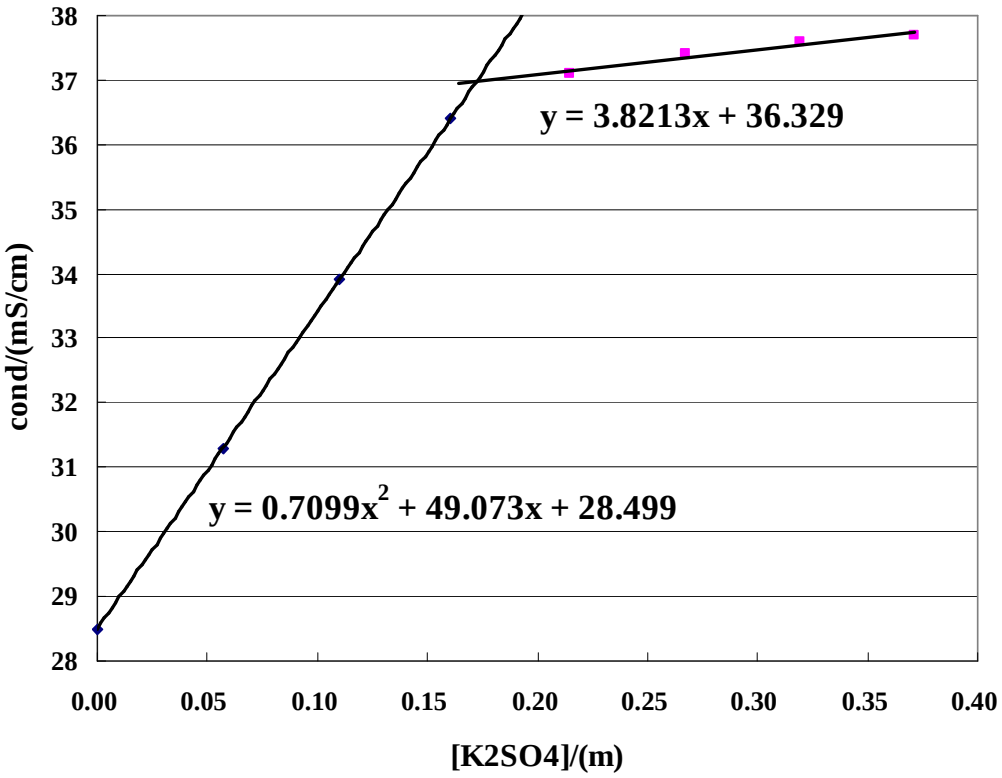

Figure 29: Conductivity dependence on concentration -1

7m MEA, $[CO_2]_t$=1.4 m, KOH=0.35m

With a decreasing solubility after the saturation point:

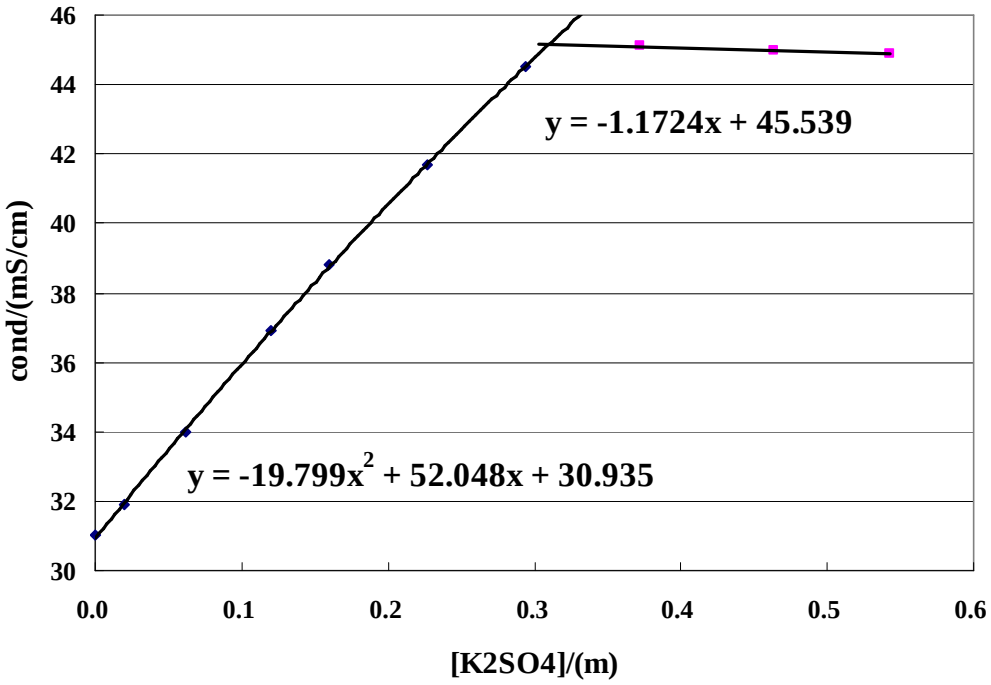

Figure 30: Conductivity dependence on concentration -2

7m MEA, $[CO_2]_t$=1.4 m, H_2SO_4=0.15m

With a flat curve after the saturation point:

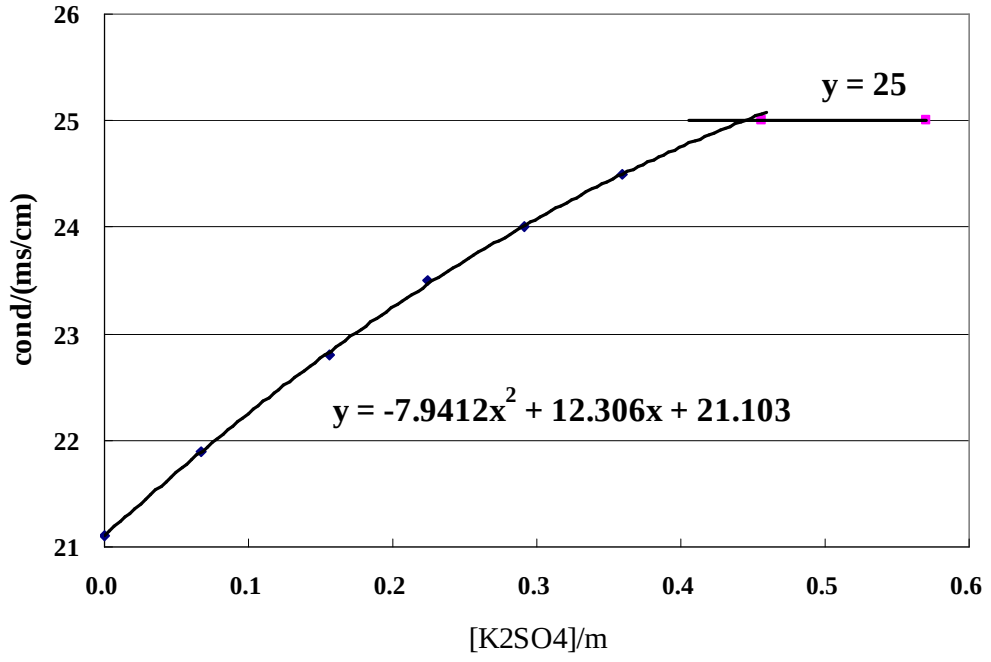

Figure 31: Conductivity dependence on concentration -3

11 m MEA, $[CO_2]_t$=5.5 m

Model Formulation

Two models of ln(Ksp), depending on $\frac{1}{T}$, I^a, and the concentration of equivalent amine, were developed.

'I' is the iron strength of the solution; 'a' is its exponent. Linear models were developed where different exponents (ranging from 0 to 0.7) are used. According to a comparison of the error and coefficients of determination from each model, the proper exponents were determined.

Model 1

Based on all the data (Söhnel, Sachde, Abesamis, and Xu),

$$\ln Ksp = 17.5I^{0.1} - 0.37[\text{equal.amine}] - \frac{1080}{T} - 15.06 \qquad (8)$$

where [equal.amine] is the concentration of equivalent amine in the solution.

The coefficient of determination $R^2 = 0.9700$ is very close to 1.

Table 37: Solubility of K_2SO_4 in amine solution

Date	T(°C)	Concentration(m)					I^a	Ksp_{exp} [b]	Kspcal/Kspexp[c]	
		K^+	$SO4^=$	CO_2	MEA	PZ			Eq. 1	Eq. 2
111306	23.45	0.614	0.307	2.8	7	0	3.72	0.116	2.277	2.192
112006	22.25	0.597	0.299	2.8	7	0	3.70	0.107	2.404	2.297
112806	23.8	0.836	0.218	2.8	7	0	3.46	0.153	1.495	1.397
2006 fall	25	0.112	0.056	0	7	0	0.168	0.001	1.877	
	25	0.183	0.035	0	7	0	0.162	0.001	1.062	
	25	0.112	0.112	0	7	0	0.336	0.001	2.684	
	45	0.190	0.095	0	7	0	0.285	0.003	1.069	
	45	0.270	0.038	0	7	0	0.114	0.003	0.342	
	45	0.170	0.190	0	7	0	0.570	0.005	2.021	
	60	0.150	0.074	0	7	0	0.222	0.002	1.752	
	60	0.260	0.057	0	7	0	0.171	0.004	0.514	
	60	0.160	0.150	0	7	0	0.450	0.004	2.287	
summer	25	0.250	0.125	0	7	0	0.375	0.008	0.574	
	25	0.080	0.040	0	11.4	0	0.121	0.000	0.618	
	25	0.097	0.049	0	15	0	0.146	0.000	0.121	
	40	0.601	0.301	0	3	0	0.902	0.109	0.923	
	40	0.239	0.119	0	7	0	0.358	0.007	0.728	

	40	0.083	0.042	0	11.4	0	0.125	0.000	0.693	
	40	0.016	0.008	0	15	0	0.024	0.000	2.882	
	60	0.733	0.367	0	3	0	1.10	0.197	0.887	
	60	0.302	0.151	0	7	0	0.452	0.014	0.646	
	60	0.128	0.064	0	11.4	0	0.192	0.001	0.440	
	60	0.017	0.008	0	15	0	0.025	0.000	3.380	
	80	0.692	0.346	0	3	0	1.04	0.166	1.145	
	80	0.305	0.152	0	7	0	0.457	0.014	0.766	
	80	0.129	0.065	0	11.4	0	0.194	0.001	0.520	
	80	0.022	0.011	0	15	0	0.033	0.000	2.497	
Söhnel	20	1.268	0.634	0	0	0	1.90	1.020	0.904	0.861
	25	1.375	0.688	0	0	0	2.06	1.300	0.877	0.852
	30	1.477	0.738	0	0	0	2.22	1.610	0.860	0.853
	40	1.700	0.850	0	0	0	2.55	2.456	0.827	0.862
	50	1.899	0.950	0	0	0	2.85	3.427	0.817	0.898
	60	2.105	1.053	0	0	0	3.16	4.665	0.811	0.944
	70	2.301	1.150	0	0	0	3.45	6.091	0.814	1.003
	80	2.468	1.234	0	0	0	3.70	7.519	0.828	1.077
1.31	24.15	0.205	0.103	0	7	0	0.308	0.004	0.754	1.275
2.5	24.6	0.119	0.060	0	11	0	0.179	0.001	0.385	0.882
2.6	23.95	0.685	0.343	5.5	11	0	5.18	0.161	0.733	0.789
2.12	23.95	0.756	0.378	5.5	11	0	5.28	0.216	0.569	0.621
2.13	22.9	0.766	0.383	5.5	7	2	6.65	0.225	0.874	1.155
2.14	24.1	0.346	0.173	2.2	7	2	2.72	0.021	1.581	1.271
2.20	24.8	0.539	0.270	2	0	4	2.81	0.078	1.358	1.171
2.21	22.85	0.719	0.359	4	0	4	5.08	0.186	1.827	2.052
2.27	40.2	0.887	0.444	5.5	11	0	6.83	0.349	0.728	1.044
2.28	40.1	0.831	0.415	5.5	7	2	6.75	0.287	0.863	1.223
3.5	39.95	0.742	0.371	2.2	3.7	0.8	3.31	0.204	2.328	2.336
3.20	39.9	0.419	0.210	2.2	11	0	2.83	0.037	1.148	0.981
3.21	40	0.618	0.309	1.4	7	0	2.33	0.118	1.083	0.968

3.22	39.95	0.910	0.455	2.8	7	0	4.17	0.377	1.062	1.139
3.25	39.95	0.735	0.193	1.4	7	0	2.15	0.104	1.061	0.942
3.26	40	0.949	0.300	4.4	11	0	0.270	0.270	0.591	0.698
3.28	40	0.594	0.122	2.2	7	2	0.043	0.043	0.927	0.787
3.29	40	0.614	0.457	1.4	7	0	2.62	0.172	0.932	0.849
3.30	39.85	0.678	0.489	4.4	11	0	5.72	0.225	0.774	0.946
3.31	39.9	0.432	0.366	2.2	7	2	3.15	0.068	0.765	0.673
4.2	39.85	0.695	0.173	1.4	7	0	2.09	0.083	1.252	1.109

a. I: ionic strength;

b. $Ksp=[K^+]^2[SO_4^=]$;

c. Ksp_{cal} is calculated from Model 1 and Model 2.

Model 2 is based on data from Söhnel & Xu except data on the dates of 11/13/06, 11/20/06, 2/21/07 and 3/5/07, because these data were outliers; but the values of Ksp_{cal}/Ksp_{exp} of these experiments are calculated from Model 2.

To find out how well the model fits the experimental data, and the relationship between Ksp(cal)/Ksp(exp)=error and equivalent amine concentration(equals to [MEA]+2*[PZ]), temperature, and concentration of CO_2 loading, plot the following graphs:

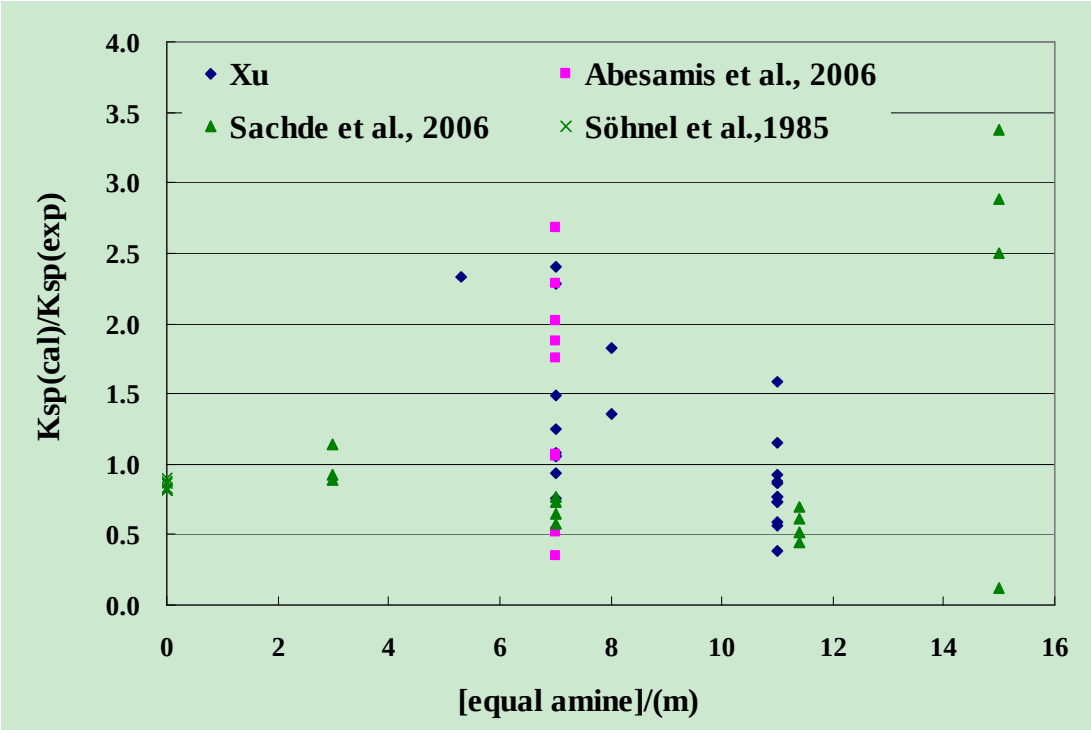

Figure 32: Accuracy of model 1 for K_2SO_4 solubility, effect of equal amine concentration

The data of Sachde and Sivaram (2006) at high amine concentration are substantially lower than the model. The data of Söhnel et al. on solubility in water agree well with the model. With all of the data, larger amine concentrations give larger errors.

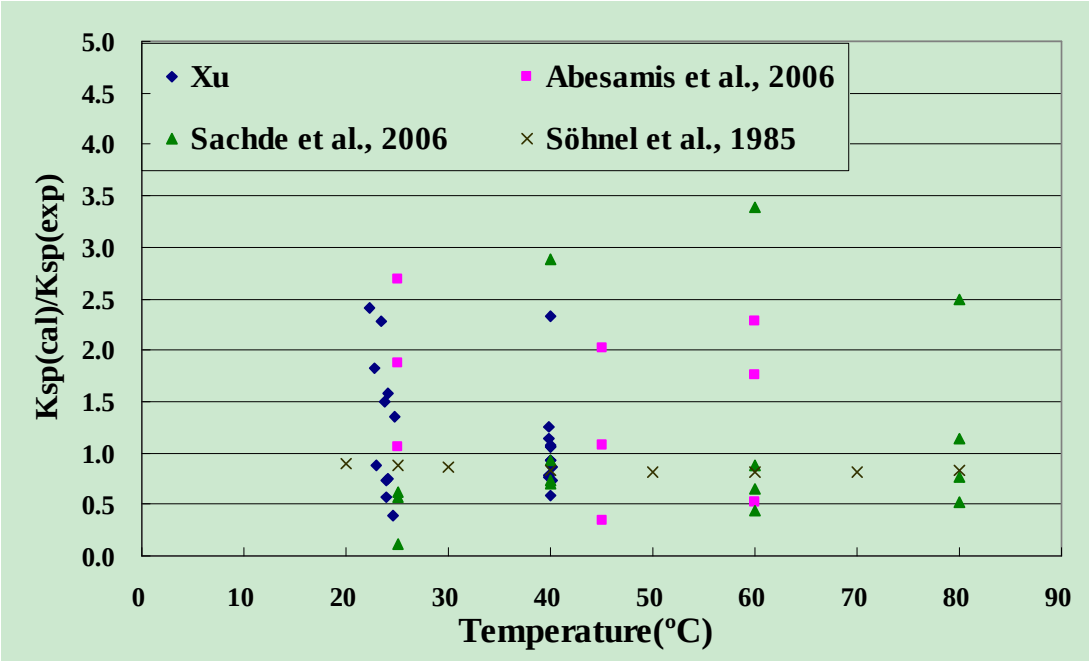

Figure 33: Accuracy of model 1 for K_2SO_4 solubility, effect of temperature

Figure 33 shows that temperature does not have an obvious effect on the errors.

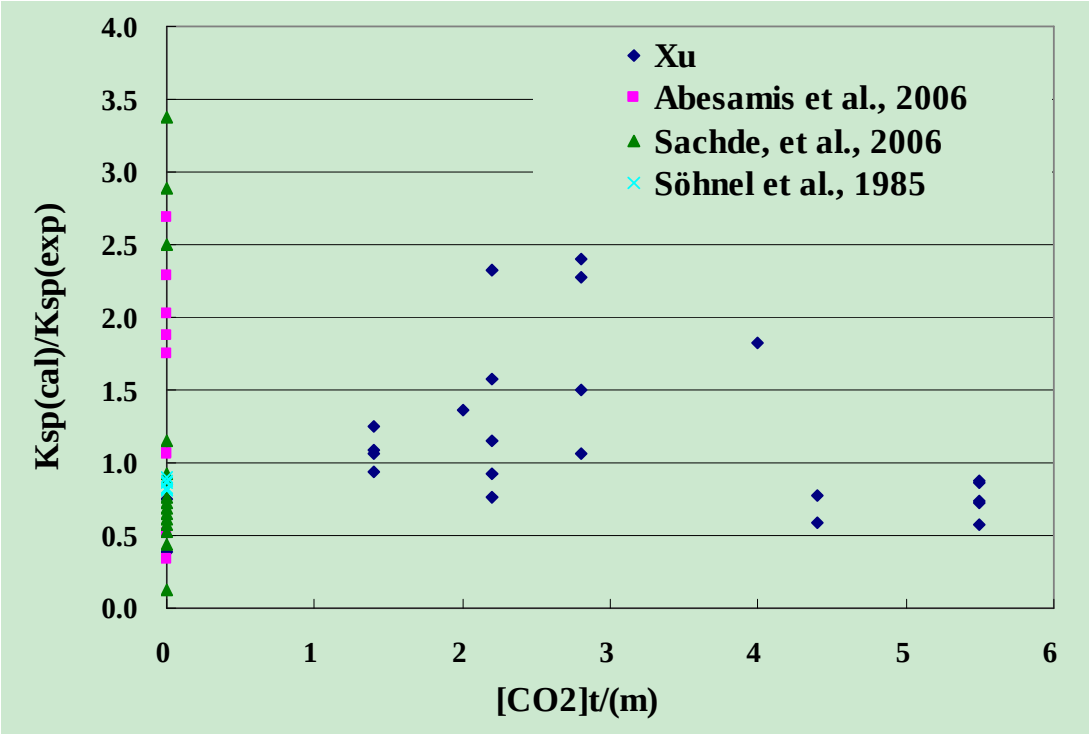

Figure 34: Accuracy of model 1 for K_2SO_4 solubility, effect of CO_2 loading

We can conclude that the effect of loaded CO_2 concentration is much less than that of the experimental method.

Model 2

Based on data from Söhnel and Xu:

$$\ln Ksp = 3.6I^{0.4} - 0.39[\text{equal.amine}] - \frac{1382}{T} - 0.072 \qquad (2)$$

where [equal.amine] is the concentration of equivalent amine in the solution.

The coefficient of determination $R^2 = 0.9909$ is very close to 1.

As with Model 1, to find out how well the model fits the experimental data, and the relationship between Ksp(cal)/Ksp(exp)=error and equivalent amine concentration(equals to [MEA]+2*[PZ]), temperature, and concentration of CO_2 loading, plot the following graphs:

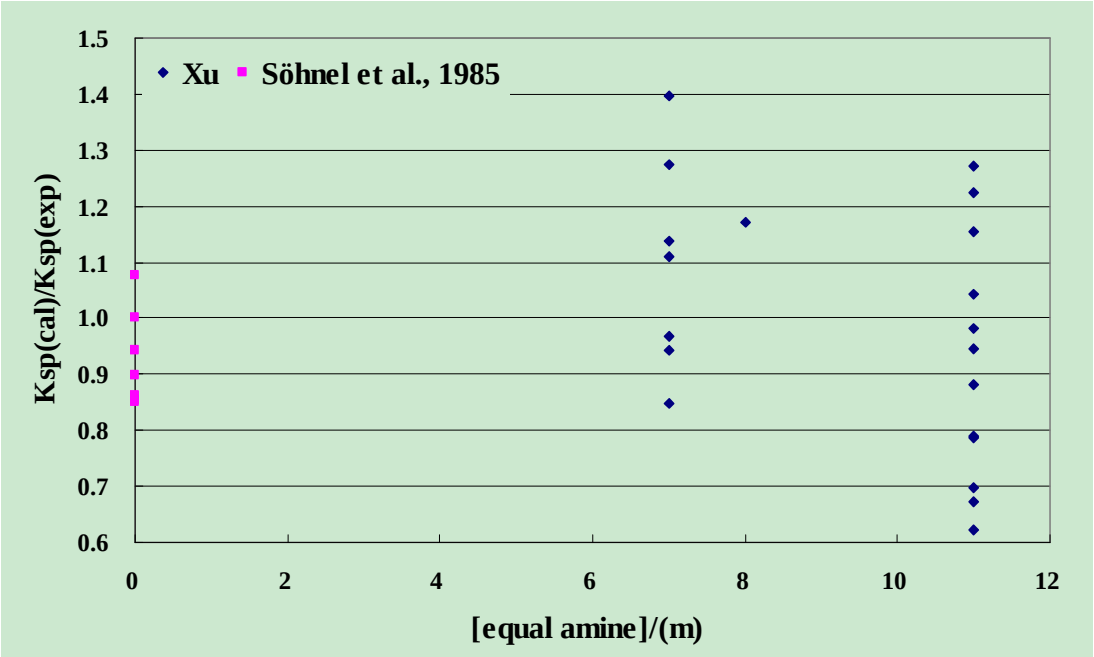

Figure 35: Accuracy of model 2 for K_2SO_4 solubility, effect of equal amine concentration

We can see that by using the same experimental method, low amine concentration usually results in an error range from 0.8~1.4, while higher amine concentration usually results in an error range from 0.6~1.3.

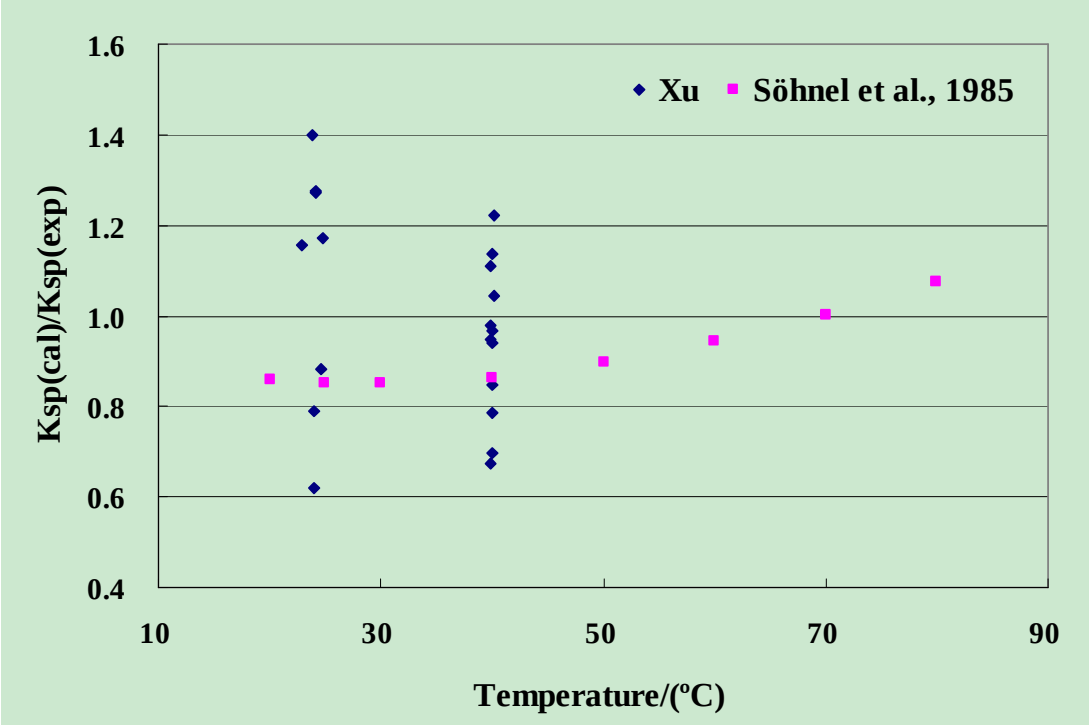

Figure 36: Accuracy of model 2 for K_2SO_4 solubility, effect of temperature

From figure 36 we can conclude that a higher temperature yields a lower error rate. That might be because at high temperature experiments were carried out in a water bath so temperature was less fluctuant.

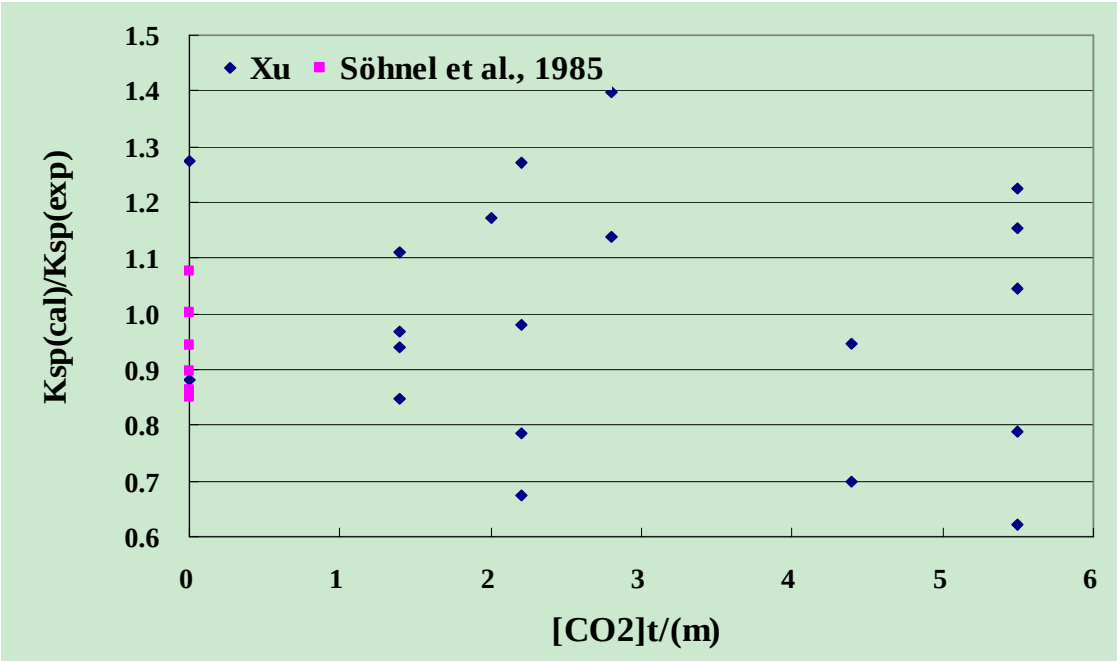

Figure 37: Accuracy of model 2 for K_2SO_4 solubility, effect of CO_2 loading

From Figure 37 we can see that, generally, the error rate of high CO_2 loaded solutions is slightly higher that that of low loading solutions.

Results and Discussion

Compare the two models above:

Coefficient of determination R^2

$$\text{Model 1: } R^2 = 0.9700$$

$$\text{Model 2: } R^2 = 0.9909$$

Thus model 2 fits the data better.

Error=Ksp(cal)/Ksp(exp).

Its dependence on equivalent amine concentration (equals to [MEA]+2*[PZ]), temperature, and concentration of loaded CO_2:

From Figures 32-37, we find that different experimental methods bring different results. Experimental method 1 brings large errors at high amine concentration. Reference data fits best with the model. For a certain method, larger amine concentrations give larger errors; low amine concentration usually results in an error from 0.8~1.4, while higher amine concentration usually results in an error from 0.6~1.3. The effect of loaded CO_2 concentration is much less than that of experimental method. Generally, according to data from the same experimental method, the errors of high CO_2 loaded solutions are a little larger than those of low loading solutions. Maybe because of the experimental methods, higher temperature has smaller error.

Effect of I on Ksp

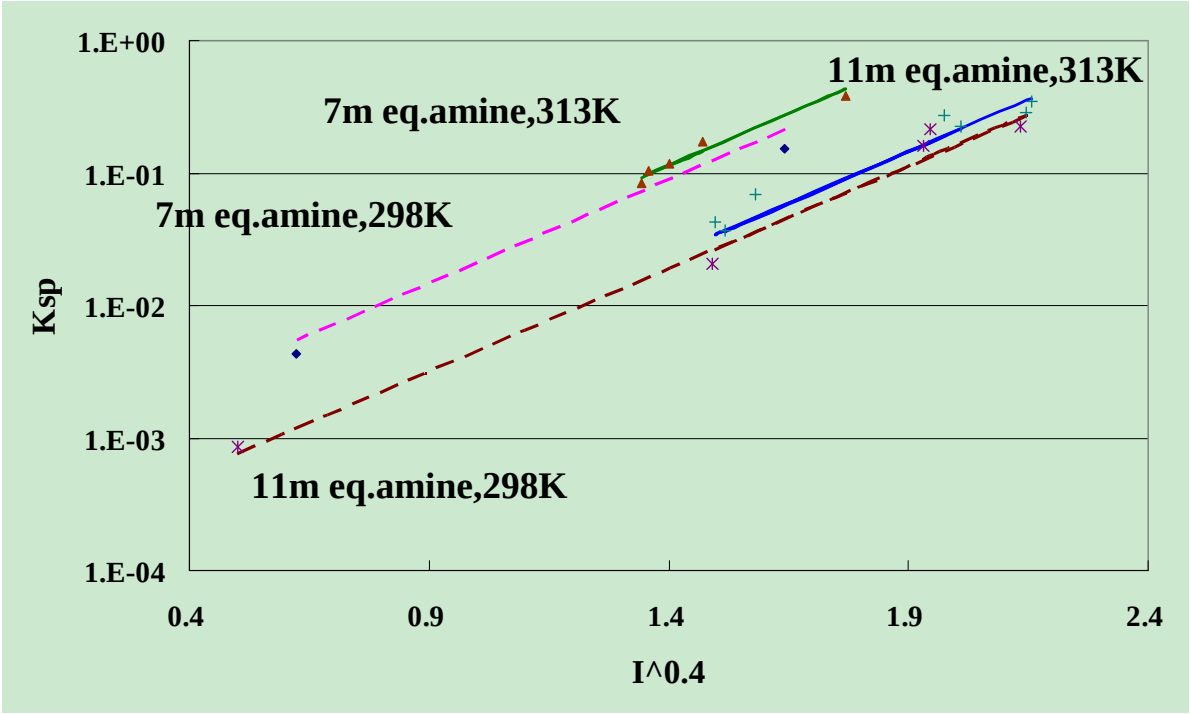

Figure 38: Solubility of K_2SO_4 under different ionic strength

Curves are calculated from Model 2, and points are from experimental data. From Figure 38, we can clearly see that lower temperature, higher amine concentration, and higher ionic strength, will result in lower Ksp.

Conclusions

Two models concerning about solubility of potassium sulfate in amine(MEA, PZ) solution have been developed and tested by the data from both experiments and references. Both of them can fit the data well.

Future work

Data about the solubility of Na_2SO_4 in CO_2 loaded amine solution is needed, so that a better salt can be chosen for reclaiming.

An Aspen NRTL/electrolyte model will be used to regress and compare with experimental data.

Table 38: Raw data

date	T/°C	Concentrations (m)						I	Equation 1 *				Equation 2		
		Sat. K_2SO_4	MEA	PZ	CO_2	KOH	H_2SO_4		a_1	b_1	c_1	R_1^2	a_2	b_2	R_2^2
Data in 2006 by Xu															
111306	23.45	0.3069	7	0	2.8	0	0	3.721	0	1.9377	6.5358	0.9898	0	9.88	1
112006	22.25	0.2987	7	0	2.8	0	0	3.696	0.1711	1.484	6.3105	0.9988	0.1263	9.0718	1
112006	22.6	0	7	0	2.8	2.79	0	2.800	N/A	N/A	N/A	N/A	N/A	N/A	N/A
112806	23.8	0.2182	7	0	2.8	0.4	0	3.455	-1.7058	3.0388	2.989	0.9996	0.045	3.5611	0.7169
Data in 2007 by Xu															
1.31	24.15	0.1025	7	0	0	0	0	0.308	0	23.226	0.5256	0.9923	-0.0939	2.916	1
2.5	24.6	0.0597	11	0	0	0	0	0.179	0	12.500	0.2503	0.9973	0.0741	0.9918	1
2.6	23.95	0.3426	11	0	5.5	0	0	5.178	4.8226	7.1018	13.39	0.991	0.0449	16.374	0.0597
2.12	23.95	0.3781	11	0	5.5	0	0	5.284	-7.3645	10.734	13.554	0.9994	0.1961	16.47	1
2.13	22.9	0.3829	7	2	5.5	0	0	6.649	-6.0614	9.1086	12.285	0.9977	0.141	14.83	1
2.14	24.1	0.1728	7	2	2.2	0	0	2.718	1.8301	8.9956	8.0186	0.996	-0.1693	9.6574	1
2/20	24.8	0.2695	0	4	2	0	0	2.809	-31.387	24.443	7.1306	0.9982	0.4313	11.322	1
2.21	22.85	0.3594	0	4	4	0	0	5.078	-14.434	28.821	6.228	0.9999	-0.6671	14.962	1
2.27	40.2	0.4437	11	0	5.5	0	0	6.831	-7.9412	12.306	21.103	0.9997	0	25	1
2.28	40.1	0.4153	7	2	5.5	0	0	6.746	-3.5975	10.751	18.753	0.9998	-0.5272	22.816	0.6184
3.5	39.95	0.3710	3.7	0.8	2.2	0	0	3.313	-8.1059	27.827	16.656	0.9999	-0.325	25.985	0.227
3.20	39.9	0.2097	11	0	2.2	0	0	2.829	4.5985	27.842	22.627	0.9991	-1.0679	28.893	0.904
3.21	40	0.3091	7	0	1.4	0	0	2.327	-36.931	60.042	25.424	0.9994	2.3081	39.74	0.753
3.22	39.95	0.4551	7	0	2.8	0	0	4.165	-12.532	48.791	41.707	0.9998	-0.3285	61.465	0.0657
3.25	39.95	0.1927	7	0	1.4	0.35	0	2.153	-11.732	53.141	28.747	0.9868	-0.9512	38.734	0.7492

3.26	40	0.2995	11	0	4.4	0.35	0	5.474	-25.14	26.611	35.924	0.9969	-1.1751	41.991	0.9999
3.28	40	0.1219	7	2	2.2	0.35	0	2.741	-29.388	27.283	23.337	0.9933	1.5112	26.041	0.878
3.29	40	0.3070	7	0	1.4	0	0.15	2.621	-19.799	52.048	30.935	0.9999	-1.1724	45.539	0.9983
3_30	39.85	0.3392	11	0	4.4	0	0.15	5.718	-8.7994	23.017	36.502	0.9996	-0.5715	43.49	0.7425
3.31	39.9	0.2158	7	2	2.2	0	0.15	3.147	-56.099	33.455	24.124	0.9985	1.7102	28.362	0.9998
4.2	39.85	0.1726	7	0	1.4	0.35	0	2.093	0.7099	49.073	28.499	1	3.8213	36.329	0.9534

* The formula of equation 1 is: conductivity=$a_1x^2+b_1x+c_1$; the formula of equation 2 is: conductivity=a_2x+b_2, x is the concentration of K_2SO_4 in the amine solutions. They represent the curve before and after the saturation point, respectively. R^2 is the coefficient of determination for each equation.

Task 5 – Corrosion

Corrosion in CO2 absorption process using aqueous solution of blended potassium carbonate/piperazine

by Amorvadee (Amy) Veawab, University of Regina

(Supported by subcontract)

Objective

The carbon dioxide (CO_2) absorption process using aqueous chemical solutions is subject to a number of operational difficulties, of which the most severe is corrosion of process equipment and solvent degradation. Corrosion problems have been receiving a great deal of attention because they have substantial impacts on the plant's economy, especially in terms of unplanned downtime, production losses, reduced equipment life, and extra expenditure for restoring the corroded equipment and for treatment systems initiated to mitigate the corrosion. The corrosion problems also prevent the absorption process from achieving energy efficient operations.

The aqueous solution of blended potassium carbonate and piperazine has shown itself to be a promising solvent for CO_2 capture from coal-fired power plant flue gas due to its capture performance and energy efficiency. It is our goal to explore further the promise of this solvent in an aspect of the potential operational problems. This project focuses on the investigation of corrosion of materials during CO_2 absorption and solvent regeneration in the presence and absence of solvent degradation products and chemical additives including oxidative inhibitors and corrosion inhibitors.

The research involves comprehensive literature review on the corrosion in CO_2 absorption process using potassium carbonate and piperazine, and experimental evaluations in the following sequences:

Task 1: Evaluation of corrosion in base solution (the blended potassium carbonate and piperazine) against the corrosion in an aqueous solution of monoethanolamine (MEA).

Task 2: Evaluation of corrosion in base solution containing degradation products.

Task 3: Evaluation of corrosion in base solution containing degradation products and oxidative inhibitors.

Task 4: Evaluation of inhibition performance of corrosion inhibitor in the presence of degradation products and oxidative inhibitors.

Based on our discussion with Dr. Rochelle, we would like to expand our project to cover the corrosion study in both K_2CO_3-piperazine and MEA-piperazine since MEA-piperazine is another promising piperazine-based solvent for cost-effective CO_2 capture. The original tasks for K_2CO_3-MEA will be kept minimum, and the tasks with similar objectives will be carried out for MEA-piperazine system.

Progress

Over the past three months, we have successfully obtained additional electrochemical corrosion data of carbon steel immersed in aqueous solutions of blended MEA-piperazine containing heat-stable salt and two corrosion inhibitors (copper carbonate ($CuCO_3$) and sodium metavanadate ($NaVO_3$)). We have also conducted weight loss corrosion tests and obtained corrosion data of the uninhibited and inhibited aqueous solutions of MEA-piperazine under long-term exposure. Results and discussion are given below.

Electrochemical corrosion tests

Performance of $CuCO_3$ corrosion inhibitor

The inhibition performance of $CuCO_3$ was examined in aqueous solutions of blended 5M MEA/ 1.2M piperazine containing 0.20 mol/mol CO_2 loading at 80^{o}C. As illustrated in Figures 39-40, $CuCO_3$ is an anodic corrosion inhibitor that shifts the corrosion potential of metal from active to passive state where a passive film is formed on the metal surface. The passive film acts as a separator of metal surface and solution, thus retarding the diffusion of Fe^{2+} and electrons from the metal surface to the solution. As a result, the corrosion reactions proceed in a slower rate. The cyclic polarization curves also exhibit positive hysteresis, suggesting that $CuCO_3$ tends to induce pitting.

The results also show that oxygen plays an important role in inhibition performance of $CuCO_3$. As shown in Figure 41, corrosion rate of carbon steel decreases significantly when 500 ppm $CuCO_3$ is added in the presence of oxygen. However, in the absence of oxygen, the corrosion rate does not decrease, but increases from the uninhibited system. This suggests that $CuCO_3$ performs more effectively in the presence of dissolved oxygen. This is due to the nature of passive film formed on the metal surface as discussed in our previous progress report.

Performance of CuCO3 in the presence of heat-stable salt

The inhibition performance of $CuCO_3$ was further evaluated in the presence of acetic acid. The acetic acid was chosen to represent heat-stable salts present in service solutions since it is the most corrosive salt in the uninhibited aqueous solution of blended 5M MEA/1.2M piperazine (according to our previous results). Results in Figures 42-44 show that $CuCO_3$ performs well in the presence of heat-stable salt. Corrosion rate of carbon steel is greatly reduced from 168 to 16.2 mpy in the absence of oxygen, and can be further reduced to 0.9 mpy in the presence of oxygen. However, the cyclic polarization curves show positive hysteresis, indicating pitting tendency.

Performance of $CuCO_3$ under high CO_2 loading environment

The inhibition performance of $CuCO_3$ was examined in aqueous solutions of blended 5M MEA/1.2M piperazine containing 250 ppm $CuCO_3$ and 0.55 mol/mol CO_2 loading at 80^{o}C. The polarization curve in Figure 45 shows that even in the presence of high CO_2 content in the

solution, passive film can be formed on the carbon steel surface to retard corrosion process. The corrosion rate was found to be 17.2 mpy. This shows the effectiveness of $CuCO_3$ inhibitor. The cyclic polarization curve, however, shows positive hysteresis, indicating pitting tendency.

Performance of $NaVO_3$ corrosion inhibitor

The inhibition performance of $NaVO_3$ was examined in aqueous solutions of blended 5M MEA/1.2M piperazine containing 0.20 mol/mol CO_2 loading at 80^oC. The concentrations of $NaVO_3$ used for these experiments are 50, 250, and 500 ppm. Results in Figures 46-54 show that, in the absence of oxygen, the inhibition performance of $NaVO_3$ decreases with increasing concentration of $NaVO_3$, whereas it increases slightly with $NaVO_3$ concentration in the presence of oxygen. It is apparent that 50 ppm is an optimum $NaVO_3$ concentration since it gives the lowest corrosion rates in both the presence and absence of oxygen. Corrosion rate of carbon steel is reduced to 1 mpy with an addition of 50 ppm $NaVO_3$ in the presence of oxygen, while that in the absence of oxygen is reduced to 5.7 mpy.

Weight loss corrosion tests

A series of weight loss experiments were carried out in four 2-liter jacketed cylindrical glass cells connected to accessories as illustrated in Figure 54. Carbon steel specimens are flat and rectangular in shape with dimensions of 1 inch x 1 inch x 1/8 inch and a 600 grit surface finish. The corroded specimens were cleaned after the tests according to the ASTM standard G1-90 (Re-approved 1999). The corrosion rate of the specimens was estimated by using the following equation:

$$\text{Corrosion rate (mpy)} = (K \times W)/ (A \times T \times D) \quad (9)$$

where $K = 3.45 \times 10^6$

W = mass loss in g, (corrected for any loss during cleaning)

A = area in cm^2

T = time of exposure in hours

D = density in g/cc

Performance of $CuCO_3$

The inhibition performance of $CuCO_3$ was evaluated in aqueous solutions of blended 5M MEA/1.2M piperazine containing 0.20 mol/mol CO_2 loading and 10% oxygen at 80^oC under long-term exposure (7, 14, 21, and 28 days). Results in Figure 56 show that the corrosion rate of carbon steel in uninhibited systems increases with time and then stabilizes at a certain value. The corrosion rate increases from 6.8 mpy after 7 days to 8.4 mpy after 14 days, eventually stabilizing at 13 mpy after 21 days. When 250 ppm $CuCO_3$ is added to the solutions, weights of specimens remain unchanged for 28 days. This clearly indicates an excellent inhibition performance of $CuCO_3$ in the presence of oxygen, thus confirming the results obtained from previous electrochemical tests.

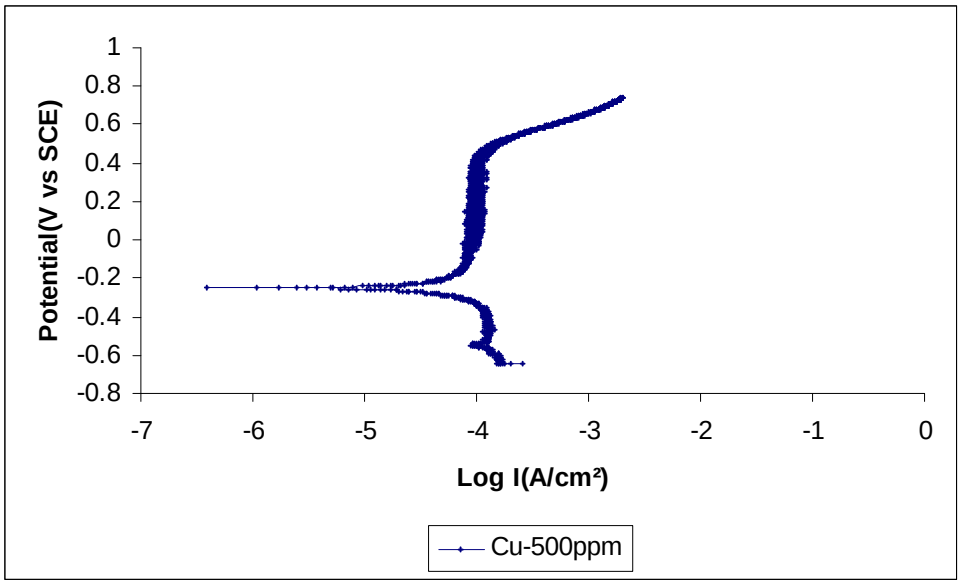

Figure 39: Cyclic polarization curve of carbon steel in 5 M MEA-1.2 M PZ containing 500 ppm $CuCO_3$ and 0.20 mol/mol CO_2 loading at 80°C

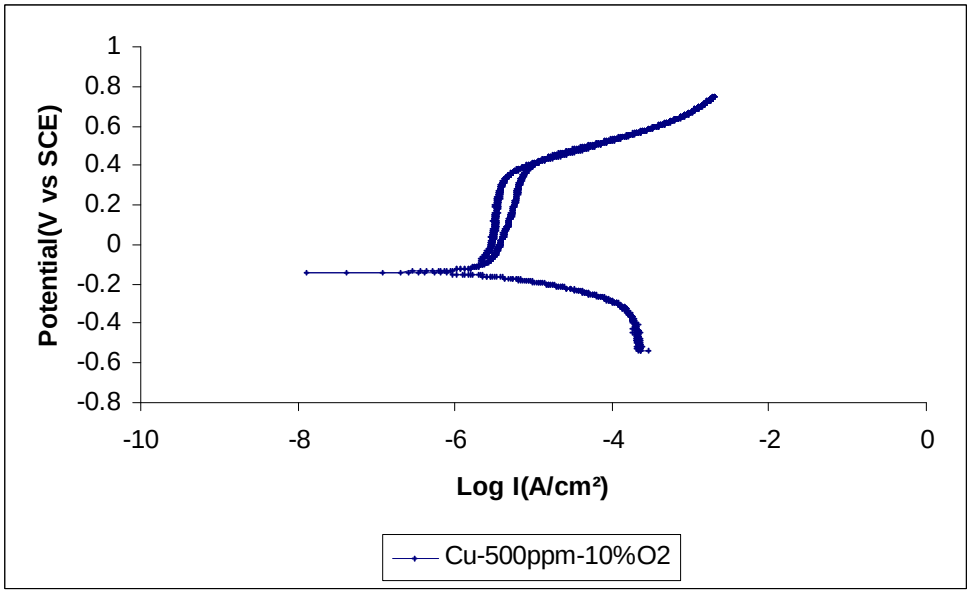

Figure 40: Cyclic polarization curve of carbon steel in 5 M MEA-1.2 M PZ containing 500 ppm $CuCO_3$ and 0.20 mol/mol CO_2 loading at 80°C with 10% oxygen.

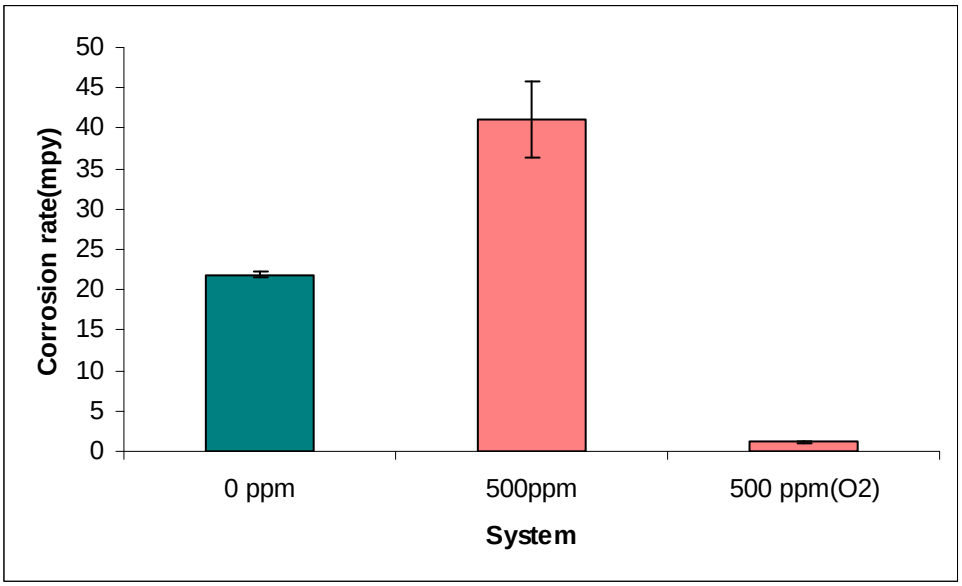

Figure 41: Corrosion rate of carbon steel in 5 M MEA-1.2 M PZ containing 500 ppm $CuCO_3$ and 0.20 mol/mol CO_2 loading at 80°C

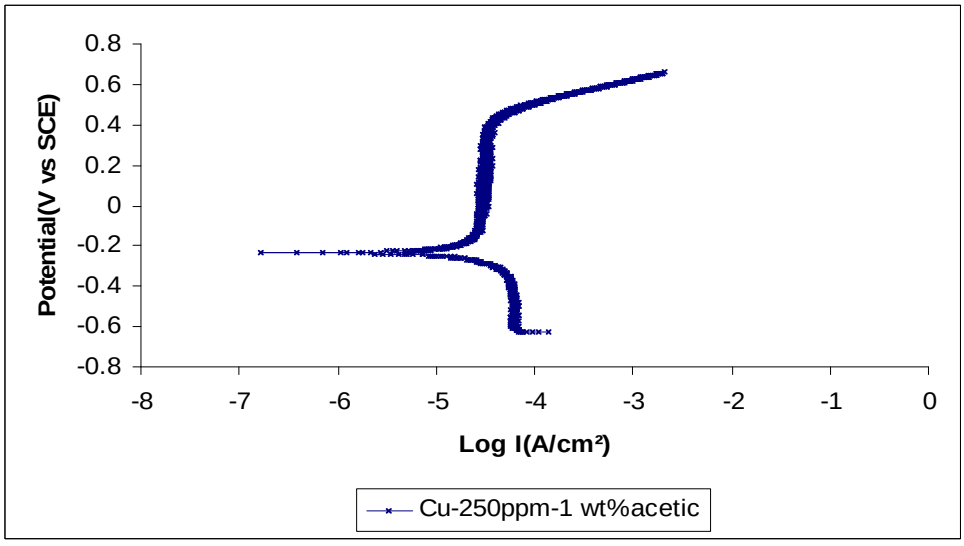

Figure 42: Cyclic polarization curve of carbon steel in 5 M MEA-1.2 M PZ containing 250 ppm $CuCO_3$, 1 wt % acetic acid and 0.20 mol/mol CO_2 loading at 80°C

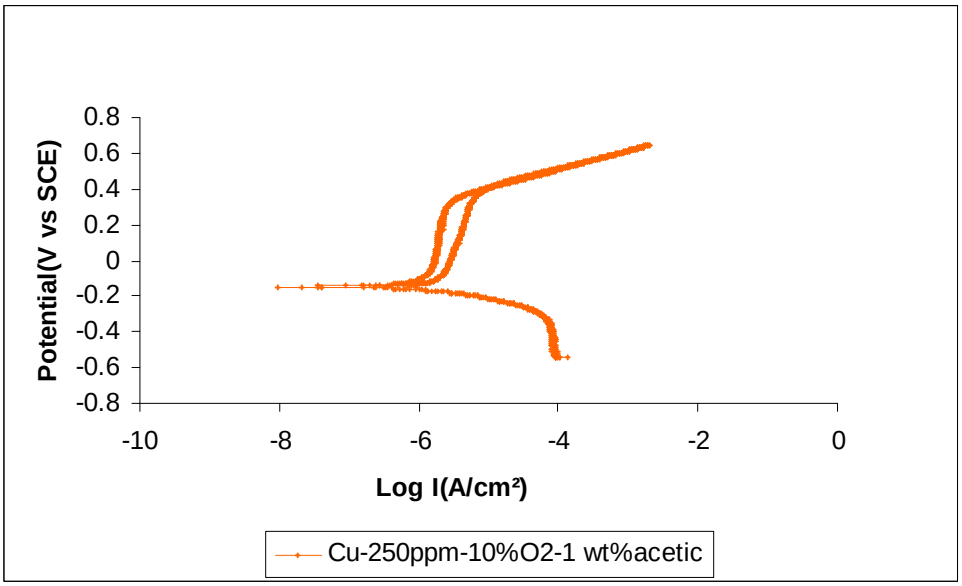

Figure 43: Cyclic polarization curve of carbon steel in 5 M MEA-1.2 M PZ containing 250 ppm $CuCO_3$, 1 wt % acetic acid and 0.20 mol/mol CO_2 loading at 80^{o}C with 10% O_2

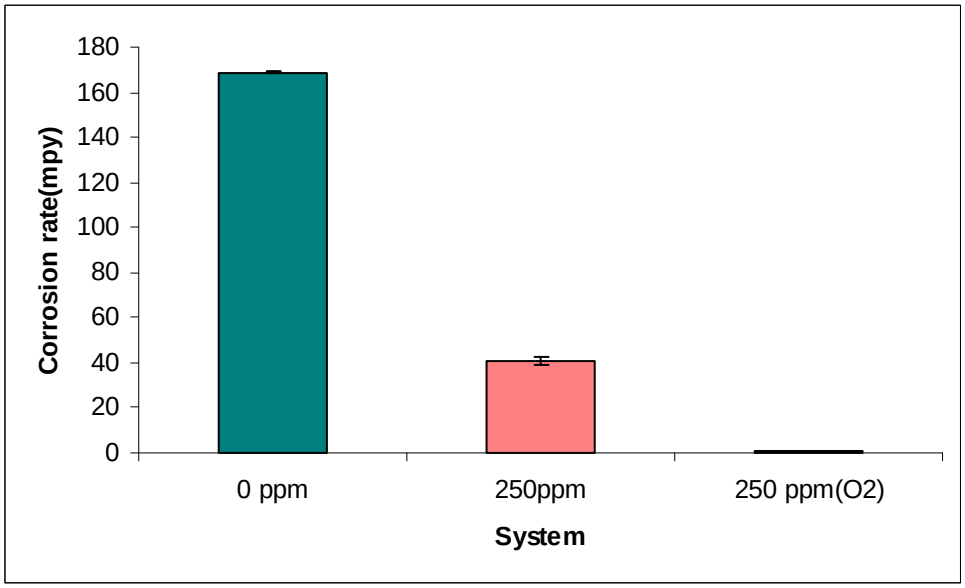

Figure 44: Corrosion rates of carbon steel in 5 M MEA-1.2 M PZ containing 250 ppm $CuCO_3$, 1 wt % acetic acid and 0.20 mol/mol CO_2 loading at 80^{o}C

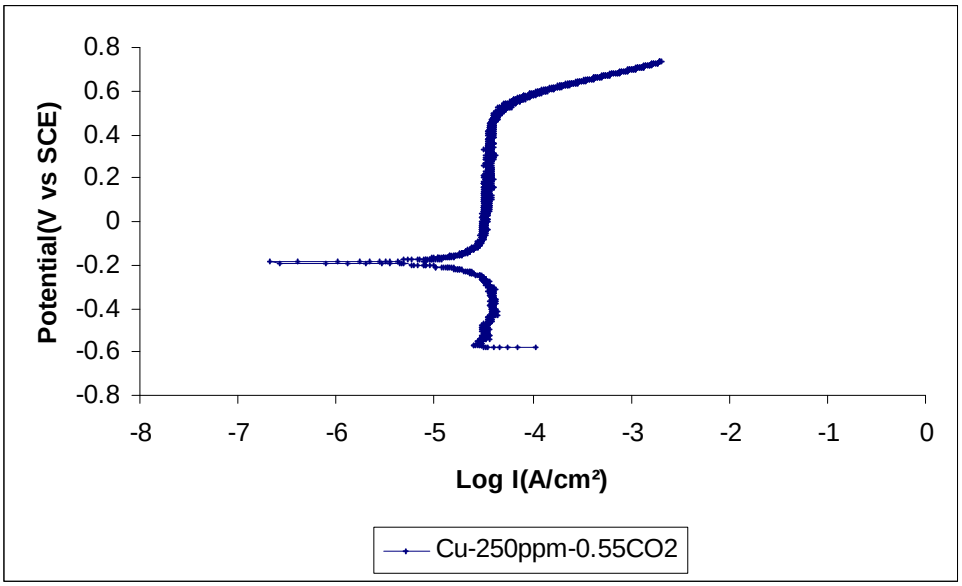

Figure 45: Cyclic polarization curve of carbon steel in 5 M MEA-1.2 M PZ containing 250 ppm $CuCO_3$ and 0.55 mol/mol CO_2 loading at 80°C

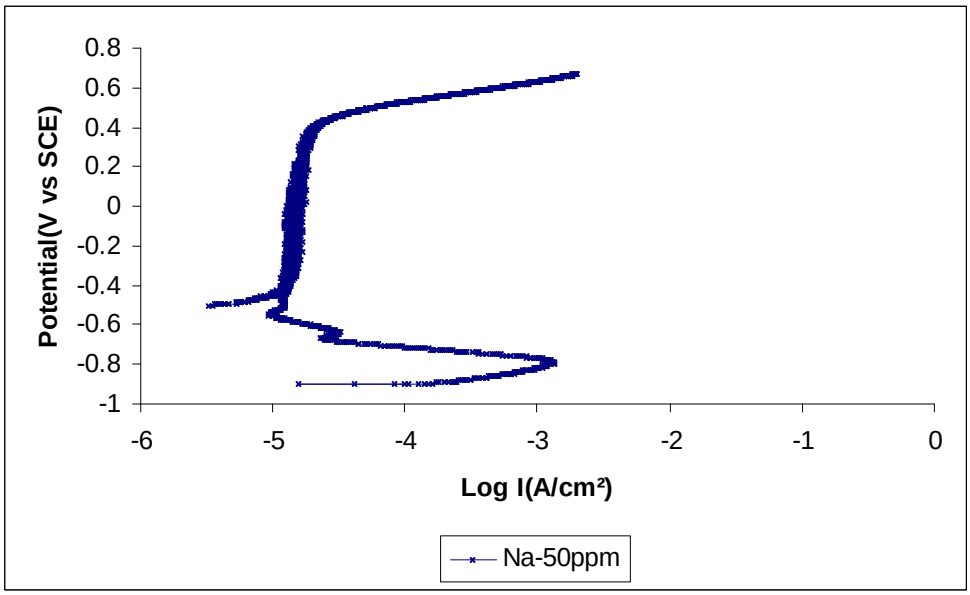

Figure 46: Cyclic polarization curve of carbon steel in 5 M MEA-1.2 M PZ containing 50 ppm $NaVO_3$ and 0.20 mol/mol CO_2 loading at 80°C

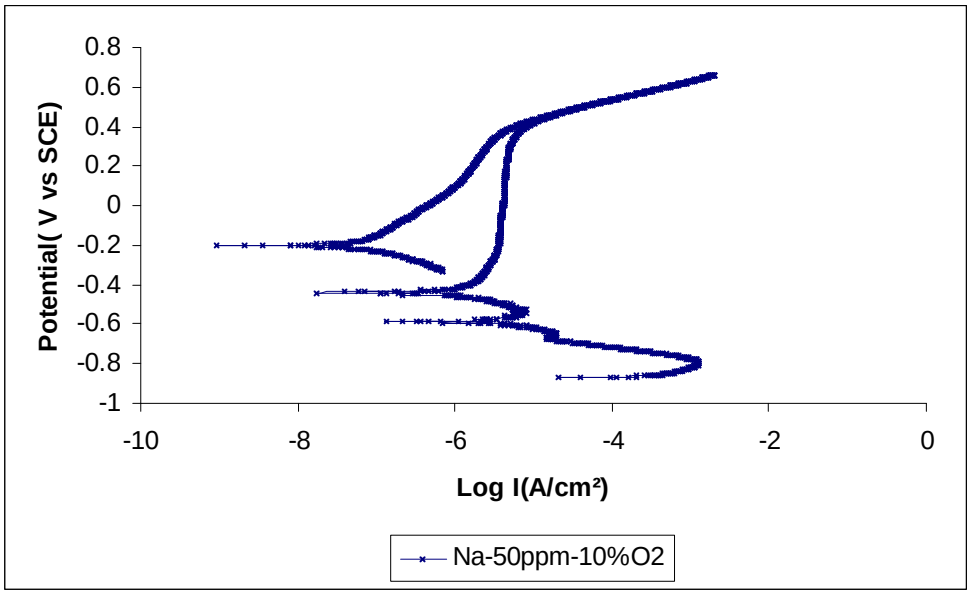

Figure 47: Cyclic polarization curve of carbon steel in 5 M MEA-1.2 M PZ containing 50 ppm $NaVO_3$ and 0.20 mol/mol CO_2 loading at 80°C with 10% O_2

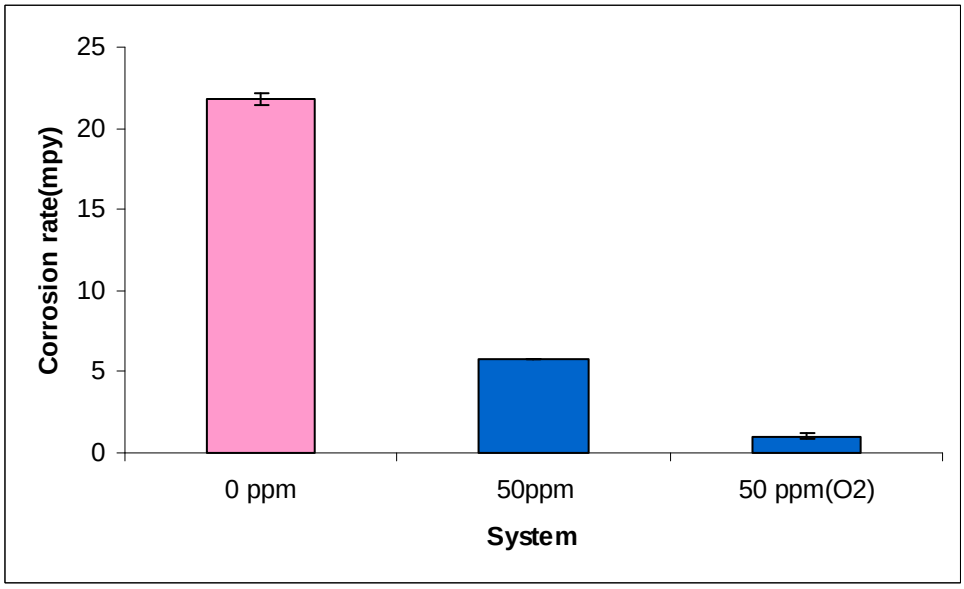

Figure 48: Corrosion rates of carbon steel in 5 M MEA-1.2 M PZ containing 50 ppm $NaVO_3$ and 0.20 mol/mol CO_2 loading at 80°C

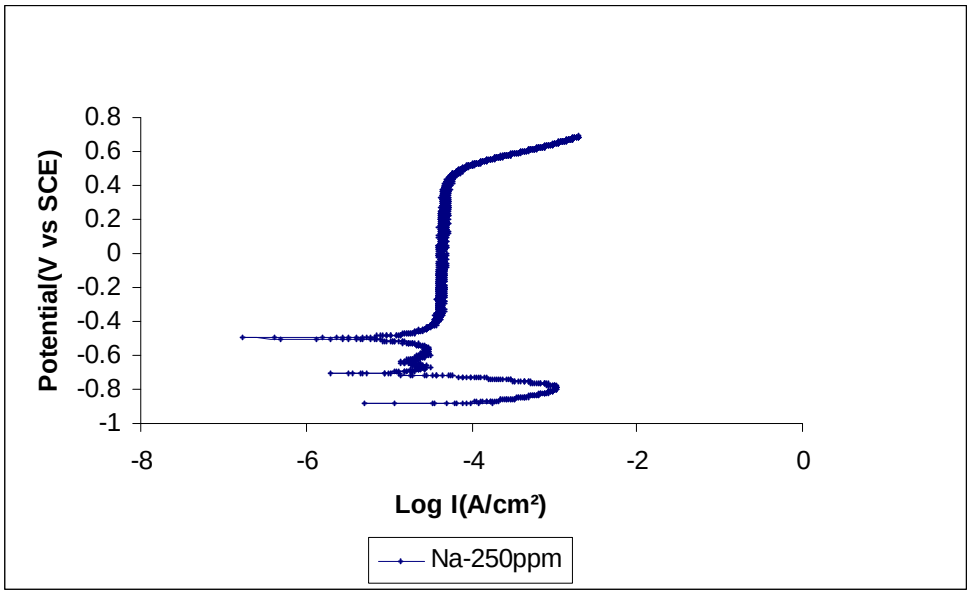

Figure 49: Cyclic polarization curve of carbon steel in 5 M MEA-1.2 M PZ containing 250 ppm $NaVO_3$ and 0.20 mol/mol CO_2 loading at 80^{o}C

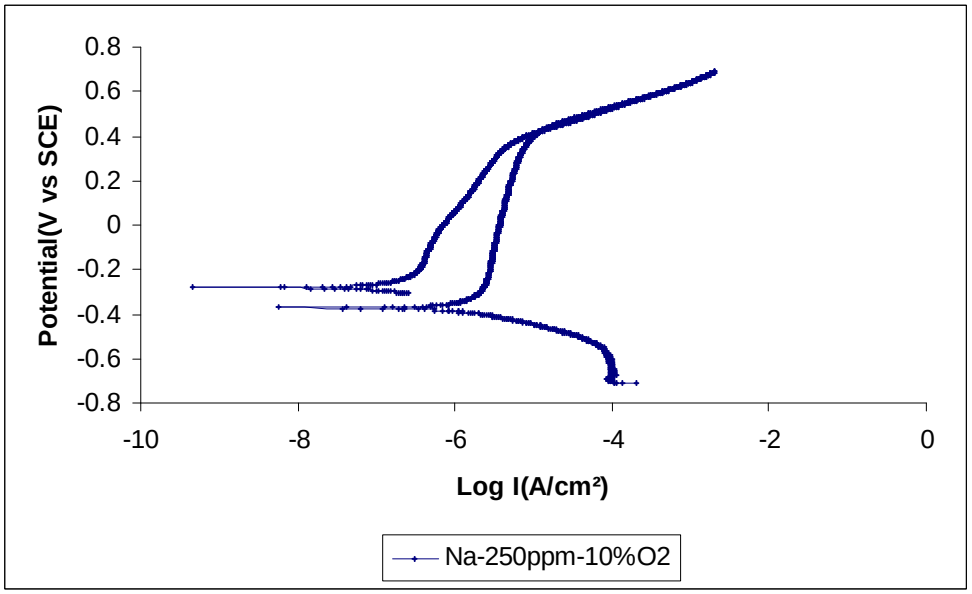

Figure 50: Cyclic polarization curve of carbon steel in 5 M MEA-1.2 M PZ containing 250 ppm $NaVO_3$ and 0.20 mol/mol CO_2 loading at 80^{o}C with 10% O_2

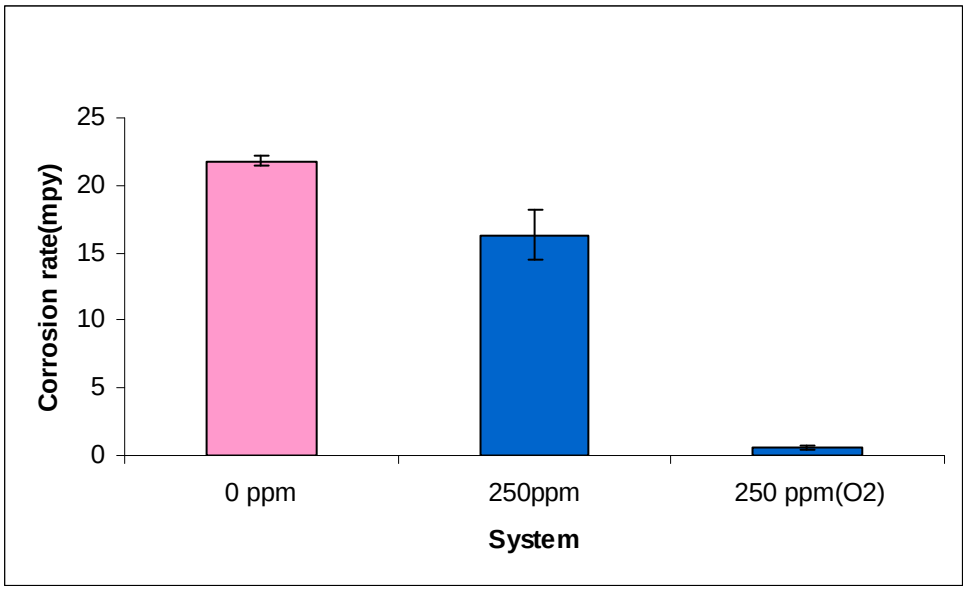

Figure 51: Corrosion rates of carbon steel in 5 M MEA-1.2 M PZ containing 250 ppm $NaVO_3$ and 0.20 mol/mol CO_2 loading at 80°C

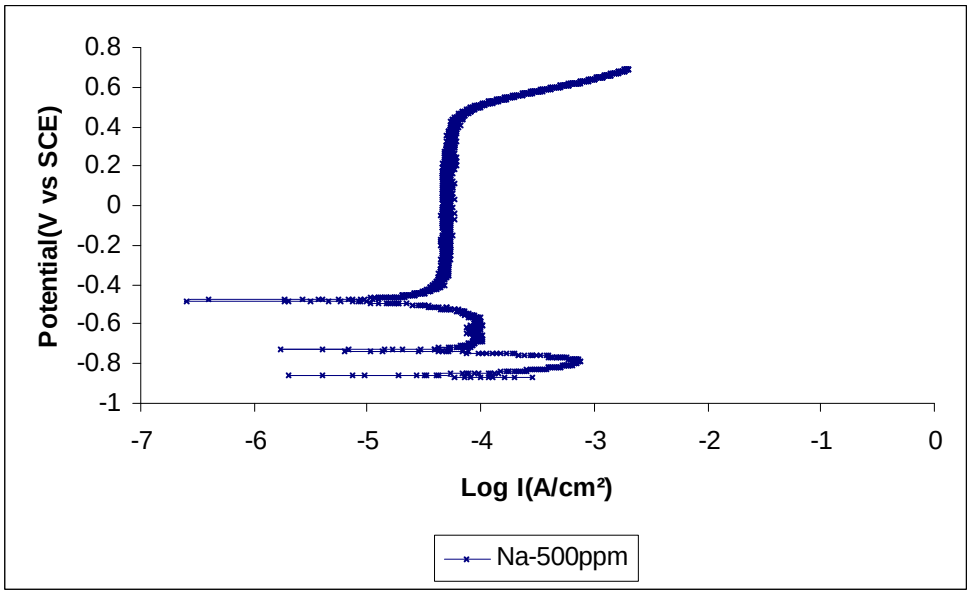

Figure 52: Cyclic polarization curve of carbon steel in 5 M MEA-1.2 M PZ containing 500 ppm $NaVO_3$ and 0.20 mol/mol CO_2 loading at 80°C

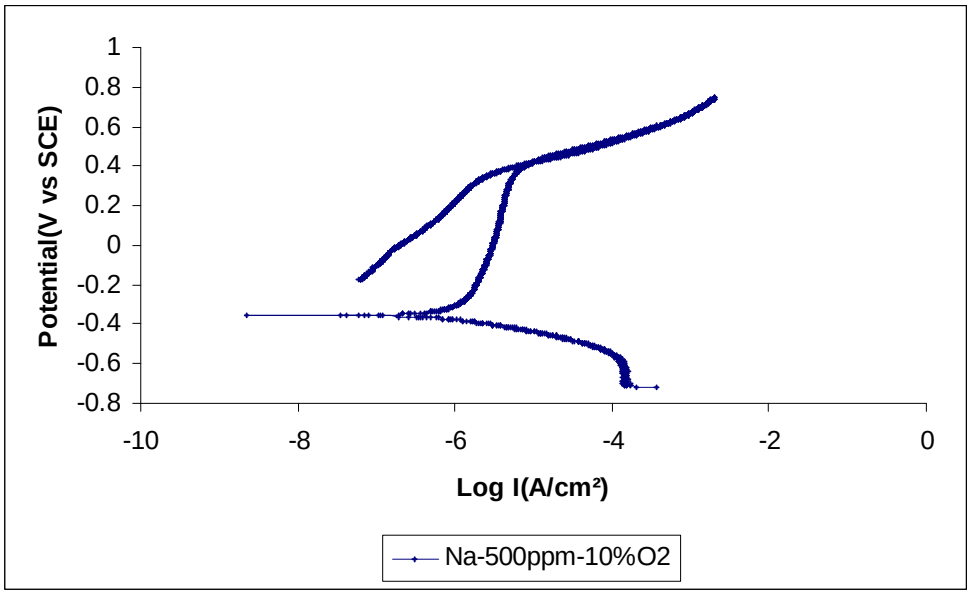

Figure 53: Cyclic polarization curve of carbon steel in 5 M MEA-1.2 M PZ containing 500 ppm $NaVO_3$ and 0.20 mol/mol CO_2 loading at 80°C with 10% O_2

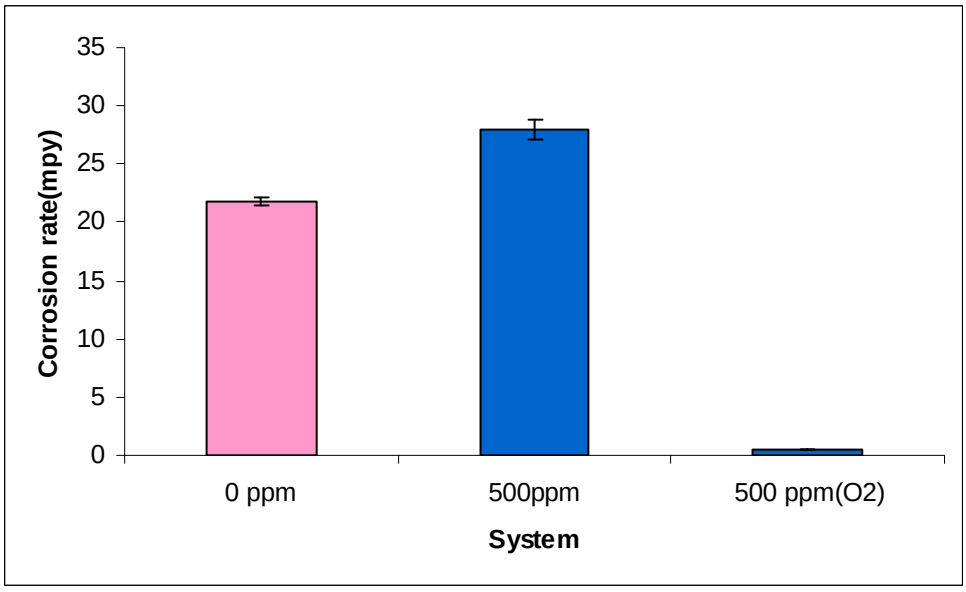

Figure 54: Corrosion rates of carbon steel in 5 M MEA-1.2 M PZ containing 500 ppm $NaVO_3$ and 0.20 mol/mol CO_2 loading at 80°C

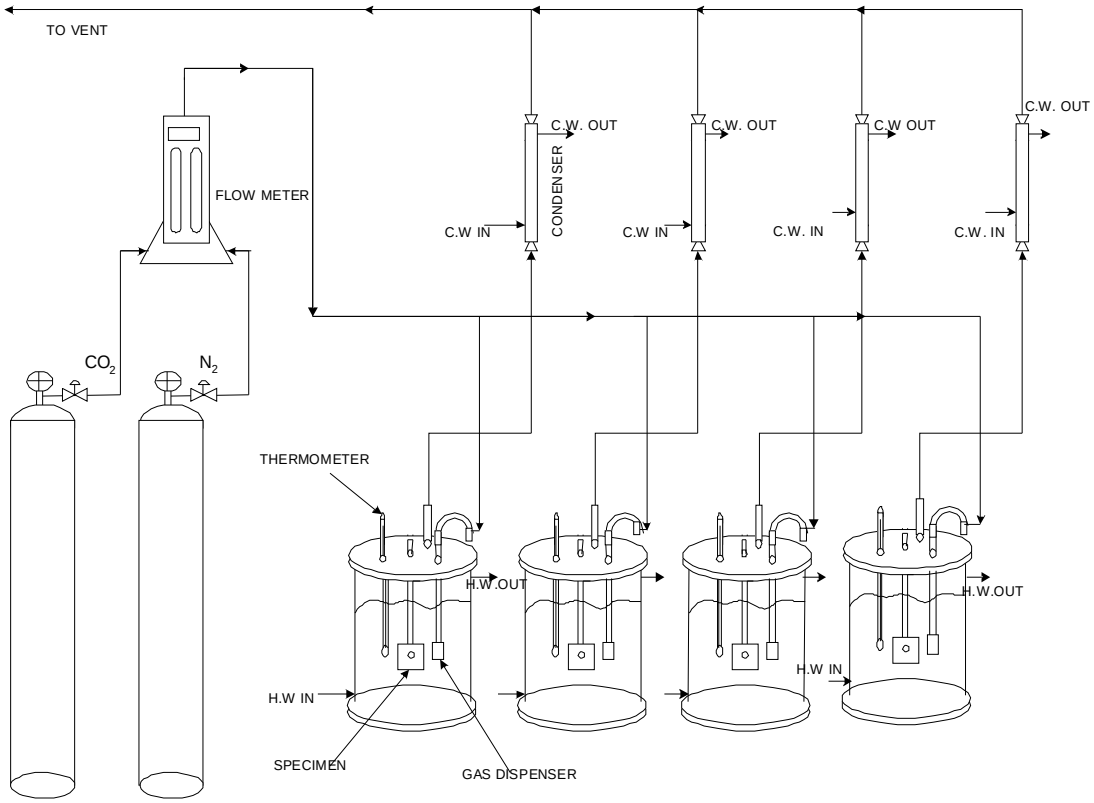

Figure 55: Experimental setup of weight loss test

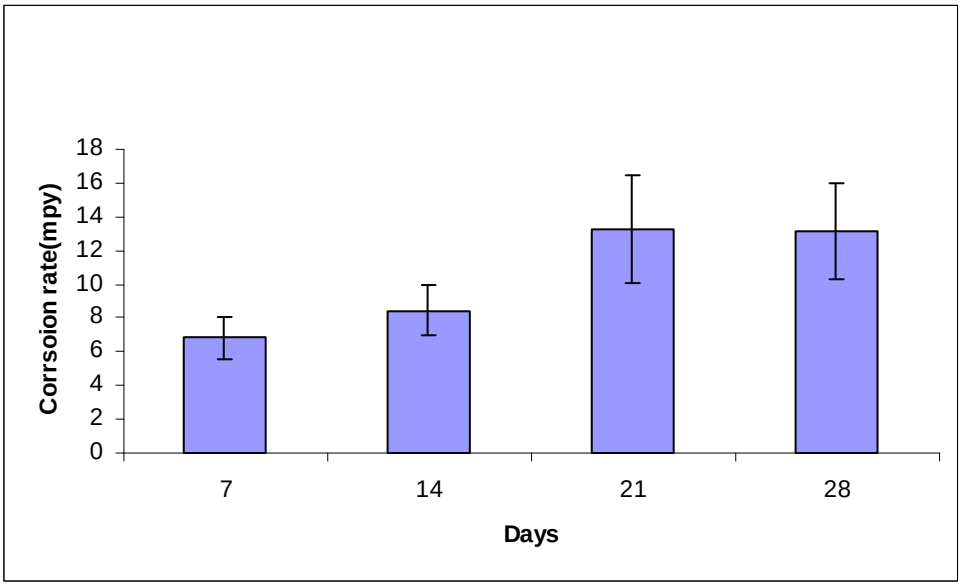

Figure 56: Corrosion rates of carbon steel in 5 M MEA-1.2 M PZ, 0.20 mol/mol CO_2 loading at 80^{o}C and 10% O_2

References

Abesamis A, Bayer B, Hai R. *Crystallization of Potassium Sulfate.* ChE 264 special project report. Fall 2006.

Cullinane, JT. Thermodynamics and Kinetics of Aqueous Piperazine with Potassium Carbonate for Carbon Dioxide Absorption, PhD dissertation, University of Texas, Austin, 2005.

Chang H and Shih C. Simulation and Optimization for Power Plant Flue Gas CO_2 Absorption-Stripping Systems. *Separation Science and Technology*. 2005;40:877-909.

CRC Handbook of Chemistry and Physics, 87th edition, online, section 8-114, http://www.hbcpnetbase.com/articles/08_21_86.pdf

Dawodu OF, Meisen A. Gas chromatographic analysis of alkanolamine solutions using capillary and packed columns. *J Chrom*. 1993;629(2):297-307.

Dionex IonPac CS17 Analytical Column Product Manual. Revision 03. May 2003. http://www1.dionex.com/en-us/webdocs/manuals/ic/31747-03_CS16_V19.pdf (Accessed January 2005)

Freguia S, Rochelle GT. Modeling of CO_2 Capture by Aqueous Monoethanolamine, *AIChE J*. 2003;49:1676-1686.

Goff GS, Rochelle, GT. Monoethanolamine Degradation: O_2 Mass Transfer Effects under CO_2 Capture Conditions. *Ind Eng Chem Res.* 2004;43(20):6400-6408.

Hilliard M. Thermodynamics of Aqueous Piperazine/ Potassium Carbonate/ Carbon Dioxide Characterized by the Electrolyte NRT Model in AspenPlus®. MS thesis, University of Texas, Austin, 2005.

Hilliard M. Oral Communication. March 2007.

Jimenez et al. Optimization of a Diabatic Column with Sequential Heat Exchangers. *Ing Eng Chem Res.* 2004:7566-7571.

Johannessen & Røjorde**.** Equipartition of entropy production as an approximation to the state of minimum entropy production in diabatic distillation. *Energy.* 2007;32:467-473.

Mellin J. Preliminary CHE 264 Report on AMP Degradation. Submitted March 24, 2007.

Oyenekan BA, Rochelle GT. Alternative Stripper Flow Schemes for CO2 Capture by Aqueous Amines. Submitted to *AIChE J*. 2007.

Polderman LD, Dillon CP, Steele AB. Why monoethanolamine solution breaks down in gas-treating service. *Oil Gas J*. 1955;54(2):180-183.Waters LC/MS: Interfacing HPLC and MS. http://www.waters.com/WatersDivision/ContentD.asp?watersit=EGOO-66YNU9. (Accessed March 2007).

Sachde D, Sivaram S. *CO_2 capture: Solubility of Potassium Sulfate in Amine Solutions.* ChE 264 special project report. Summer 2006.

Söhnel O, Novotny P. *Densities of Aqueous Solutions of Inorganic Substances*. Elsevier, Amsterdam, 1985.

Supap T, et al. Analysis of Monoethanolamine and its Oxidative Degradation Products During CO_2 Absorption from Flue Gases: A Comparative Study of GC-MS, HPLC-RID and CE-DAD Analytical Techniques and Possible Optimum Combinations. *Ind Eng Chem Res.* 2006;45(8):2437-2451.

Yazvikova NV, Zelenskaya LG, Balyasnikova LV. Mechanism of Side Reactions during removal of Carbon Dioxide from Gases by Treatment with Monoethanolamine. *Zhurnal Prikladnoi Khimii.* 1975;48(3):674-676.